Argonaute identity defines the length of mature mammalian microrna

Juvvuna Prasanna Kumar

2013

Juvvuna Prasanna Kumar. (2013). Argonaute identity defines the length of mature mammalian microrna. Doctoral thesis, Nanyang Technological University, Singapore.

https://hdl.handle.net/10356/51099

https://doi.org/10.32657/10356/51099

NANYANG TECHNOLOGICAL UNIVERSITY

ARGONAUTE IDENTITY DEFINES THE LENGTH OF MATURE MAMMALIAN MICRORNAS

JUVVUNA PRASANNA KUMAR

SCHOOL OF BIOLOGICAL SCIENCES

2013

ARGONAUTE IDENTITY DEFINES THE LENGTH OF MATURE MAMMALIAN MICRORNAS

JUVVUNA PRASANNA KUMAR

SCHOOL OF BIOLOGICAL SCIENCES

A thesis submitted to the Nanyang Technological University in partial fulfilment of the requirement for the degree of Doctor of Philosophy

2013

ACKNOWLEDGEMENTS

Words are not always enough to convey what one means but then they have to be said, and hence these acknowledgements. One person without whom this thesis wouldn't be a reality is my research supervisor, Nanyang Assistant Professor Dr. Eugene Makeyev. I sincerely thank him for excellent guidance, constant support and encouragement for doing this work. I thank him for providing excellent research facilities and giving me complete freedom to carry out this work. I am greatly indebted to him for everything he has done for me.

I would like to acknowledge my thesis advisory committee members Dr. Ravi Kambadur and Dr. Zhang Li-Feng for their valuable guidance and encouragement. My sincere thanks to Dr. G. Hannon, Dr. A. McMahon, Dr. G. Meister, Dr. M. Siomi and Dr. T. Tuschl for their kind help with plasmids, cell lines and antibodies we requested for.

Since maximum time of my research period has been spent in the lab, I couldn't have asked for a better company. I would like to thank all my lab people for extending help whenever I needed. At this point, I cannot forget the unconditional support, encouragement and help I received from Piyush, without which it would have been impossible to do this work.

I thank the present Chair, Prof. Mark Featherstone and the past chairpersons for providing excellent research facilities in the department. A special note of thanks to Dr. F. Xavier Roca and Dr. Su I-Hsin for all their encouragement, interest in my work

and valuable advice. I also acknowledge office staff of School of Biological Sciences for their support.

My special thanks are due to Dr. Eugene Makeyev for the generous help in getting my thesis ready. I thank Piyush, Sandhya and Manish for all their help in preparing my thesis.

I have been fortunate to make some really good friends, who have always stood by me. My heartfelt thanks to my friends, Piyush, Sandhya and their families for their constant encouragement and moral support.

I express my deepest gratitude to Nanyang Technological University for financially supporting me with NTU Research Scholarship during the course of my PhD studies.

Finally, however hard I try I won't be able to do justice in thanking my parents, who have been tremendous support to me throughout my life. Last but not the least, I am lucky to have the constant support and encouragement of my family, specially my brother and sister.

TABLE OF CONTENTS

LIST OF FIGURES

Introduction

MATERIALS AND METHODS

RESULTS

DISCUSSION

LIST OF TABLES

MATERIALS AND METHODS

RESULTS

ABBREVIATIONS

µg	Microgram
µl	Microliter
Amp	Ampicillin
AMV	Avian megalo virus
APS	Ammonium persulphate
ATP	Adenosine-5'-triphosphate
BCA	Bicinchoninic acid
BSA	Bovine serum albumin
$CaCl_2$	Calcium chloride
cDNA	Complementary DNA
Ci	Curie units
Cm	Centimetre
DEPC	Diethyl pyrocarbonate
DMEM	Dulbecco's Modified Eagle Medium
DNase	Deoxyribonuclease
dNTP	Deoxyribonucleotide triphosphate
Dox	Doxycycline
dsRNA	Double stranded RNA
DTT	Dithiothreitol
E12.5	12.5 days post-conception embryos
ECDFs	Empirical cumulative distribution functions
EDTA	Ethylenediaminetetraacetic acid
EGFP	Enhanced Green fluorescence protein

FBS	Fetal bovine serum
FITC	Fluorescein isothiocyanate
fmol	Femto Molar
GAPDH	Glyceraldehyde 3-phosphate dehydrogenase
hAGO	Human Argonaute
HCl	Hydrogen chloride
HEK293T	Human Embryonic Kidney 293T
HEPES	4-(2-hydroxyethyl)-1-piperazineethanesulfonic acid
HILO-RMCE	High-efficiency low-background recombination-mediated cassette exchange
HPRT	Hypoxanthine-guanine phosphoribosyltransferase
HRP	Horseradish peroxidase
IPTG	Isopropyl-β-D-thio-galactoside
KCl	Potassium chloride
LB	Luria-Bertani
LM-RT-PCR	Ligation-Mediated RT-PCR
mAgo	Mouse Arognaute
$MgCl_2$	Magnesium chloride
miRISC	miRNA-Induced Silencing Complex
miRNA	micro RNA
miRNP	micro RNA Ribonucleo protein complex
mmol	Milli Molar
mRNA	Messenger Ribo nucleic acid
NaCl	Sodium chloride
ncRNA	Non-coding RNA
NEB	New England Biolabs

ng	Nanogram
nt	Nucleotide
^{o}C	Degree centigrade
PACT	Protein kinase R (PKR)-activating protein
PAG	Polyacrylamide Gel
PAGE	Polyacrylamide Gel Electrophoresis
PBS	Phosphate-buffered saline
PCR	Polymerase Chain Reaction
piRNA	Piwi-interacting RNA
PMSF	Phenylmethanesulfonylfluoride
PNK	Polynucleotide Kinase
Pol	Polymerase
pre-miRNA	Precursor micro RNA
pri-miRNA	Primary micro RNA
PTBP	Polypyrimidine tract-binding protein
REST	RE1-silencing transcription repressor
RISC	RNA-Induced Silencing Complex
RNA	Ribonucleic acid
RNase	Ribonuclease
rRNasin	Recombinant RNase Inhibitor
rpm	Revolutions per minute
rRNA	Ribosomal RNA
RT-qPCR	Reverse transcription-quantitative PCR
RT	Reverse transcription
RT-PCR	Reverse transcription-PCR

SDS	Sodium dodecyl sulfate
siRISC	siRNA-Induced Silencing Complex
siRNA	Small interfering RNA
snRNA	Small nuclear RNA
sncRNA	Short ncRNA
snoRNA	Small nucleolar RNA
SSC	Saline-sodium citrate
ssRNA	Single-stranded RNA
TBE	Tris/Borate/EDTA
TBST	Tris Buffered Saline with Tween
TE	Tris EDTA
TEMED	Tetramethylethylenediamine
Temp	Temperature
TET promoter	Tetracycline controlled promoter
TRBP	Transactivating response RNA-binding protein
tRNA	Transfer RNA
tTA	Tetracycline trans activator
UTR	Untranslated region
X-gal	5-bromo-4-chloro-3-indolyl-b-D-galactopyranoside

ABSTRACT

Regulation of eukaryotic gene expression by microRNAs, 19-25 nt long non-coding RNAs, plays a major part in organismal development and function. Individual miRNAs often exist as populations of length variants but the mechanisms underlying this heterogeneity are poorly understood. Here we identified a large set of miRNAs that are significantly shortened during mouse nervous system development. This phenomenon, which we refer to as miRNA trimming, occurs at the 3' end of mature miRNAs following the Dicer processing step. Of the four miRNA-interacting Argonaute paralogs encoded in mammalian genomes, Ago2-bound miRNAs are trimmed with the highest efficiency. This is consistent with the high expression of Ago1 in embryonic brain and an increase in the relative abundance of Ago2 at the later developmental stages. We further show that the trimming efficiency is defined by the structure of the Argonaute PAZ domain interacting with the miRNA 3' end as well as the identity of the 3'-terminal nucleotide. These results uncover the previously unknown Argonaute role in developmentally regulated changes in the composition of miRNA isoforms.

1. INTRODUCTION

The information encoded in genomes of higher eukaryotes is sufficient to program the development from a unicellular zygote to a fully grown multicellular organism. Expression of this genetic information stored in the form of DNA requires its transcription into RNA. A fraction of transcripts called messenger RNAs (mRNAs) is further translated into proteins, the major building blocks of contemporary cell-based life forms. In addition to mRNAs, a number of non-coding RNAs (ncRNAs), both short (<200 nt) and long (>200 nt), are known to be synthesized in eukaryotic cells. Of these, short ncRNAs form a major class of regulatory ncRNAs mediating post transcriptional control of gene expression.

1.1 Short ncRNAs

Short ncRNAs (sncRNAs) have been amongst the first RNA molecules discovered in the cell (Holley *et al*., 1965). Despite their modest size, sncRNAs are known to play a variety of important roles ranging from structural and catalytic to adaptor and regulatory (Aalto & Pasquinelli, 2012; Ambros, 2004; Bartel, 2004; Bartel, 2009; Bushati & Cohen, 2007; Kim, 2005). The originally identified sncRNAs were typically 30-200 nt long and included 5S and 5.8S ribosomal RNAs (rRNAs), transfer RNAs (tRNAs), small nuclear (sn) and small nucleolar (sno) RNAs as well as the 7SL RNA component of the cytoplasmic signal recognition particle (Bachellerie *et al*., 2002; Bishop *et al*., 1970a; Bishop *et al*., 1970b; Matera *et al*., 2007; Zieve & Penman, 1976). Recent studies have shown that a substantially more diverse class of sncRNAs encoded in eukaryotic genome comes within 18-30 nt size range. These sncRNAs function as important players in spatiotemporal regulation of gene expression through mRNA degradation, translational repression and transcriptional silencing mechanisms.

Based on the mechanism of biogenesis and interacting protein partners these 18-30 nt sncRNAs can be classified into three classes (Kim *et al*., 2009).

i) Piwi-interacting RNAs (piRNAs)

ii) Small interfering RNAs (siRNAs)

iii) MicroRNAs (miRNAs)

Despite important differences in their biogenesis and function, these sncRNAs share several similar features including their relatively uniform lengths, presence of a 5' phosphate and association with a specific member of the Argonaute protein family (Czech & Hannon, 2011).

1.1.1 *piRNAs*

piRNAs were initially identified in germ line cells of *Drosophila* and later discovered in other organisms including mammals (Aravin *et al*., 2003; Grivna *et al*., 2006; Horwich *et al*., 2007; Watanabe *et al*., 2006). These are single-stranded RNAs with a typical length of 24-30 nts. piRNAs feature phosphorylated 5' ends and a 2'-O-methyl (2'-O-me) modifications at their 3' ends. piRNAs associate with members of the PIWI clade of the Argonaute super-family (hence the name "piRNAs") and play a key role in the maintenance of the germ line stability of various organisms by repressing diverse transposable elements (Girard *et al*., 2006; Grivna *et al*., 2006; Houwing *et al*., 2007; Stefani & Slack, 2008; Vagin *et al*., 2006).

1.1.2 *siRNAs*

siRNAs are sncRNAs of ~21 nt size found in invertebrates (e.g., *Drosophila, C. elegans*), vertebrates (e.g., human or mouse) and plants. siRNAs are produced from longer double-stranded (ds) RNA precursors by Dicer endonuclease (Dicer in mouse

and Dicer-2 in flies). Unlike miRNAs (section 1.1.3), this reaction does not require Drosha (Babiarz *et al*., 2008; Jones-Rhoades *et al*., 2006; Kawamura *et al*., 2008; Kim *et al*., 2009; Okamura *et al*., 2008; Watanabe *et al*., 2008). Naturally occurring dsRNAs are derived from transposons, sense-antisense transcript pairs and specialized long stem-loop structures of endogenous origin. Furthermore, siRNAs can also be generated by processing of exogenous long dsRNAs delivered into cells under laboratory conditions or as a result of viral infection (Elbashir *et al*., 2001b; Fire *et al*., 1998; Jones *et al*., 1998; Liu *et al*., 2004; Zhao *et al*., 2003). Moreover, synthetic exogenous (exo) siRNAs are a commonly used research tool for knocking down the expression of specific genes in mammalian cells (Elbashir *et al*., 2001a). siRNAs associate with the Ago clade of Argonaute super–family. siRNA-loaded Ago proteins additionally associate with other proteins to form so-called siRNA-induced Silencing Complex (siRISC). This complex functions as the central part of the RNA interference (RNAi) machinery by inducing sequence-specific endolytic cleavage of target mRNAs. siRNAs in plants and worms are generated by a more complex pathway that relies on RNA-dependent RNA polymerases (RdRPs) (Chapman & Carrington, 2007).

1.1.3 *miRNAs*

miRNAs are sncRNAs of about 22 nt that are expressed in tissue-specific and developmentally regulated manner. Human and mouse genomes encode hundreds of distinct miRNAs, each potentially targeting an extensive set of mRNA targets (Ambros, 2004; Bartel, 2004; Bartel, 2009; Bushati & Cohen, 2007; Kim, 2005). miRNAs contribute in shaping the post transcriptional regulatory landscape of an eukaryotic cell. They base-pair to the target mRNAs within the 3'UTR or sometimes other mRNA regions and normally lead to mRNA translational repression or/and

degradation. A number of miRNAs have been shown to play critical roles in diverse aspects of development and physiology (Bushati & Cohen, 2007; Carrington & Ambros, 2003; Fineberg *et al*., 2009; Kim, 2005; Leung & Sharp, 2010; Wienholds & Plasterk, 2005).

The first miRNA *lin-4* was discovered in *Caenorhabditis elegans* by Victor Ambros and Gary Ruvkun in 1993 as post transcriptional regulator of *lin-14* transcript resulting in reduced protein levels (Lee *et al*., 1993; Wightman *et al*., 1993). With advancements in molecular biology approaches including RNA deep sequencing technologies and computational prediction methods a large number of miRNAs and their potential targets have been identified.

1.2 miRNA Biogenesis

1.2.1 *miRNA genes and transcription*

miRNAs are found at diverse genomic locations including both protein coding (intragenic miRNAs) as well as non-protein-coding regions (intergenic miRNAs). Interestingly, in the latter case, mammalian miRNAs are often expressed from gene paralogues (Lagos-Quintana *et al*., 2001; Lau *et al*., 2001; Mourelatos *et al*., 2002). Within transcripts undergoing splicing, miRNAs can be intronic or exonic in origin (Kim *et al*., 2009; Lee *et al*., 2002). Individual miRNAs are often transcribed from separate gene promoters. In addition, a fraction of miRNAs is encoded in clusters and expressed in this case as a single poly-cistronic transcription unit (Baskerville & Bartel, 2005; Kim & Nam, 2006; Yu *et al*., 2006).

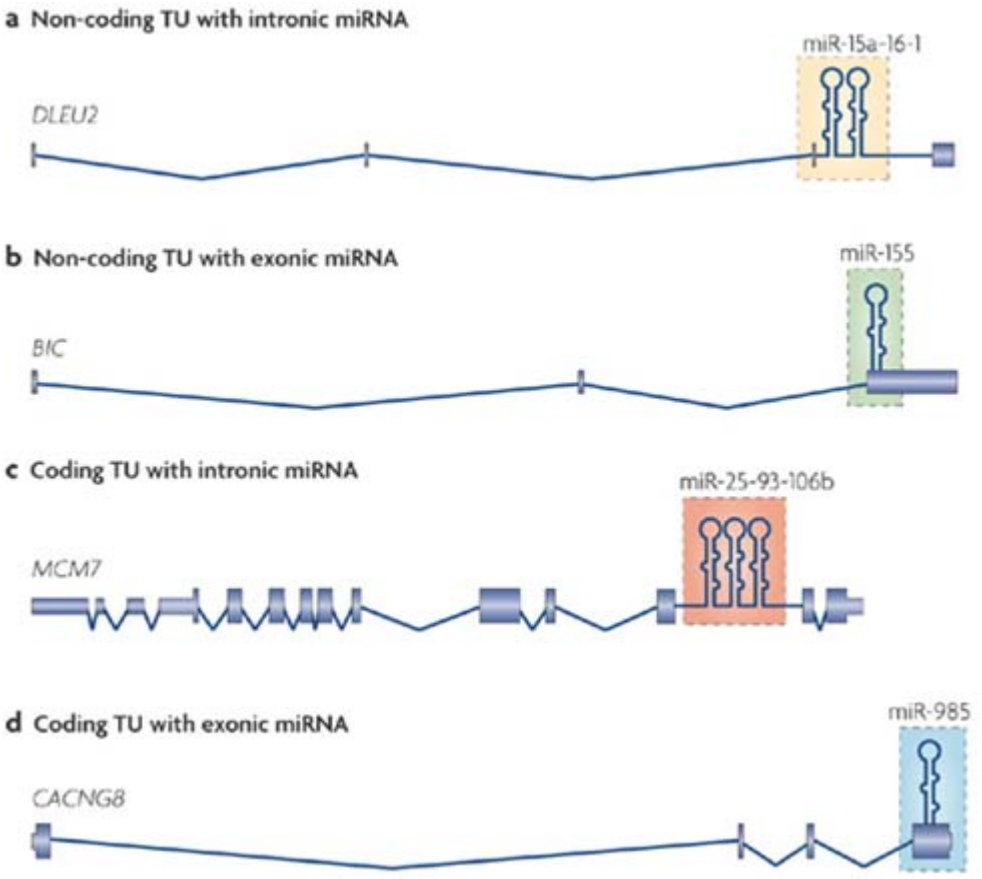

Figure 1.1: Examples of a few miRNAs expressed from different genomic locations in various transcriptional units (Kim *et al*., 2009).

miRNA genes of intergenic origin are transcribed by RNA Pol II or Pol III, whereas intragenic miRNAs are transcribed only by Pol II. Most miRNA genes are transcribed by RNA polymerase II as long primary miRNA (pri-miRNA) transcripts containing a 5' 7-methyl guanosine cap and 3' poly(A) tail. On the other hand, a few of the pri-miRNAs are transcribed by RNA Pol III from corresponding promoter sequences associated with Alu repeats, tRNA genes, mammalian wide interspersed repeat (MWIR) promoter units. miRNA encoded by mouse gammaherpes virus or adenoviruses are also thought to be generated through Pol III transcription (Andersson *et al*., 2005; Borchert *et al*., 2006; Bracht *et al*., 2004; Cai *et al*., 2004; Lee *et al*., 2004; Pfeffer *et al*., 2005).

1.2.2 *Processing of pri-miRNA transcript*

The pri-miRNAs are processed into ~70 nt hairpin-shaped precursor miRNA (pre-miRNA) by so-called microprocessor complex containing the catalytic subunit Drosha and the DGCR8 (humans) or Pasha (*D. melanogaster*) protein as its core subunits. Drosha is an RNaseIII type endonuclease with two RNaseIII and one dsRNA binding domains. Drosha cuts partially double-stranded elements of pri-miRNAs releasing the stem-loop pre-miRNA elements with 5' phosphate and 3' hydroxyl groups featuring a 2 nt 3' overhang (Denli *et al*., 2004; Gregory *et al*., 2004; Han *et al*., 2004).

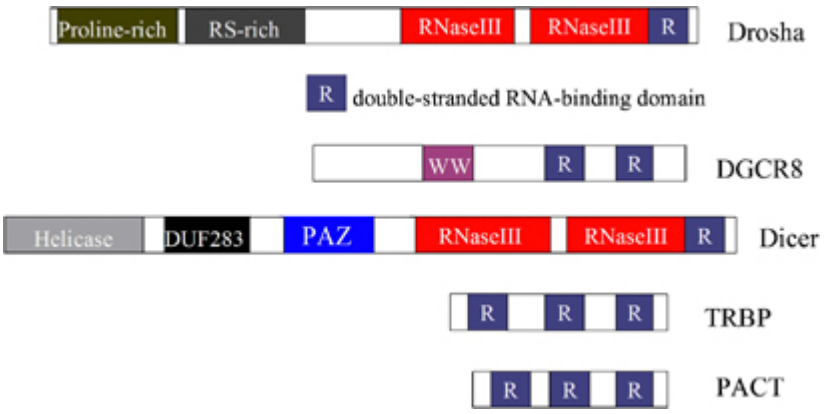

Figure 1.2: Diagram showing the domain structure of Drosha, Dicer and their associated proteins (Zeng, 2006).

Drosha recognizes the presence of a ~33 base-pair stem with a terminal loop and the flanking 5' and 3' ssRNA segments. DGCR8 has two double-stranded RNA binding domains that interact with the stem and the flanking segments of the pri-miRNA substrate and helps Drosha to position its cleavage site approximately 11 bases away from the Y-shaped junction formed by the ssRNA and the dsRNA elements (Han *et al*., 2006; Zeng & Cullen, 2005).

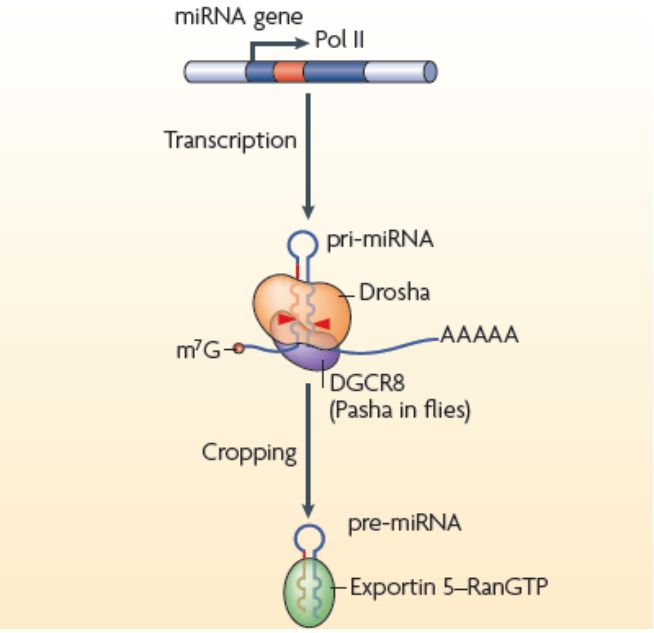

Figure 1.3: Schematic representation of pri-miRNA biogenesis from canonical miRNA genes (Kim *et al*., 2009).

As mentioned above, a number of miRNAs are encoded within introns of protein-encoding or long non-coding RNA genes. In this case, the pre-miRNA excision has to be coordinated with the splicing reaction. Interestingly, the Drosha processing step may precede splicing of the host intron without perturbing correct joining of the exons (Kim & Kim, 2007). Precise substrate recognition of Drosha does not depend on 5'cap or 3' poly (A) tail of pri-miRNA. Moreover, Drosha processing is generally independent of splicing in the case of intronic miRNAs. These considerations allow Drosha to process pri-miRNAs in a co-transcriptional manner, before the primary transcript is completely synthesized (Morlando *et al*., 2008; Pawlicki & Steitz, 2008).

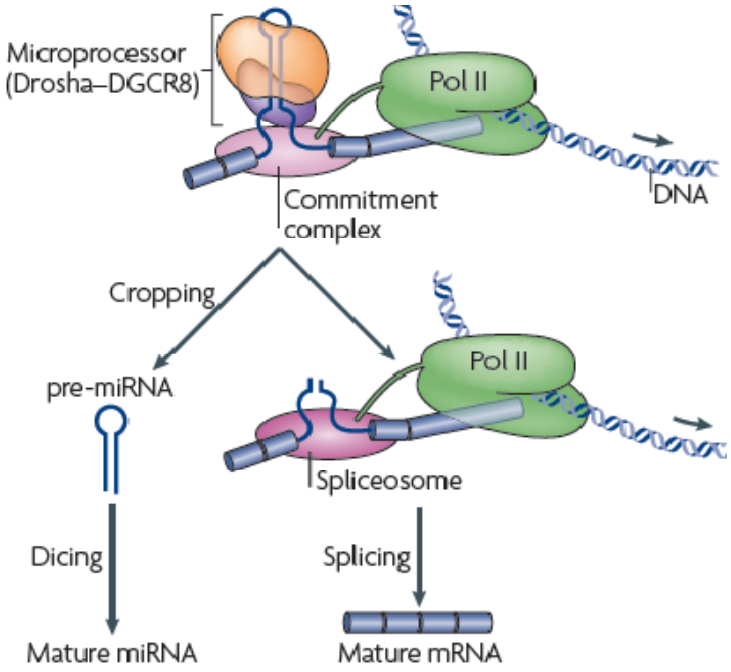

Figure 1.4: Schematic representation of intronic pri-miRNA processing by Drosha (Kim *et al*., 2009).

In a handful of cases, short miRNA-containing introns called 'mirtrons' are spliced out of the primary mRNA transcripts and processed into pre-miRNA hairpin-like structures by intron lariat debranching enzyme and exoribonucleases rather than the Drosha/Microprocessor complex (Okamura *et al*., 2007; Ruby *et al*., 2007).

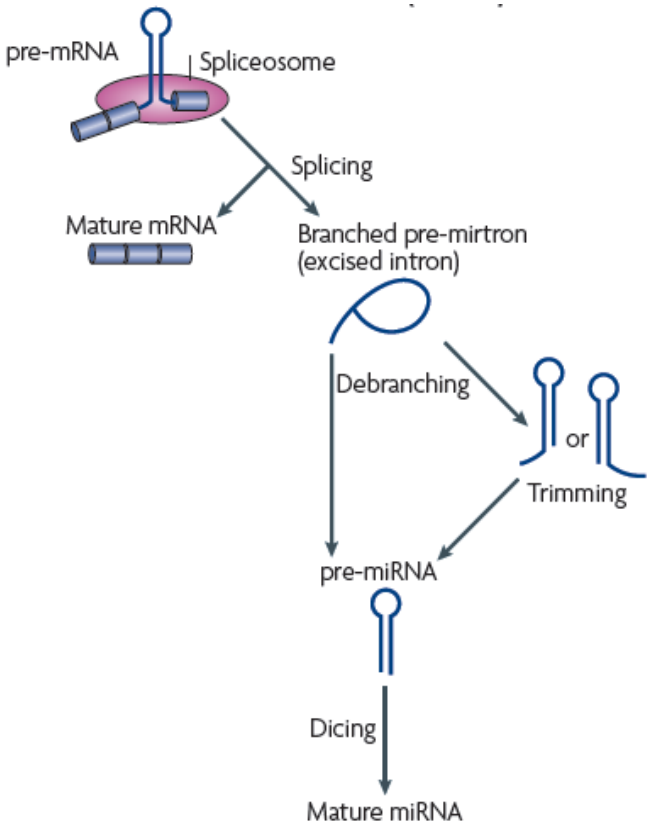

Figure 1.5: Schematic representation of the pre-miRNA biogenesis in the mirtron pathway (Kim *et al*., 2009).

Regardless of their nuclear biogenesis mechanisms, pre-miRNAs (normally containing a 2 nt overhang at the 3' end) are exported from nucleus to the cytoplasm through an Exportin-5/Ran-GTPase-dependent mechanism (Bohnsack *et al*., 2004; Lund *et al*., 2004).

1.2.3 *Processing of pre-miRNA and RISC loading of miRNA*

Once exported to the cytoplasm, pre-miRNAs are processed by Dicer in association with TRBP, PACT and other RNA-binding proteins. Dicer is an enzyme with two catalytic RNaseIII type endonuclease domains and a PAZ domain that recognizes the 3' nucleotide overhang of the precursor miRNA (Chendrimada *et al*., 2005; Lee *et al*., 2006). Dicer is highly conserved in most of the eukaryotic organisms.

Some organisms (e.g., *A. thaliana, D. melanogaster*) contain more than one Dicer homologue, each specific for distinct substrates including dsRNA and precursor miRNA. In other organisms (e.g., *S.pombe, C. elegans* and mammals), a single Dicer catalyzes biogenesis of both miRNAs and siRNAs (Meister & Tuschl, 2004). The Dicer cleavage gives rise to a duplex of mature miRNA with the partially complementary miRNA* strand (Ketting *et al*., 2001; Saito *et al*., 2005). Interestingly, a Dicer-independent mechanism is used for generating evolutionarily conserved miRNA miR-451, wherein Argonaute protein Ago2 cuts the corresponding pre-miRNA precursor (Cheloufi *et al*., 2010; Cifuentes *et al*., 2010; Yang *et al*., 2010).

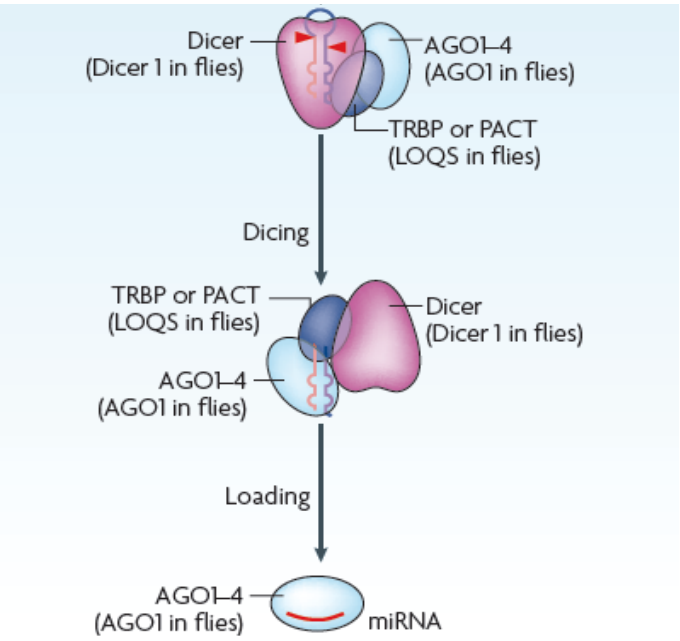

Figure 1.6: Schematic representation of pre-miRNA processing by Dicer leading to generation of mature miRNA (Kim *et al*., 2009).

The miRNA strand of the miRNA:miRNA* duplex gets incorporated into RNA-induced silencing complex (RISC), while the miRNA* strand (also called passenger stand) is normally degraded (Bernstein *et al*., 2001; Knight & Bass, 2001).

RISC strand preference is determined by the thermodynamic stability of the duplex ends. Strand that has less stability at the 5' end in the mature miRNA duplex is normally selected as the miRNA/guide strand (Khvorova *et al*., 2003; Schwarz *et al*., 2003). miRNA loading into RISC is mediated by Dicer, TRBP and Argonaute (Ago) proteins (Gregory *et al*., 2005).

1.3 Argonaute protein family

Argonaute proteins are key factors in many different RNA silencing pathways and play vital roles in embryonic development, cell differentiation and stem cell maintenance. Based on sequence similarities and phylogenetic analysis, the Argonaute protein super-family can be broadly divided into three clades, or subfamilies: Ago subfamily, PIWI subfamily and a recently identified new subfamily the *Caenorhabditis elegans*-specific group 3 Argonautes or Wagos (Carmell *et al*., 2002; Hutvagner & Simard, 2008; Joshua-Tor & Hannon, 2011; Peters & Meister, 2007; Yigit *et al*., 2006). PIWI proteins are predominantly expressed in the germ line, where they interact with piRNAs in a variety of organisms including *Drosophila*, Zebrafish and mouse. In contrast, Argonaute proteins tend to be expressed in a more ubiquitous manner (Hock & Meister, 2008). The number of Argonaute super-family genes varies in different organisms: 5 in *Drosophila melanogaster* (2 Argonaute-like and 3 Piwi-like), 10 Argonaute-like in *Arabidopsis thaliana*, only 1 Argonaute-like in *Schizosaccharomyces pombe* and at least 26 Argonaute genes in *C. elegans* (5 Argonaute-like, 3 Piwi-like and 18 group 3 Argonautes) (Hutvagner & Simard, 2008). Based on sequence similarity mammalian Argonaute super-family can be classified into Ago and PIWI subfamilies. In mammals including mouse, rat and humans, there are eight Argonaute-like genes (Carmell *et al*., 2002; Meister & Tuschl, 2004; Peters

& Meister, 2007). The human and mouse Ago subfamilies consist of four (human AGO1-4) and five (mouse Ago1-5) members, respectively, whereas four members of the PIWI subfamily are encoded in human genome and only three are found in the mouse (Peters & Meister, 2007). In humans, AGO1, 3 and 4 are clustered on the chromosome 1 and AGO2 is present on the chromosome 8.

1.4 Functional domains of Argonautes

Argonautes (Agos) have a molecular weight of about 100kDa and are characterized by the presence of N, PAZ, MID and PIWI domains.

Figure 1.7: Domain structure of Argonaute2 (Hutvagner & Simard, 2008).

1.4.1 *PAZ domain*

PAZ domain has a binding pocket that anchors the two nucleotide 3' overhang of RNA produced by RNaseIII cleavage (Lingel *et al*., 2004; Ma *et al*., 2004; Song *et al*., 2003; Yan *et al*., 2003). The binding of PAZ to the guide RNAs is mediated by highly conserved aromatic residues, two tyrosines and a histidine that interact with the phosphates of the two terminal bases on the 3' end of small RNA (Lingel *et al*., 2004; Ma *et al*., 2004).

1.4.2 *Mid domain*

Mid domain present between the PAZ and PIWI domains has a highly basic pocket that binds to the 5' phosphate of small RNAs and facilitates the anchoring to

Argonaute protein. The mid domain of metazoan Argonautes that participate in miRNA pathway has a MC motif that shares homology with cap structure binding motif of translation initiation factor eIF4E and this MC motif can bind to cap of mRNAs and plays a role in efficient repression of translation (Kiriakidou *et al*., 2007).

1.4.3 *PIWI domain*

PIWI domain is the catalytic domain of Argonaute proteins with a catalytic triad. PIWI domain has RNase-H like fold with three residues forming a catalytic triad: DDR in Ago1, DGR in Ago4 and DDH in Ago2, Ago3 of both mouse and human (Peters & Meister, 2007). The catalytic triad of human Ago2, D (597), D (669) and H (807) endows the protein with an endonuclease activity (slicer activity) that cleaves the target mRNA perfectly bound to miRNA (Liu *et al*., 2004; Meister *et al*., 2004).

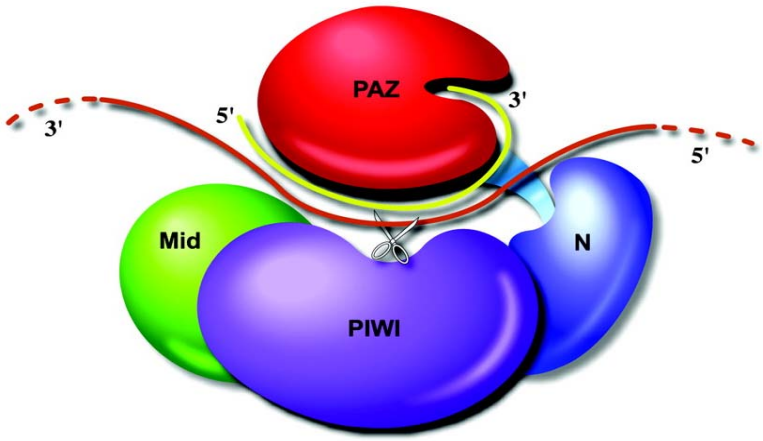

Figure 1.8: Diagram of Argonaute domain structure. The protein is shown interacting with siRNA (yellow) and its target mRNA (brown) (Song *et al*., 2004).

1.5 Mechanisms of miRNA-mediated gene silencing

miRNAs normally regulate the expression of mRNA targets either by repression of translation or destabilization by deadenylation or cleavage followed by

degradation (Du & Zamore, 2005; Meister & Tuschl, 2004; Zhao & Srivastava, 2007). miRNAs may bind to the target mRNAs with either imperfect or perfect/nearly perfect complementarity. Based on the extent of complementarity between miRNA and target mRNA the mechanisms of target regulation can be broadly divided into two categories:

1. Target mRNA cleavage
2. Inhibition of target translation and degradation

1.5.1 *Target mRNA cleavage*

When a miRNA comes in contact with target of perfect or nearly perfect complementarity, the miRNA-loaded RISC complex can catalyze endonucleolytic cleavage, or "slicing", of the mRNA target (Hutvagner & Zamore, 2002; Martinez & Tuschl, 2004). Of the four human Ago paralogs (Ago1 to 4), only Ago2 has the slicer activity, whereas Ago1, 3 and 4 have apparently lost this activity during evolution.

Figure 1.9: Schematic representation of endonucleolytic cleavage (slicing) of a perfectly complementary target (Krol *et al*., 2010).

1.5.2 *Inhibition of target translation and degradation*

On the other hand, miRNAs partially complementary to their targets bring about translational repression or slicer-independent destabilization of the mRNA (Hutvagner & Zamore, 2002; Martinez & Tuschl, 2004; Nilsen, 2007). Although we

are still far from complete understanding of this regulatory network, several underlying molecular mechanisms have emerged over the years.

Under different circumstances, miRNAs can inhibit target mRNA translation at either the initiation or the elongation step and both of these mechanisms obviously reduce the protein production output. Studies on the role of 5'-cap and 3'-poly(A)+ tail of target mRNA in the phenomenon of miRNA mediated gene silencing showed that miRNAs regulate the targets by affecting the initiation of translation (Humphreys *et al*., 2005; Pillai *et al*., 2005). Moreover the presence of miRNA and mRNA in actively translating polysomes support the translational inhibition mediated RNA silencing and the reduced protein levels were the result of premature translational termination (premature ribosome drop off) or inhibition of translational elongation followed by protein degradation (Nottrott *et al*., 2006; Petersen *et al*., 2006).

miRNA mediated destabilization of mRNAs by deadenylation followed by 5' decapping of target mRNAs has been studied in several organisms. The association of deadenylase complex CCR4-NOT and decapping complex DCP1:DCP2 with miRNP in several cases further supports the phenomenon of miRNA mediated mRNA deadenylation and eventual degradation. However there have been reports questioning the significance of mRNA polyadenylation affecting the extent of miRISC mediated target deadenylation (Behm-Ansmant *et al*., 2006; Giraldez *et al*., 2006; Wu *et al*., 2006).

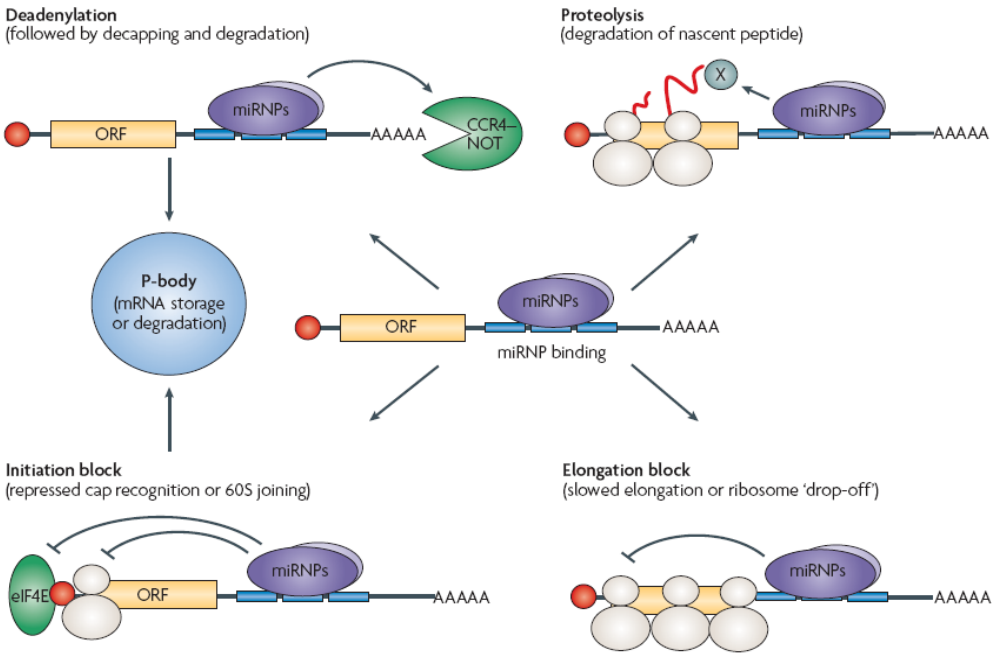

Figure 1.10: Different mechanisms of miRNA gene silencing for mRNAs with imperfect complementarity (Filipowicz *et al*., 2008).

mRNAs that are silenced by various mechanisms can be transported to special cytoplasmic foci called Processing or P bodies. The presence of miRISC components like miRNA, Argonaute proteins, target RNAs, decapping, deadenylation complexes and exonucleases suggest that P bodies act as sites of miRISC mediated mRNA degradation. Also, GW182 protein localized to P bodies was found to interact with Ago proteins suggesting the transfer of miRISC associated mRNAs to P bodies for degradation (Eulalio *et al*., 2007; Liu *et al*., 2005; Meister *et al*., 2005; Pillai *et al*., 2005; Valencia-Sanchez *et al*., 2006).

Interestingly, miRNA-mediated gene silencing often reduces the steady-state levels of target mRNAs (Guo *et al*., 2010). In this case, translational repression is quickly followed by target destabilization (Bazzini *et al*., 2012; Djuranovic *et al*., 2012). However, in a few cases considerable repression of target mRNA translation was not accompanied by changes in the mRNA levels. Thus, under certain conditions,

miRNAs may act purely at the level of translation (Boutz *et al*., 2007; Chen *et al*., 2006; O'Donnell *et al*., 2005; Saito *et al*., 2006; Zhao *et al*., 2005).

Of all base-pairing interactions that a miRNA forms with its targets, perfect binding of nucleotides 2 to 8 at the miRNA 5' end (so-called seed sequence) to complementary mRNA sequences plays the most critical role in the activity of miRNA and further target repression. Due to the apparent simplicity of this major determinant of the miRNA-mRNA interaction, a single miRNA may regulate multiple mRNA targets and on the other hand, a single mRNA can be targeted by more than one miRNA (Bartel, 2009; Lewis *et al*., 2005). In addition to the seed sequence, mismatches (bulges) and the complementarity between the 3' end of miRNA and the corresponding sites within the mRNA target also plays a role in determining the recognition and efficient repression of target mRNAs (Brennecke *et al*., 2005; Brodersen & Voinnet, 2009; Doench & Sharp, 2004; Grimson *et al*., 2007).

1.6 Post transcriptional modifications of miRNA

Recent deep sequencing studies suggest that individual miRNAs often exist as populations of variants (iso-miRs) that differ in length and sometimes nucleotide composition (Berezikov *et al*., 2011; Fernandez-Valverde *et al*., 2010; Krol *et al*., 2010; Landgraf *et al*., 2007; Morin *et al*., 2008; Wyman *et al*., 2011). This variability suggests that miRNAs might be prone to various modifications either during or after their biogenesis. miRNA molecules in the cell are continuously turned over by various ribonucleases.

Several exoribonucleases have been implicated in miRNA degradation (Ramachandran & Chen, 2008). Active turnover of mature miRNAs in plants is regulated by the 3'-to-5' exonuclease SDN1. On the other hand, exonuclease XRN-2

degrades miRNAs in *Caenorhabditis elegans* in the 5' to 3' direction (Chatterjee & Großhans, 2009). In some organisms, miRNAs and other short RNAs appear to be degraded 3' to 5' by the cytoplasmic RNA exosome (Bail *et al*., 2010; Schmid & Jensen, 2008). Interestingly, the 3' ends of Argonaute-associated miRNAs have recently been shown to be trimmed by the 3'-to-5' exonuclease Nibbler in *Drosophila* (Han *et al*., 2011; Liu *et al*., 2011). This reaction may potentially contribute to the developmentally regulated iso-miR dynamics detected for some miRNAs in *Drosophila* (Fernandez-Valverde *et al*., 2010).

On the other hand, a number of chemical modifications have evolved to stabilize RNAs from enzymatic degradation. For example, mRNAs have a 7-methylguanosine cap at their 5' ends and a poly A tail at the 3' ends (Garneau *et al*., 2007). Similarly, various post transcriptional modifications help miRNAs to evade the exoribonucleases (Kai & Pasquinelli, 2010). Plant miRNAs are protected at 3' end by a methyl group on the ribose moiety of the last nucleotide (Yu *et al*., 2005). A significant population of miRNAs undergo addition of one or several nucleotides on the 3' end by multiple nucleotidyl transfereases (Wyman *et al*., 2011). The addition of one or several adenosines to the 3' end of mature miR-122 by poly(A) polymerase, Gld2 was shown to stabilize the miRNA (Katoh *et al*., 2009). Also ZCCHC11 or (TUT4) an uridylyl transferase adds 1 to 3 uridines on their 3' ends of miR-26a (Jones *et al*., 2009). In some instances TUT4 also uridylates the precursor miRNA and blocks Dicer processing thus reducing the levels of the corresponding mature miRNA (Hagan *et al*., 2009; Heo *et al*., 2009; Rau *et al*., 2011). However the exact biological significance of these modifications needs to be addressed.

Recently it has been shown in *Drosophila* and mouse models that miRNAs recruited to Argonaute proteins undergo extensive 3'-terminal trimming and tailing in

the presence of a perfectly complementary target mRNA to the 3' end of miRNA and that this target-mediated trimming and tailing is accompanied by a reduction in the miRNA levels. However, the enzyme(s) involved in template-dependent miRNA trimming and tailing have not been identified so far (Ameres *et al*., 2010; Xie *et al*., 2012).

1.7 miRNAs in the nervous system

A large fraction of metazoan miRNAs are expressed in a tissue-specific manner and at different levels during the different stages of organismal development (Bartel, 2004; Borchert *et al*., 2006). This spatio-temporal expression determines the specific function of the tissues and switching of the stages during organismal development. A number of miRNAs are expressed in the nervous system (NS) where they contribute to diverse developmental and physiological programs (Ashraf *et al*., 2006; Chang *et al*., 2004; Kim *et al*., 2004; Kosik, 2006; Krichevsky *et al*., 2003; Li *et al*., 2006; Miska *et al*., 2004; Schratt *et al*., 2006; Sempere *et al*., 2004).

Nervous system in triploblastic animals (animals developed from three germinal layers) is derived from the ectoderm. During mammalian embryogenesis, the entire central nervous system is formed from neural stem cells including neuroepithelial cells, radial glia and neural stem cells. These cells eventually differentiate to form neurons and glia. Neurogenesis in the adult brain is limited to only few sites containing adult neural stem cells: dentate gyrus of hippocampus, olfactory bulb and possibly the subventricular zone (Liu & Zhao, 2009).

miRNAs are known to play an important role in both embryonic and adult neurogenesis. One interesting line of evidence comes from studies using genetic inactivation of the miRNA biogenesis pathway components. For example, maternal

zygotic Dicer mutants in Zebrafish showed morphogenesis defects during neurulation accompanied by improper brain development (Giraldez *et al*., 2005). Similarly, a reduction in all types of neurons and glial cells was noticed in Ago1 mutants of *Drosophila* (Kataoka *et al*., 2001). Non-conditional Dicer mutant mice die before the neural tube is formed (Bernstein *et al*., 2003). However, conditional inactivation of Dicer in select NS areas is known to lead to severe neurodegenerative phenotypes (Hébert *et al*., 2010; Huang *et al*., 2010; Kim *et al*., 2007; Makeyev *et al*., 2007; Schaefer *et al*., 2007).

One limitation of the above studies is that inactivation of Dicer or other components of the miRNA biogenesis machinery affects the total cellular miRNA pool and thus making it difficult to ascertain the function of a specific miRNA. To circumvent this, alternative approaches were developed wherein specific miRNAs were depleted to examine their role in cell renewal, neurogenesis, and maintenance of tissue identity or neural functions.

One striking example of regulatory network deciphered using this approach is offered by miRNAs lsy-6 and miR-273 forming a double negative feedback loop with the transcription factors Die-1 and Cog-1 in determining the asymmetry of the chemosensory neuron pairs in nematodes (Chang *et al*., 2004; Johnston & Hobert, 2003; Johnston *et al*., 2005; Kosik, 2006).

In mouse, let-7a in association with TRIM32 was found to repress proliferation and induce neuronal stem cells differentiation by inhibiting the c-Myc expression (Kawahara *et al*., 2012; Melton *et al*., 2010; Schwamborn *et al*., 2009). miR-132 whose transcription is regulated by CREB (cAMP response element-binding) plays a role in determining the dendrite length, arborization leading to the dendrite maturation in new born neurons of adult hippocampus (Magill *et al*., 2010).

1.8 miR-124 in nervous system development

Expression of some miRNAs is spatially separated restricting their abundance to specific tissues. In the nervous system, miR-124 is one of the most conserved and abundantly expressed tissue specific miRNAs (Lagos-Quintana *et al*., 2002). This miRNA has been shown to be expressed at high levels in mouse brain and as well as P19 cell line that undergoes differentiation into neuron-like cells (Lagos-Quintana *et al*., 2003; Sempere *et al*., 2004). miR-124 is expressed in neurons, but not astrocytes, and the levels of miR-124 increase over time in the developing NS (Krichevsky *et al*., 2003; Miska *et al*., 2004; Smirnova *et al*., 2005). In human and mouse, miR-124 is encoded by three distinct non-allelic genes (*pri-miR-124-1*, *124-2* and *124-3*) that have distinct exon-intron structure. Mouse miR-124-1, 2 and 3 are located on chromosomes 14, 3 and 2 respectively. miR-124-1 and 3 are exonic in origin whereas miR-124-2 is encoded in the intron of a non-coding gene. The abundance of miR-124 increases from embryonic to adult mouse with the progressive neuronal differentiation and nervous system development. Majority of mature miR-124 in P6 mouse comes from pri-miR-124-1 whose knock out (*Rncr3*$^{-/-}$) showed a 60 to 80% decrease in miR-124 abundance. The contribution of pri-miR-124-2 and pri-miR-124-3 to the overall miR-124 expression levels in the adult brain appears to be more modest (Blackshaw *et al*., 2004; Sanuki *et al*., 2011). However, the relative expression levels of the three miR-124 genes during embryonic development have not been studied.

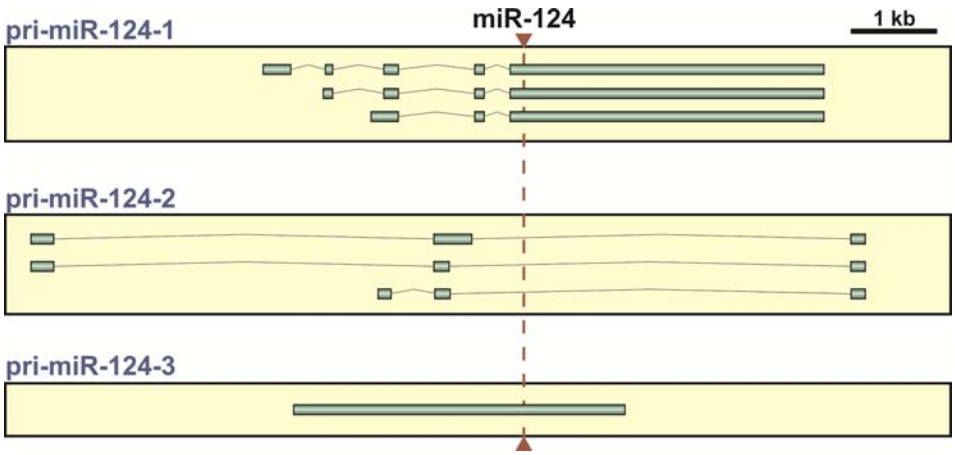

Figure 1.11: Diagram showing the structure of the three miR-124 gene paralogs in mouse.

miR-124 appears to play several important functions in developing nervous system. In combination with the nervous system specific miRNA miR-9, miR-124 stimulates neuronal and represses glial differentiation of ES cells *in vitro* (Krichevsky *et al*., 2006; Ponomarev et al., 2011). miR-124 reduces the expression of transcripts responsible for cell proliferation and/or stem cell function when introduced into non-neuronal cells (Cao *et al*., 2007; Lim *et al*., 2005). In addition, miR-124 has been shown to regulate hundreds of non-neuronal transcripts (Hendrickson *et al*., 2009) and its introduction into HeLa and other non-neuronal cells promotes a neuronal-like mRNA profile (Conaco *et al*., 2006; Lim *et al*., 2005). In neuronal cells miR-124 silences PTBP1 that encodes a global repressor of alternative pre-mRNA splicing hence plays a major role in differentiation of neurons from their progenitors (Makeyev *et al*., 2007; Smith *et al*., 2011; Spellman & Smith, 2006). SCP1, a component of the REST (RE1-silencing transcription repressor) complex that represses the transcription of neuron specific genes, is also silenced by miR-124. Interestingly, transcription of miR-124 genes is in turn repressed by REST, which provides double negative feedback regulation (Conaco *et al*., 2006; Makeyev & Maniatis, 2008; Visvanathan *et al*., 2007). miR-124 expressed in the Rncr3 non-coding RNA is found to repress the

protein levels of Lhx2 by inhibiting the translation in brain and retina leading to defects in dentate gyrus maturation and survival in mouse (Sanuki *et al*., 2011). Also Argonaute HITS CLIP studies revealed hundreds ofmRNA targets regulated by miR-124 in mouse brain (Chi *et al*., 2009). Taken together it is evident that miR-124 is a critical post transcriptional regulator of nervous system development and function.

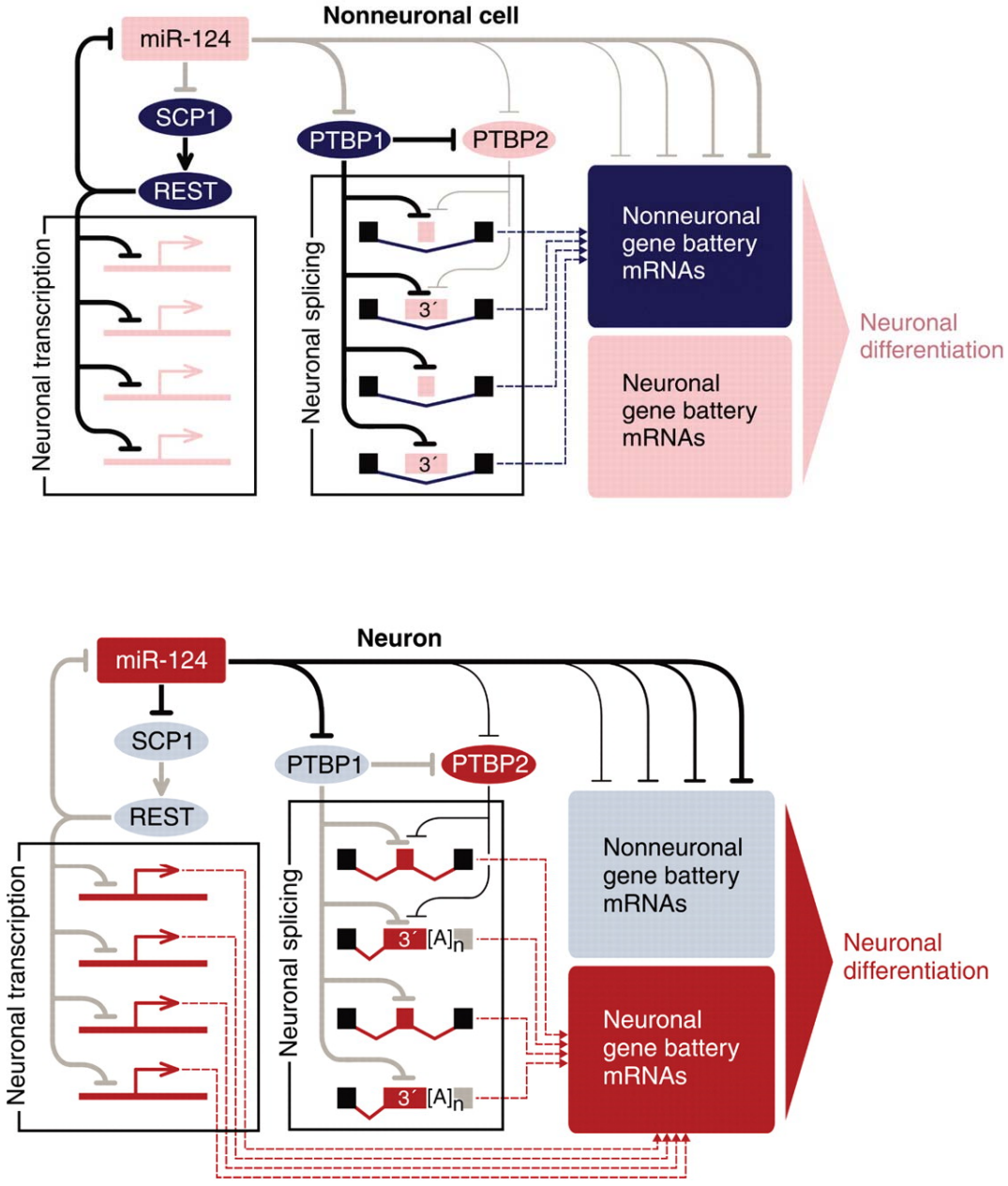

Figure 1.12: Cross talk between SCP1, PTBP1 and miR-124 in non-neuronal [top] and neuronal cells [bottom] (Makeyev & Maniatis, 2008).

1.9 Objectives

As mentioned in the section 1.6, miRNAs are known to exist as size variants, or iso-miRs, that might potentially exhibit distinct biological activities. However, not much is known about the molecular mechanisms involved in the iso-miR generation. To this end, my thesis work focused on the following specific objectives:

- To investigate the changes in miRNA size variant profile as a function of mammalian brain development
- To understand changes in the expression of the four mammalian Argonaute paralogs in developing brain
- Establishing the possible role of Argonaute proteins in post-transcriptional modification of mammalian miRNAs with a specific emphasis on the evolutionarily conserved neuron-specific miRNA miR-124
- To delineate the differences in biological activities of miR-124 recruited to either Ago1 or Ago2 in the context of neuronal differentiation.

2. MATERIALS AND METHODS

2.1 Cell lines

HEK293T and N2a cells were obtained from ATCC and cultured in Dulbecco's modified Eagle's medium (DMEM) (Hyclone) containing 10% Fetal Bovine Serum (FBS; Hyclone, characterized grade), 100 IU/ml penicillin and 100 μg/ml streptomycin (Invitrogen) and 1 mM sodium pyruvate (Invitrogen) at 37°C and 5% CO_2. Transfections were done using Lipofectamine 2000 (Invitrogen) according to manufacturer's instructions. Transgenic N2a cell populations were generated using the HILO-RMCE procedure as described in Khandelia *et al.*, 2011.

2.2 Animals

Tissue samples were prepared from adult and embryos of time pregnant C57BL/6J mice using protocols approved by the Institutional Animal Care and Use Committee. All the animals were ordered from National University of Singapore Centre for Animal Resources.

2.3 Molecular cloning techniques

2.3.1 *Restriction endonuclease reaction and gel extraction*

The host plasmid and the insert or PCR products were digested to generate compatible cohesive or blunt ends with desired restriction endonucleases (NEB) according to manufacturer's instruction. The products were electrophoresed on 1-2% agarose gel. The DNA of desired molecular weight respect to the 1 Kb DNA Ladder (Invitrogen) was extracted from the gel by using Nucleospin Extract II kit (Macherey-Nagel) in accordance with manufacturer's instructions.

2.3.2 *Klenow reaction to generate blunt ends*

In a Klenow reaction cohesive ends of Plasmid or PCR product DNA were made blunt by incubating 1µg of DNA with 0.2 mM of dNTPs, 1 unit of DNA polymerase I Klenow fragment enzyme (NEB, 5 units/µl) at room temperature for 30 minutes. The reaction was stopped by the addition of 1 µl of 0.5 M EDTA, pH 8.0 for a 25 µl reaction, followed by extraction with phenol: chloroform extraction and ethanol precipitation as described in section 2.9.

2.3.3 *Ligation of the DNA insert to plasmid vector DNA*

Gel purified vector and the insert were ligated at 1:3 to 1:5 ratio in 1X ligation buffer and T4 DNA ligase (NEB) overnight at 4°C according to the manufacturer's instructions.

2.3.4 *Bacterial transformation and plasmid DNA propagation*

For propagation of plasmid DNA, chemically competent *E. coli* cells (Top10, Invitrogen) were used. 5 µl of plasmid DNA (10-100 ng) was incubated on ice with 25 µl of thawed competent cells for 30 minutes. The cells were then subjected to heat shock for 30 seconds at 42°C on a heat block and immediately snap chilled on ice for 2 minutes. Cells were then cultured in LB broth for 1 hour and plated on LB agar plates of desired antibiotic selection.

2.3.5 *Plasmid DNA preparation*

Bacterial cells transformed with plasmid were cultured in 3 ml (miniprep) or 250 ml (midiprep) LB medium with desired antibiotic at 200rpm, overnight at 37°C.

Plasmid isolation was performed using mini or midiprep kit (Qiagen) according to manufacturer's instructions.

2.3.6 *Plasmid DNA sequencing*

Plasmid DNA sequencing was performed by AIT biotech, Singapore using BigDye Terminator chemistry. 1-1.5 µg of the plasmid DNA along with 3 µl of 10 µM sequencing primer was provided for each reaction.

2.3.7 *Site-directed mutagenesis*

To introduce site specific mutations in target sequences a slightly modified Quikchange site-directed mutagenesis protocol (Stratagene) in which the *Pfu* Turbo DNA polymerase was substituted with the KAPA HiFi DNA polymerase (KAPA Biosystems) was used. Target plasmid DNA was amplified in a PCR with KAPA HiFi PCR Kit according to manufacturer's instructions using site specific mutagenesis primers. PCR product was purified by Nucleospin Extract II kit (Macherey-Nagel) in accordance with manufacturer's instructions. The purified PCR product was treated with 2 µl of Dpn1 (New England BioLabs), 1X NEB-4 buffer and 1X BSA in a 20 µl reaction for 2 hours at 37^{o}C. Dpn1 treated DNA was then transformed in to chemically competent *E. coli* cells (Top10, Invitrogen) and the colonies were screened for mutants by plasmid DNA sequencing as described in section 2.3.4 and 2.3.6.

2.4 Immunoblotting

2.4.1 *Protein extraction*

Cells were washed twice with ice-cold 1X PBS (PAA Laboratories) and lysed in extraction buffer [20 mM Tris-HCl, pH 7.5, 150 mM NaCl, 5 mM EDTA, 10%

glycerol, 1% Nonidet P-40, 1 mM PMSF and 1X Complete EDTA free protease inhibitor cocktail (as recommended by Roche)] for 10 minutes at 4°C with continuous mixing. The lysate was collected by scraping the cells.

Mouse brain tissues were isolated from adult or E12.5 mice in cold 1X PBS (PAA Laboratories) by dissecting adult or time pregnant C57BL/6J mice after anaesthetization. Tissues were washed thrice in ice-cold 1X PBS, frozen down in liquid nitrogen and homogenized with ice cold 1X extraction buffer using a ceramic mortar and pestle followed by incubation for 15 minutes at 4°C with continuous mixing. The cell or tissue lysates were cleared by centrifugation for at 20,000g for 10-20 minutes at 4°C. Supernatant containing the protein was collected and stored at -80°C for further analysis.

2.4.2 *Estimation of protein concentration*

Protein concentration was estimated by plotting their absorbance values against the known BSA standards using BCA protein assay kit (Thermo Scientific) according to manufacturer's instructions. The absorbance was measured at 595 nm by a TECAN plate reader.

2.4.3 *SDS PAGE separation and electroblotting of proteins*

Protein samples for SDS PAGE were prepared by boiling with 1X sample buffer for 5 minutes at 98^{o}C then resolved on a 4-20% gradient SDS-PAG (Thermo Scientific) in 1X gel running buffer (100 mM Tris base, 100 mM HEPES, and 3 mM SDS at pH ~8) for 1 hour at 100 mV. Proteins were then electroblotted on a nitrocellulose membrane (Whatman) for 1-2 hours at 0.65 mA/cm^2 in 1X Transfer buffer (25 mM Tris, 192 mM glycine, and 0.1% SDS). Following the transfer,

nitrocellulose membrane was washed once with water and stained with Ponceau S (0.5% Ponceau S in 5% acetaldehyde) for 3 minutes and destained in water to confirm the transfer of proteins on to the membrane. Membrane was then washed with 1X TBST (10 mM Tris HCl, 100 mM NaCl and 0.1% Tween 20) for 2-3 times to remove Ponceau S stain.

2.4.4 *Immunological detection of proteins*

Proteins electroblotted on the membrane were blocked with 5% milk in 1X TBST for 1 hour followed by three washes in 1X TBST, each for 5 minutes. The membrane was then incubated with the following primary antibodies: rabbit polyclonal anti-Ago1 (Millipore; 1:1000 dilution); mouse monoclonal anti-Ago1 (kind gift of Mikiko Siomi); 1:500 dilution), rabbit monoclonal anti-Ago2 (Cell Signaling Technology; 1:1000), mouse monoclonal anti-β-tubulin (Invitrogen; 1:3000), mouse monoclonal anti-GAPDH (Ambion; 1:10000), mouse monoclonal anti-c-Myc (Sigma; 1:3000) in 5% milk or 1% BSA in TBST for 2 hours at room temperature or overnight at 4^{o}C. After the primary antibody probing, the membrane was washed thrice in TBST each for 5 minutes to remove excess antibody followed by incubation with secondary anti-rabbit or anti-mouse horseradish peroxidase (HRP) conjugates from (GE Healthcare; 1:5000) in 5% milk for half an hour to 1 hour at room temperature. The membrane was again washed thrice in TBST for 5 minutes each and protein bands were visualized by autoradiography using enhanced chemiluminescence (ECL) reagents from Thermoscientific according to manufacturer's instructions.

2.5 *In silico* protein analyses

Argonaute amino acid sequences were aligned using MUSCLE (http://www.ebi.ac.uk/Tools/msa/muscle/) and the similarity plots were generated in JProfileGrid (Tian *et al.,* 2008); http://www.profilegrid.org/) using a 5 aa sliding window. The structure of the AGO1-small RNA complex (1SI3; (Ma *et al.,* 2004)) was downloaded from the Protein Data Bank (http://www.pdb.org) and visualized by PyMOL (http://www.pymol.org/).

2.6 Total RNA extraction from mouse brain and cell lines

Brains from embryonic (E12.5) or adult (P60) mice were isolated in ice cold PBS (1X) (PAA Laboratories) by dissecting adult or time pregnant C57BL/6J mice after anaesthetization and homogenized with TRIzol (Invitrogen) in a Dounce homogenizer for RNA extraction. 1 ml of cold TRIzol was used for 50-100 mg of brain tissue. Cultured cells from a single well of a 6-well culture plate were lysed by pipetting in 1 ml of cold TRIzol. The homogenized samples were then incubated for 5 minutes at room temperature. To these samples 0.2 ml chloroform was added, mixed vigorously and incubated for 3 minutes at room temperature, followed by centrifugation at 12,000g for 15 minutes at 4°C for phase separation. The aqueous phase containing RNA was collected, 0.5 ml of isopropanol was added, mixed gently and incubated for 10 minutes at room temperature followed by centrifugation at 12,000g for 10 minutes at 4°C to pellet RNA. Supernatant was discarded and RNA pellet was washed with 1 ml of 75% ethanol by brief vortex followed by centrifugation at 7,500g for 5 minutes at 4^{o}C. Supernatant was carefully discarded, the RNA pellet was air dried briefly and dissolved in DEPC-treated water.

2.7 miRNA Northern blot analysis

2.7.1 *RNA electrophoresis and electroblotting*

Total RNA was extracted with TRIzol (Invitrogen) as described in section 2.6. RNA samples for electrophoresis were prepared by adding an equal volume of 2X RNA loading dye (98% formamide, 10 mM EDTA, 0.025% bromophenol blue, 0.025% xylene cyanol) to an appropriate amount of RNA (10-20 μg). Samples were denatured for 5 minutes at 95°C , snap chilled on ice and then resolved on a 15% Polyacrylamide Gel (PAG) containing 7.5 M urea, 1X TBE, 15% of 19:1 acrylamide: bisacrylamide, 0.87 μl/ml of TEMED and 0.03% ammonium persulphate (APS) at ~10-20 V/cm. The resolved RNAs were then electroblotted to Hybond N+ nylon membrane (GE Healthcare) in 0.5X TBE for 1 hour at 2.5 mA/cm^2 using a semi-dry transfer apparatus (BioRad Transblot SD) and subsequently UV cross-linked at 0.15 J/cm^2 using HL-2000 Hybri Linker (UVP Laboratories).

2.7.2 *Autoradiography, Image acquisition and data analysis*

RNA electroblotted and cross-linked to the nylon membrane was prehybridized in ExpressHyb buffer (Clontech) for 1 hour at 37°C followed by hybridization with the desired complementary end labeled DNA oligo probe for 2 hours at 37°C. The membrane was then washed for 10 minutes with wash buffers I and II successively (wash buffer I: 2X SSC and 0.05% SDS; wash buffer II: 0.1X SSC and 0.1% SDS) and exposed to a Storage Phosphor screen (GE Healthcare). Radioactive signals were scanned by a Typhoon Trio Variable Mode Imager (GE Healthcare), and the data was analyzed by ImageQuant TL software (GE Healthcare).

2.7.3 *Preparation of 5' end labeled DNA oligo probes*

DNA oligos labeled on the 5' end with ([γ]-^{32}P) ATP were used as probes for Northern blotting. For end labeling, 1.5 µM DNA oligo was incubated with 1X T4 PNK buffer, 3 µl of ([γ]-^{32}P) ATP (6000 Ci/mmol, Perkin Elmer) and 1 µl of T4 PNK enzyme (10,000 units/ml, NEB) in a 20 µl reaction volume for 30 minutes at 37°C. Labeled oligonucleotides were then purified using Sephadex G-25 spin columns (Geneaid) as per manufacturer's instructions.

2.8 RT-qPCR analysis (Reverse Transcription-quantitative Polymerase Chain Reaction)

DNase I treatment: 20 µg of total RNA was treated with 5 units of RNase-free DNase I (Promega), 1X DNase I buffer and 40 units of rRNasin (Promega) in a 100 µl reaction for 1 hour at 37°C, followed by phenol chloroform extraction and ethanol precipitation of the RNA as described in section 2.9. RNA pellet was then dissolved in an appropriate amount of DEPC-treated water and quantified using a NanoDrop 1000 spectrophotometer (Thermo Fischer Scientific).

Reverse Transcription: For first strand cDNA synthesis by reverse transcription, 5 µg of DNase I treated RNA sample was incubated with 10 pmoles of random decamer (N10) primer in 11 µl volume for 10 minutes at 70°C followed by incubation on ice. To this 9 µl of reaction mixture containing 1X RT buffer, 1 mM dNTPs, 40 units rRNasin (Promega), 200 units Superscript III RT enzyme (Invitrogen) and 10 mM DTT was added and incubated for 60 minutes at 50°C. The reverse transcriptase was then heat inactivated for 10 minutes at 70°C and the reaction mix was diluted to 200 µl with sterile DEPC-treated water and stored at -80°C or used immediately.

Quantitative/Real-Time PCR: Quantitative analysis of gene expression by real-time PCR was carried out using StepOnePlus real-time PCR systems (Applied Biosystems) and Fast SYBR Green Master Mix (Applied Biosystems). Each real-time PCR reaction (reaction volume: 20 µl) consists of 5 µl of first strand cDNA, 10 µl of 2X Fast SYBR Green Master Mix (Applied Biosystems) and forward/reverse primers at a final concentration of 0.15 µM. All reactions were performed in triplicates using the following thermal cycling conditions: Initial denaturation for 20 seconds at 95°C, followed by 45 cycles of a two-step reaction, denaturation for 5 seconds at 95°C, annealing/extension for 45 seconds at 60°C. Transcript levels were normalized to HPRT or GAPDH housekeeping transcript levels. Relative fold change in expression was determined using the comparative ΔΔCT method.

2.9 Nucleic acid precipitation

Nucleic acid samples were extracted with an equal volume of phenol-chloroform mixture (1:1). Water saturated acidic phenol (pH 4.5) for RNA and Tris HCl (pH 8.0) saturated phenol for DNA was used. The samples were mixed and allowed to stand at room temperature for 2 minutes followed by centrifugation at 14,000 rpm for 10 minutes at 4^{o}C. The aqueous phase was collected, $1/10^{th}$ volume of 3M sodium acetate and 3 volumes of 100% ethanol were added, mixed well and incubated for 30 minutes at -80^{o}C to precipitate the nucleic acids. For small amounts of nucleic acid precipitation, 10 µg/ml of glycogen to the total volume was also added. Following the incubation, samples were centrifuged at 14,000 rpm, for 10 minutes at 4^{o}C to pellet down DNA or RNA. The nucleic acid pellet was washed with 75% ethanol followed by centrifugation at 5,000 rpm for 5 minutes, air dried and dissolved in DEPC-treated water (for RNA) or 1X TE buffer (for DNA).

2.10 Gel extraction of RNA

RNA was resolved on a 5-10% PAG containing 7.5 M urea and the RNA fraction of desired size corresponding to the ssRNA marker (Takara Biosciences) was excised from the PAG. The excised gel pieces were crushed with a 1 ml pipette tip and incubated in gel extraction buffer [2% SDS, 0.3 M sodium acetate at pH 5.5 and 0.02 U/μl of rRNasin (Promega)] overnight. RNA was precipitated from the above mixture as per the nucleic acid precipitation protocol described in section 2.9.

2.11 Preparation of miRNA duplex

miRNA duplexes were prepared by annealing complementary synthetic RNA oligos (Dharmacon). Reaction mix containing 20 μM each of the two oligos to be annealed in 1X siRNA buffer (Dharmacon) was incubated for 1 minute at 90^{o}C and then slowly cooled down to the room temperature to promote annealing. 22-mer duplexes were prepared by annealing the 5'GGUGUUCACAGCGGACCUUGAU3' antisense strand and either the 5'pUAAGGCACGCGGUGAAUGCCAA3' or the 5'pUAAGGCACGCGGUGAAUGCCAmA3' miRNA strands (5'p indicates a 5' phosphate and mA3' is a 2'-OMe-modified 3' adenosine). 21-mer duplexes were prepared by annealing the 5'GUGUUCACAGCGGACCUUGAU3' antisense and the 5'pUAAGGCACGCGGUGAAUGCCA3' miRNA strands.

2.12 Co-immunoprecipitation analysis

Co-immunoprecipitation of mature miR-124 and Argonaute proteins was done in principle as described in Karginov *et al.,* 2007. In brief, 10 cm cell culture dishes containing ~60% confluent HEK293T cell cultures were typically co-transfected with a 3xMyc-tagged Argonaute expression plasmid and a miR-124 expression plasmid

(Table 2.1 and section 2.21) and incubated for 48 hours. Alternatively, cells were first transfected with a 3xMyc-tagged Argonaute expression plasmid for 24 hours followed by transfection with a synthetic miRNA duplex. Cells were then washed with ice-cold 1X PBS (PAA Laboratories) followed by 15 minutes incubation in 1 ml hypotonic lysis buffer containing 10 mM Tris HCl pH 7.5, 10 mM KCl, 2 mM $MgCl_2$, 5 mM DTT and 1X Complete EDTA-free protease inhibitor cocktail (Roche). The cells were scraped off the plate and the suspensions were supplemented with the 5X ATP depletion mix [450 mM KCl, 100 mM glucose, 1 mg/ml yeast tRNA (Invitrogen), 0.4 units/µl rRNasin (Promega) and 0.5 units/ml hexokinase (Sigma)] added to a final concentration of 1X. The cells were then homogenized in a Dounce homogenizer by 15 strokes of pestle B. The lysates were cleared by centrifugation at 16,000g for 30 minutes at 4^{o}C. To immunoprecipitate the 3xMyc-tagged Argonaute complexes, anti-c-Myc agarose beads (Sigma) were pre-blocked for 2 hours at 4^{o}C in W1 buffer (0.5% Nonidet P-40, 150 mM NaCl, 2 mM $MgCl_2$, 2 mM $CaCl_2$, 20 mM Tris-HCl, pH 7.5, 5 mM DTT, and 1X Complete EDTA-free protease inhibitor cocktail) additionally containing 1 mg/ml yeast tRNA and 1 mg/ml BSA. The beads (~35 µl resin) were then incubated with the cleared lysates for 4 hours at 4^{o}C, washed once with 1 ml of ice-cold W1 buffer and twice with 1 ml of ice-cold W2 buffer (0.5% Nonidet P-40, 650 mM NaCl, 2 mM $MgCl_2$, 2 mM $CaCl_2$, 20 mM Tris, pH 7.5, 5 mM DTT, and 1X Complete EDTA-free protease inhibitor cocktail), for 5 minutes each. The co-immunoprecipitated RNAs were eluted from the beads using TRIzol and analyzed by Northern blotting and phosphorimaging. “Input” lanes contained RNAs, TRIzol-extracted from 5% aliquots of the cleared lysates.

2.13 Pulse-chase experiments

HEK293T cells were co-transfected with the pTet-Off plasmid and an appropriate miR-124 expression plasmid (pEM405) or control plasmid (pEM142) [Table 2.1] and incubated for 24 hours. Doxycycline (Dox) was then added to the cultures to a final concentration of 2 μg/ml in order to repress the interaction of tTA with TET promoter and the incubation was continued for another 48 hours. Total RNA from samples isolated at different points of this time course was analyzed by Northern blotting and phosphorimaging as described in section 2.7.

2.14 *In vitro* dicer assay

20 μg of total RNA isolated from RIP-miR-124-1, 2 or 3 (section 2.21) transfected HEK293T cells, 24 hours post-transfection was incubated for 1 hour at 37°C in 20 μl reactions with 0.125-0.5 units of the purified human Dicer enzyme (Roche) in 1X reaction buffer containing 30 mM Tris HCl pH 6.8, 50 mM NaCl, 3 mM $MgCl_2$, 0.1% Triton X-100, 15% glycerol, 1 mM DTT and 2 units/μl rRNasin (Promega). Reaction products were extracted with a 1:1 mixture of acidic phenol/chloroform, precipitated with ethanol and analyzed by Northern blotting and phosphorimaging as described in section 2.7.

2.15 Ligation-Mediated RT-PCR (LM-RT-PCR)

The LM-RT-PCR protocol was modified from Morin *et al.,* 2008. Briefly, 500 μg of total RNA from E12.5 or adult mouse brain was resolved by 10% PAGE containing 7.5 M urea and the 14-30 nt RNA fraction was extracted using a miRNA gel extraction kit (Abnova) according to manufacturer's instructions. One half of the gel-purified RNA was ligated with 200 pmoles of the 3' RNA adapter (5'P-

UCGUAUGCCGUCUUCUGCUUGidT; Dharmacon) for 12 hours at 16°C in a 10 µl reaction containing 5 units of T4 RNA ligase, 1X ligation buffer (Ambion), and 20units of RNase Out (Invitrogen, 40 U/µl). The ligation mixtures were heat inactivated for 8 minutes at 68°C, resolved by 10% PAGE containing 7.5 M urea and the 36-46 nt RNA fraction was extracted from the gel (Abnova) and subjected to reverse transcription with the 3'_RT primer and SuperScript III RT (Invitrogen). The gel purified RNA was subjected to reverse transcription by incubating with 5 µM 3'_RT primer in 11 µl volume for 2 minutes at 70°C followed by incubation on ice. To this a 9 µl of reaction mixture (1X RT buffer, 0.75 mM dNTPs, 40 units rRNasin [Promega], 200 units Superscript III RT enzyme, 10 mM DTT) was added and incubated for 60 minutes at 50°C, followed by heat inactivation of reverse transcriptase for 5 minutes at 85°C. miR-124 specific sequences were then PCR amplified using miR-124_F1 and 3'_PCR primers (Table 2.2) and KAPATaq HotStart DNA Polymerase (KAPA Biosystems) as per manufacturer's instructions. PCR reaction was performed using the following thermal cycling parameters: 95°C for 2 minutes, followed by 28 cycles of a three-step reaction, denaturation at 95°C for 30 seconds, annealing at 59°C for 30 seconds and extension at 72°C for 10 seconds and terminating the reaction with a final extension at 72°C for 10 minutes. The PCR products were then purified using a Nucleospin Extract II Kit (Macherey-Nagel) as recommended, ligated with pGEM-T vector (Promega) and transformed into chemically competent Top10 *E. coli* cells (Invitrogen). A total of 30 clones were screened by sequencing with T7 sequencing primer.

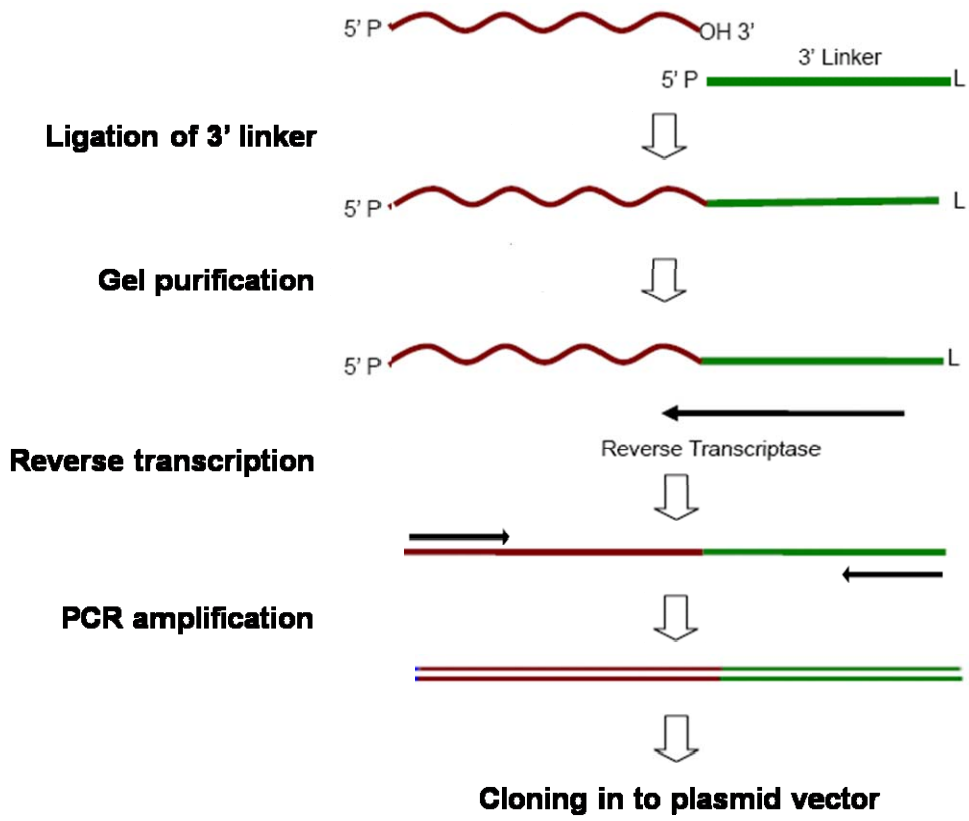

Figure 2.1: Flow chart of the miRNA cloning methodology

2.16 Primer extension analysis

10 µg of total RNA from the E12.5 or the adult mouse brain was annealed to 200 fmoles of 5' [^{32}P]-labeled miR-124_p_ext primer (Table 2.2) complementary to the 3' end of the mature miR-124 in 10 µl reaction mixture containing 10 mM Tris pH 7.4, 0.5 mM EDTA, and 50 mM KCl. The above reactions were incubated for 5 minutes at 70°C, 20 minutes at 37°C and finally for 10 minutes at 20°C. The annealed RNA-DNA hybrids were supplemented with 10 µl of the 2X reverse transcription mixture containing 4 µl of the 5X AMV reverse transcription buffer (Promega), 2 µl of 10 mM dNTPs, 2 µl of DEPC-treated water (Invitrogen), 1 µl of rRNasin (40 units/µl; Promega) and 1 µl of the AMV reverse transcriptase (10 units/µl; Promega) and

incubated for 20 minutes at 42°C. The reaction products were extracted with phenol-chloroform, separated by 15% Polyacrylamide Gel Electrophoresis (PAGE) containing 7.5 M urea and the gel was exposed to an X-ray film.

2.17 miRNA deep sequencing

Total RNA from adult and E12.5 mouse brain was extracted with cold TRIzol (Invitrogen) as described in section 2.6 and sent to BGI-Hong Kong for deep sequencing. Deep sequencing of small RNAs from E12.5 and adult mouse brains was done as recommended by Illumina using a GAIIx sequencing platform. The fastq files were pre-filtered to remove reads containing bases with phred scores <10, followed by clipping the adapter sequences and post-filtering to remove reads containing bases with phred scores <20 and discarding reads <18 nt long using `FASTX` (http://hannonlab.cshl.edu/fastx_toolkit/). The collapsed reads (Friedlander *et al.*, 2008) were parsed with a `bowtie` (Langmead *et al.*, 2009) index containing mature mouse miRNA sequences (miRBase v17; miRBase) extended by 3 nt at the 5' ends and by 6 nt at the 3' ends. No mismatches were allowed. To analyze reads with non-templated 3'-terminal nucleotides, parsing was repeated with reads computationally clipped by 1-3 nucleotides at their 3' ends. Sequences represented by <100 reads in either of the two brain samples were discarded. This filter was relaxed to <10 reads for the pair-wise analysis of trimming efficiencies of pre-miRNA "siblings". We further discarded miRNA entries that could not be unambiguously distinguished from other miRNAs after removing three 3'-terminal nucleotides from either the experimental reads of the miRBase sequences. Downstream statistical analyses were carried out using in-house Perl and R scripts.

2.18 High-efficiency low-background recombination-mediated cassette exchange (HILO-RMCE) protocol

N2a-A5 acceptor cells were seeded in 6-well plate at 0.5×10^6 cells per well in an antibiotic-free medium and cultured for a day. Then co-transfected with an RMCE donor plasmid pEM911 [Ago1(shAgo2-3'UTR)] or pEM912 [Ago1(shAgo2-3'UTR)] (Table 2.1) mixed with 1% (wt/wt) of Cre-encoding plasmid, pCAGGS-nlCre (section 2.21). Each well was transfected with a mixture of 2 μg total DNA, 5 μl Lipofectamine 2000 in 250 μl Opti-MEM I (Invitrogen) as per manufacturer's instructions. Cells were incubated with the transfection mixtures overnight, following which the medium was replaced with fresh media and the incubation continued for another 24 hours. Next, three-step selection regime was used beginning with one-half of the maximal puromycin concentration (2.5 μg/ml) for the first 24 to 48 h of selection, followed by the maximal concentration (5 μg/ml) for a few days until the puromycin-sensitive cells were eliminated and then returned to one-half maximal concentration to accelerate the proliferation of the puromycin-resistant cells. The cultures were incubated until the appearance of visible puromycin-resistant colonies, which were then pooled and expanded in medium containing one-half maximal puromycin concentration.

2.19 Microscopy

The expression of dsRed2 fluorescent marker protein from RIP-miR-124 or the control vector, RI vector (section 2.21) and EGFP from Dox induced pEM911 [Ago1(shAgo2-3'-UTR)], pEM912 [Ago2(shAgo2-3'-UTR)] cassettes or pEM830 [EGFP(shLuc)] control transgene (table 2.1) was analyzed by epifluorescence microscopy using an Eclipse Ti microscope (Nikon) equipped with a CoolSNAP HQ2 CCD camera (Photometrics) using FITC filter at 10x magnification.

2.20 Luciferase assay

Luciferase assay was conducted as described in Makeyev *et al.,* 2007. In brief, $3x10^4$ cells were seeded per well of a 96 well plate, and immediately transfected with a mixture of plasmid for firefly luciferase reporter containing the mouse Ptbp1 3'UTR (100 ng), RIPmiR-124 (pEM208) plasmid (100 ng) and 20 ng of *Renilla reniformis* luciferase encoding plasmid (pRL-TK; Promega) using lipofectamine 2000 (Invitrogen). Luciferase activity was measured after 24 hours of transfection using a Dual-Glo Luciferase Assay System (Promega) in accordance with manufacturer's instructions. *Renilla reniformis* luciferase was used as normalization control.

2.21 Plasmids and primers

Plasmids encoding miR-124 (RIP-miR-124-1 [pEM183] or RIP-miR-124-2 [pEM208] or RIP-miR-124-3 [pEM209]) and the corresponding control vector (RI vector [pEM157]), as well as the human AGO2 (pcDNA3-3xMyc-AGO2) and nlCre (pEM784) expression constructs have been described previously (Karginov *et al.,* 2007; Khandelia *et al.,* 2011; Makeyev *et al.,* 2007). We normally used the RIPmiR-124-2 (pEM208) to express miR-124 unless otherwise mentioned. The pTet-Off plasmid encoding a tetracycline transactivator (tTA) protein was from Clontech. We used standard molecular cloning techniques (Sambrook, 2001 #5) and enzymes from NEB to generate several new constructs described in the Table 2.1. Site-specific mutations were introduced in plasmid DNA using modified Quikchange site-directed mutagenesis protocol (Stratagene) as described in section 2.3.7. All primers used in this study are listed in Table 2.2.

Table 2.1: Plasmids generated in this study

Name	Purpose	Promoter	Vector	Insert or Treatment
pEM 142	Control for Dox-repressible miRNA expression	TRE	pTRE-Tight (Clontech) cut with *Bam*HI and *Eco*RV	~1.1 kb dsRed2-intron cassette from the RI vector (pEM157) (Makeyev *et al.*, 2007)
pEM 405	Dox-repressible expression of the wild-type miR-124	TRE	pEM142 cut with *Kpn*I-*Hpa*I to remove the dsRed2-intron cassette	~1.8 kb KpnI-HpaI fragment from RIPmiR-124-2 (pEM208) (Makeyev *et al.*, 2007)
pEM 455	Control for 3xMyc-tagged Argonaute expression experiments	CMV	pcDNA3-3xMyc-AGO2 (Karginov *et al.*, 2007) treated with *Bam*HI and *Bsp*DI and then the Klenow enzyme to remove the AGO2 ORF	The vector fragment was re-circularized with T4 DNA ligase
pEM 590	Constitutive expression of the 3xMyc-tagged human AGO1	CMV	pcDNA3-3xMyc-AGO2 (Karginov *et al.*, 2007) digested with *Bam*HI, ends filled in with Klenow, followed by digestion with *Xba*I to remove the AGO2 ORF	AGO1 ORF released from pIRESneo-FLAG/HA-AGO1 (Meister *et al.*, 2004) by *Not*I digestion, Klenow treatment and *Spe*I digestion
pEM 591	Constitutive expression of the 3xMyc-tagged human AGO3	CMV	pcDNA3-3xMyc-AGO2 (Karginov *et al.*, 2007) digested with *Bam*HI, ends filled in with Klenow, followed by digestion with *Xba*I to remove the AGO2 ORF	AGO3 ORF released from pIRESneo-FLAG/HA-AGO3 (Meister *et al.*, 2004) by *Not*I digestion, Klenow treatment and *Spe*I digestion
pEM 592	Constitutive expression of the 3xMyc-tagged human AGO4	CMV	pcDNA3-3xMyc-AGO2 (Karginov *et al.*, 2007) digested with *Bam*HI, ends filled in with Klenow, followed by digestion with *Xba*I	AGO4 ORF released from pIRESneo-FLAG/HA-AGO4 (Meister *et al.*, 2004) by *Not*I digestion, Klenow treatment and *Spe*I digestion

			to remove the AGO2 ORF	
pEM 694	Constitutive expression of the human AGO2 D597A mutant	CMV	pcDNA3-3xMyc-AGO2 (Karginov *et al.*, 2007)	Mutagenized using EMO1505 and EMO1506 primers
pEM 695	Constitutive expression of the AGO1 KY>RH mutant	CMV	pEM590	Mutagenized using EMO2508 and EMO2509 primers
pEM 697	Constitutive expression of the 3xMyc-tagged human AGO4	CAG	pCIG digested with *Eco*RV and *Bgl*II to remove the IRES-nls-EGFP cassette	~2.7 kb fragment encoding 3xMyc-AGO4 released from pEM592 by *Ase*I digestion, Klenow treatment and *Bam*HI digestion
pEM 698	Constitutive expression of the miR-124 3'C mutant	CMV	RIPmiR-124-2 (pEM208) (Makeyev *et al.*, 2007)	Mutagenized using EMO1288 and EMO1289 primers
pEM 699	Constitutive expression of the miR-124 3'G mutant	CMV	RIPmiR-124-2 (pEM208) (Makeyev *et al.*, 2007)	Mutagenized using EMO1290 and EMO1291 primers
pEM 700	Constitutive expression of the miR-124 3'U mutant	CMV	RIPmiR-124-2 (pEM208) (Makeyev *et al.*, 2007)	Mutagenized using EMO1681 and EMO1682 primers
pEM 728	Constitutive expression of 3xMyc-tagged human AGO1(AGO2 PAZ)	CMV	PCR product amplified from pEM590 using KAPA HiFi and EMO1120 and EMO1121 primers and cut with *Age*I	PCR product amplified from pcDNA3-3xMyc-AGO2 (Karginov *et al.*, 2007) using KAPA HiFi and EMO1126 and 5'-phosphorylated EMO1127 primers and cut with *Age*I
pEM 729	Constitutive expression of 3X Myc-tagged human AGO2(AG	CMV	PCR product amplified from pcDNA3-3xMyc-AGO2 (Karginov *et al.*, 2007) using KAPA HiFi and	PCR product amplified from pEM590 using KAPA HiFi and EMO1124 and 5'-phosphorylated EMO1125 primers and cut with *Age*I

	O1 PAZ)		EMO1122 and EMO1123 primers and cut with *Age*I	
pEM 830	Dox inducible expression of the EGFP(shLuc) cassette	TRE	pRD-RIPE (pEM791) (Khandelia *et al.*, 2011) cut with *Bsm*BI.	Annealed EMO1321/EMO1322 oligonucleotides
pEM 911	Dox inducible reprogramming of N2a Argonaute expression pattern	TRE	pRD-RIPE (pEM791) backbone was amended with two mouse Ago2 3'UTR-specific shRNAs (Khandelia *et al.*, 2011); EMO1530/EMO1531 and EMO1536/ EMO1537), digested with *Bsr*GI, followed by filling in the ends with Klenow and *Age*I digestion to remove the EGFP ORF	Mouse Ago1 ORF amplified from the corresponding cDNA clone using KAPA HiFi and EMO1687/ EMO1267 primers and cut with *Age*I
pEM 912	Dox inducible reprogramming of N2a Argonaute expression pattern	TRE	Same as above	Mouse Ago2 ORF amplified from the corresponding cDNA clone using KAPA HiFi and EMO1688/ EMO1269 primers and cut with *Age*I
pEM 919	Dox-repressible expression of the miR-124 3'C mutant	TRE	pEM142 digested with *Sac*II and *Spe*I	~0.6 kb pre-miR-124-2 fragment released from pEM698 by *Sac*II and *Spe*I digestion
pEM 920	Dox-repressible expression of the miR-124 3'G mutant	TRE	pEM142 digested with *Sac*II and *Spe*I	~0.6 kb pre-miR-124-2 fragment released from pEM699 by *Sac*II and *Spe*I digestion
pEM 921	Dox-repressible expression	TRE	pEM142 digested with *Sac*II and *Spe*I	~0.6 kb pre-miR-124-2 fragment released from pEM700 by *Sac*II and *Spe*I

	of the miR-124 3'U mutant			digestion
pEM 924	Constitutive expression of the AGO2 RH>KY mutant	CMV	pcDNA3-3xMyc-AGO2 (Karginov *et al.*, 2007)	Mutagenized using EMO2484 and EMO2485 primers

Table 2.2: Oligonucleotides used in this study

ID	Name	Sequence, 5' to 3'
RT-qPCR		
EMO592	mHPRT1_up1	CCAGACAAGTTTGTTGTTGGA
EMO593	mHPRT1_down1	TTTACTAGGCAGATGGCCACA
EMO863	mPTBP1_up5	AGTGCGCATTACACTGTCCA
EMO864	mPTBP1_down5	CTTGAGGTCGTCCTCTGACA
EMO1094	mAgo1_F2	TCTATCCCAGCACCTGCCTA
EMO1095	mAgo1_R2	GCGAAGTACATGGTGCGTAGA
EMO1098	mAgo2_F2	TGCACACGCTCTGTGTCAAT
EMO1099	mAgo2_R2	CAGTGTGTCCTGGTGGACCT
EMO1100	mAgo3_F1	GGTATGGCACTATGGGCAAA
EMO1101	mAgo3_R1	CATAAACTGGTCTACGGTCTCCA
EMO1106	mAgo4_F2	ATTCCGGGCAAGGTATCATT
EMO1107	mAgo4_R2	CATTTTGAGGATGCGTGAGAT
EMO1134	mGAPDH_F1	AAATGGGGTGAGGCCGGTGC
EMO1135	mGAPDH_R1	ATCGGCAGAAGGGGCGGAGA
EMO1160	mCTDSP1_F1	ACCGGGGGAACTACGTAAAG
EMO1161	mCTDSP1_R1	CGGCTGAGTTGCTCAAAGAA
EMO1162	mVAMP3_F2	AGAAGCTCTCGGAGCTAGATGA
EMO1163	mVAMP3_R2	TGATGACAATGATCACCAGGA
Cloning		
EMO1120	hAGO1_F1	GCTGTATTAAAAAGCTGACCGACAACCA
EMO1121	hAGO1_R1	CAATCACCGGTTGTGCCTTATAAAAGGCAGTG GCT
EMO1122	hAGO2_F1	GCTGTATTAAAAAATTAACGGACAATCAGACC T
EMO1123	hAGO2_R1	CGATTACCGGTTGTGCCTTGTAAAACGCTGTTG CT
EMO1124	hAGO1_PAZ_F1	GCACAACCGGTGATTGAGTTCATGTGTGAGGT
EMO1125	hAGO1_PAZ_R1	GCTGCCCAGCCACAATGTTACA
EMO1126	hAGO2_PAZ_F1	GCACAACCGGTAATCGAGTTTGTTTGTGAAGTT TTG
EMO1127	hAGO2_PAZ_R1	GCTGTCCTGCCACAATGTTACAGAC
EMO1266	mAgo1_cDNA_FP	CCCGGAATTCATGGAAGCGGGACCCTCGGGAG CAG
EMO1267	mAgo1_cDNA_RP	CGATGCGGCCGCTCAAGCGAAGTACATGGTGC GTAGA
EMO1268	mAgo2_cDNA_FP	CCCGGAATTCATGTACTCGGGAGCCGGCCCCG TTC
EMO1269	mAgo2_cDNA_RP	CGATGCGGCCGCTCAAGCAAAGTACATGGTGC GCAGT
EMO1321	ffLuc_shRNA_FP	TGCTGTATTCAGCCCATATCGTTTCAGTTTTGG CCACTGACTGACTGAAACGATGGGCTGAATA
EMO1322	ffLuc_shRNA_RP	CCTGTATTCAGCCCATCGTTTCAGTCAGTCAGT GGCCAAAACTGAAACGATATGGGCTGAATAC

EMO1530	mAgo2_shRNA1_FP	TGCTGAATCCAACTTGGTACACAATCGTTTTGG CCACTGACTGACGATTGTGTCAAGTTGGATT
EMO1531	mAgo2_shRNA1_RP	CCTGAATCCAACTTGACACAATCGTCAGTCAG TGGCCAAAACGATTGTGTACCAAGTTGGATTC
EMO1536	mAgo2_shRNA4_FP	TGCTGCAAAGACGTCTCATGTTCGATGTTTTGG CCACTGACTGACATCGAACAAGACGTCTTTG
EMO1537	mAgo2_shRNA4_RP	CCTGCAAAGACGTCTTGTTCGATGTCAGTCAGT GGCCAAAACATCGAACATGAGACGTCTTTGC
EMO1687	mAgo1_Age1_F1	CCACCGGTCGCCACCATGGTGGACTACAAAGA CGACGATGACAAGTCCATGGAAGCGGGACCCTC
EMO1688	mAgo2_Age1_F1	CCACCGGTCGCCACCATGGTGGACTACAAAGA CGACGATGACAAGTCCATGTACTCGGGAGC
EMO1744	mAgo3_cDNA_F1	CATGGAAATCGGCTCCGCAGGA
EMO1745	mAgo3_cDNA_R1	GTCACGGAGAATAAGCGGCCGCTTGTTAAGCG AAGTACATTG
EMO1746	mAgo4_cDNA_F1	CATGGAGGCGCTGGGAC
EMO1747	mAgo4_cDNA_R1	CAAATTTGTTGAGTGCGGCCGCAAGACTCTCA GGCAAAATAC

Site-specific mutagenesis

EMO1288	miR-124_A>C_F1	GCACGCGGTGAATGCCACGAGCGGAGCCTAC GGCTG
EMO1289	miR-124_A>C_R1	CAGCCGTAGGCTCCGCTCGTGGCATTCACCGC GTGC
EMO1290	miR-124_A>G_F1	GCACGCGGTGAATGCCAGGAGCGGAGCCTAC GGCTG
EMO1291	miR-124_A>G_R1	CAGCCGTAGGCTCCGCTCCTGGCATTCACCGC GTGC
EMO1505	hAGO2_D597A_F1	CATCTTTCTGGGAGCAGCCGTCACTCACCCCC CC
EMO1506	hAGO2_D597A_R1	GGGGGGGTGAGTGACGGCTGCTCCCAGAAAG ATG
EMO1681	miR-124_A>T_F1	GCACGCGGTGAATGCCATGAGCGGAGCCTAC GGCTG
EMO1682	miR-124_A>T_R1	CAGCCGTAGGCTCCGCTCATGGCATTCACCGC GTGC
EMO2484	hAGO2_KY>RH_F1	CGGTGGCCCAGTATTTCAAGGACAAATATAAG CTTGTTCTGCGCTACCCCCACC
EMO2485	hAGO2_KY>RH_R1	GGTGGGGGTAGCGCAGAACAAGCTTATATTTG TCCTTGAAATACTGGGCCACCG
EMO2508	hAGO1_RH>KY_F1	GGCACAGTATTTCAAGCAGAGGCACAACCTTC AGCTCAAGTATCCCC
EMO2509	hAGO1_RH>KY_R1	GGGGATACTTGAGCTGAAGGTTGTGCCTCTGC TTGAAATACTGTGCC

Primer extension and LM-RT-PCR

EMO222	miR-124_p_ext	TGGCATTCACCGCGT
EMO465	miR-124_F1	TAAGGCACGCGGTGAATG
EMO1013	3'_RT	TCTGTACAAGCAGAAGACGGCATAC

EMO1014	3'_PCR	TCTGTACAAGCAGAAGACGGCA

Northern probes

EMO12	anti_miR-124	TGGCATTCACCGCGTGCCTTAA
EMO30	anti_U6	GCCATGCTAATCTTCTCTGTATC
EMO1615	anti_miR-186	AGCCCAAAAGGAGAATTCTTTG
EMO1736	anti_miR-541	AGTGTGACCAACATCAGAATCCCTT
EMO1769	anti_miR-148b	ACAAAGTTCTGTGATGCACTGA
EMO1770	anti_miR-411	CGTACGCTATACGGTCTACTA
EMO1771	anti_miR-381	ACAGAGAGCTTGCCCTTGTATA
EMO1773	anti_miR-125a-5p	TCACAGGTTAAAGGGTCTCAGGGA

3. RESULTS

3.1 Mammalian Argonaute identity affects miRNA length

To understand the biological significance of the mammalian Argonaute paralog expansion, we co-transfected HEK293T cells with expression plasmids encoding 3xMyc-tagged versions of the human AGO1-4 under the control of the CMV or CAG promoters (Figure 3.1A) together with the RIPmiR-124 construct encoding miR-124, an evolutionarily conserved nervous system-specific miRNA studied in our laboratory (Makeyev & Maniatis, 2008; Makeyev *et al*., 2007). Cells were harvested 72 hours post transfection and expression of 3xMyc-tagged Argonautes and miR-124 was examined by immunoblotting and Northern blotting respectively. The AGO1-3 proteins were well expressed from a CMV promoter, whereas a CAG promoter was required to express AGO4 at an optimal level (Figure 3.1B).

A high-resolution Northern blot analysis of the miR-124 RNA revealed that (i) Argonaute over-expression led to dramatically increased steady-state levels of the mature miRNA as compared to the control plasmid (Figure 3.1C) and (ii) the miR-124 isoform population was dominated by 21-mers in the presence of recombinant AGO2 and by 22-mers in the presence of AGO1, AGO3 or AGO4 (Figure 3.1C-D). The abundance of 21-mers relative to 22mers was calculated by the ratio of 21-mer to 22-mer band intensities from Figure 3.1C and it was observed that there is a significant increase in this ratio with respect to recombinant AGO2 as compared to AGO1, AGO3 or AGO4 (Figure 3.1D).

When expression plasmids encoding 3xMyc-tagged versions of the mouse Ago1-4 under CMV (Figure 3.2A) were co-transfected with the RIPmiR-124 construct encoding miR-124 in HEK293T, mouse Argonautes behaved similar to human Argonautes with respect to miR-124. RNA and protein samples were harvested 72

hours post transfection and analysed by urea and SDS PAGE respectively. Northern blot analysis of the miR-124 RNA revealed an increased steady-state levels of the mature miR-124 and its isoform population was dominated by 21-mers in the presence of recombinant Ago2 and by 22-mers in the presence of Ago1, Ago3 or Ago4 (Figure 3.2A-C) which is evident from the significant increase in the ratio of 21-mer to 22-mer with respect to recombinant Ago2 as compared to Ago1, Ago3 or Ago4 (Figure 3.2C).

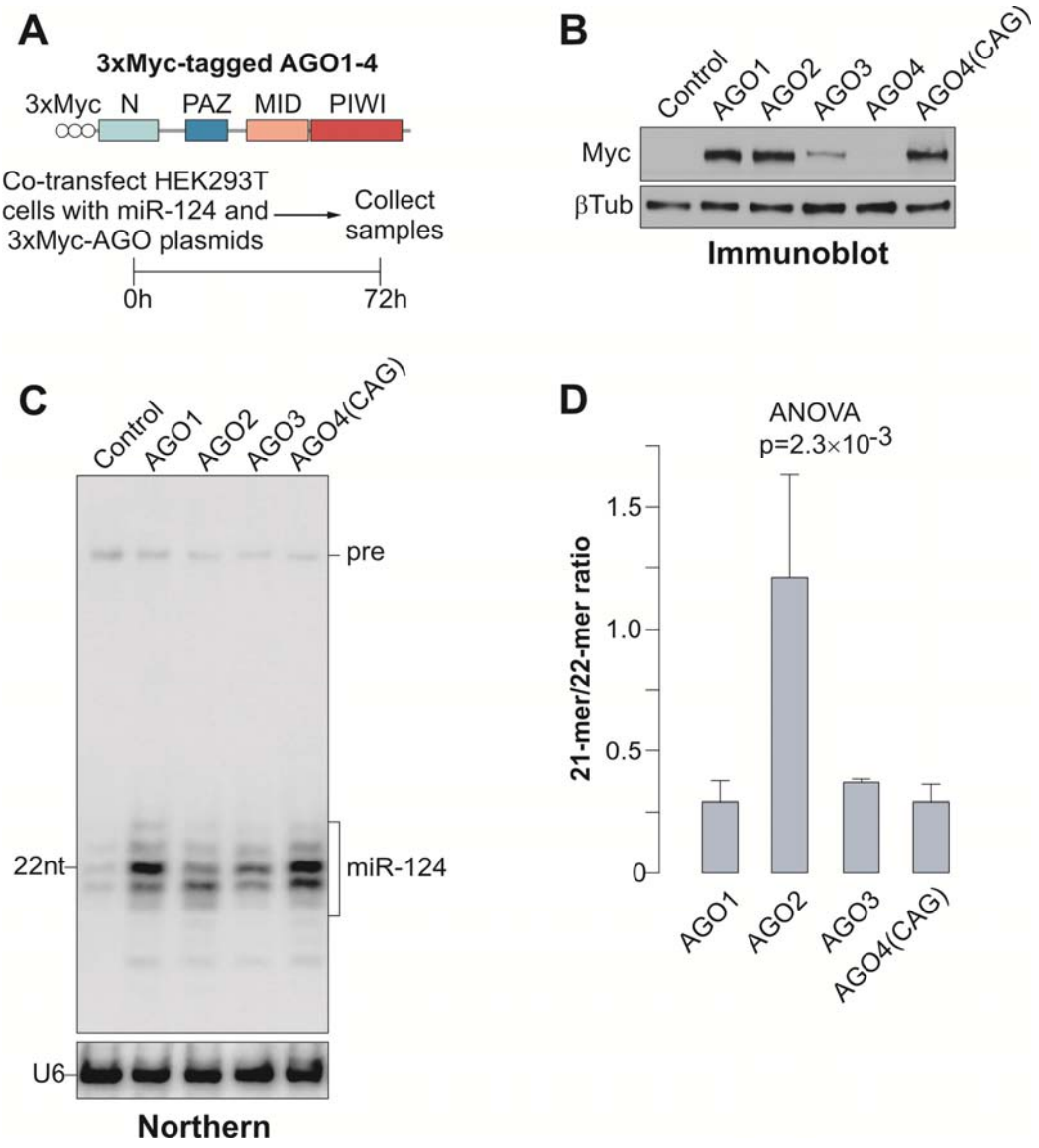

Figure 3.1: Human Argonautes modulate the mature miRNA length. (**A**) Top, diagram of the 3xMyc-AGO constructs and bottom, workflow of the 3xMyc AGO/miR-124 co-expression experiment. (**B**) Immunoblot analysis of the 3xMyc-tagged AGO1-4 proteins expressed from a CMV promoter and AGO4 expressed from a CAG promoter using a Myc tag-specific antibody. β-tubulin is a lane loading control. (**C**) Northern blot analysis of miR-124 co-expressed with the corresponding 3xMyc AGO proteins or a control plasmid. The positions of the mature miR-124 and the pre-miR-124 precursor (pre) are marked on the right. U6 snRNA specific probe is used as a loading control. (**D**) Quantification of the results in (C) showing a significantly increased ratio between the 21- and 22-mers in cells over-expressing 3xMyc AGO2 as compared to the other three Argonautes. Data are averaged from 3 independent transfection experiments ±SD.

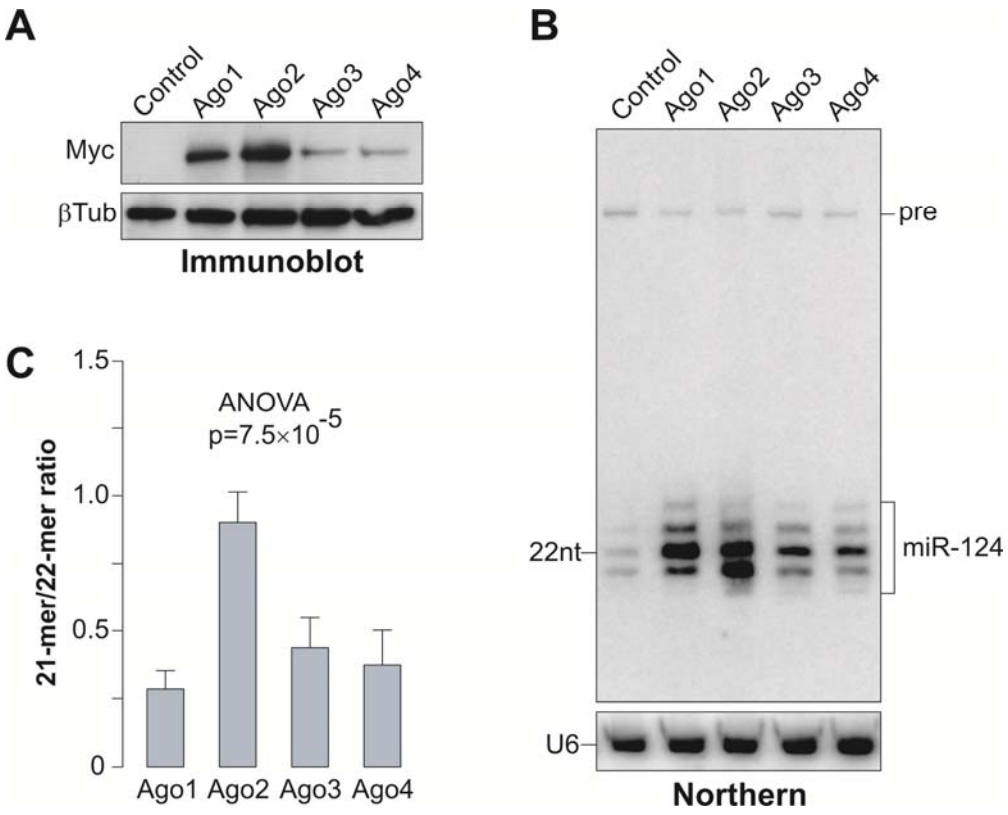

Figure 3.2: Role of mouse Argonautes in defining the mature miRNA length. (**A**) Immunoblot analysis of 3xMyc-tagged mouse Ago1-4 expressed from a CMV promoter. The recombinant Ago proteins were detected with a Myc tag-specific antibody; β-tubulin is a loading control. (**B**) Northern blot analysis of miR-124 co-expressed with the corresponding 3xMyc Ago proteins or a control plasmid. U6 snRNA-specific probe is used as a loading control. (**C**) Quantification of the results in (B) showing a significantly increased ratio between the 21- and 22-mers in cells over-expressing 3xMyc Ago2 as compared to the other three Argonautes. Data are averaged from 3 independent transfection experiments ±SD.

3.1.1 *Accumulation of mature miRNA in Ago-overexpressing cells is due to the miRNA-Ago interaction*

The mature miRNA accumulated in the Argonaute over-expressing cells was likely associated with the corresponding AGO proteins, as discussed previously (Diederichs & Haber, 2007). To test this prediction, we co-expressed miR-124 and the 3xMyc-tagged AGO proteins in HEK293T cells, pulled down the complexes using a Myc tag-specific antibody and analyzed the co-immunoprecipitated miR-124 by Northern blotting (Figure 3.3A). Similar to the distributions observed in Figure 3.1C-D, the most abundant AGO2-associated form was 21-mer, whereas 22-mer was predominant in the AGO1, AGO3 and AGO4 pull-downs (Figure 3.3A-B). Thus, the miR-124 isoform composition of the total RNA samples corresponded to the miRNA patterns physically associated with the over-expressed Argonautes.

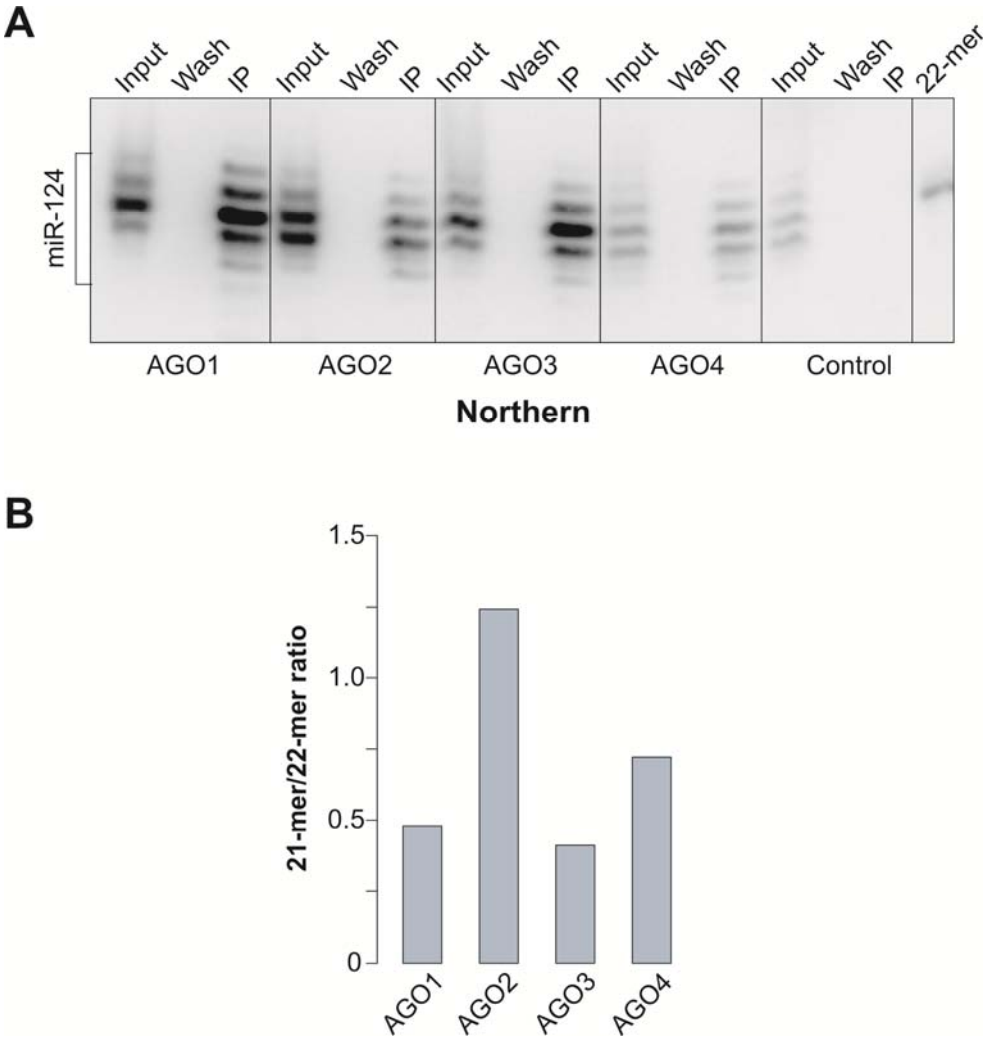

Figure 3.3: Mature miRNA accumulates in the abundant Argonaute. (**A**) HEK293T cells were co-transfected with a miR-124 expression plasmid and either of the 3xMyc-tagged AGO1-4 plasmids. Argonaute-associated mature miR-124 species were pulled down with anti-Myc antibody 72 hours post transfection and analyzed by Northern blotting. (**B**) Quantification of the data in (A).

3.2 Increase in fractional abundance of Ago2 correlates with shortening of mature miR-124 during mouse brain development

3.2.1 *Increase in fractional abundance of Ago2 in developing mouse brain*

Since the above results suggested that Argonaute identity might affect the length of mature miRNAs. We examined the Ago1-4 expression in developing mouse brain both at transcript and protein levels. Quantitative RT-PCR (RT-qPCR) analyses showed that the embryos of 12.5 days post conception (E12.5) brain expressed readily detectable amounts of the Ago1 and Ago2 mRNAs (Figure 3.4A). Notably, the apparent Ago1 mRNA abundance decreased ~8 fold in the adult brain, while the Ago2 expression decreased only ~2 fold (Figure 3.4A-B). The expression of Ago3 and Ago4 was negligible at both developmental stages (Figure 3.4A). Immunoblot analyses confirmed that the originally high Ago1 protein levels in the E12.5 brain were dramatically reduced in the adult sample, whereas the Ago2 expression was relatively uniform at both developmental stages (Figure 3.4C).

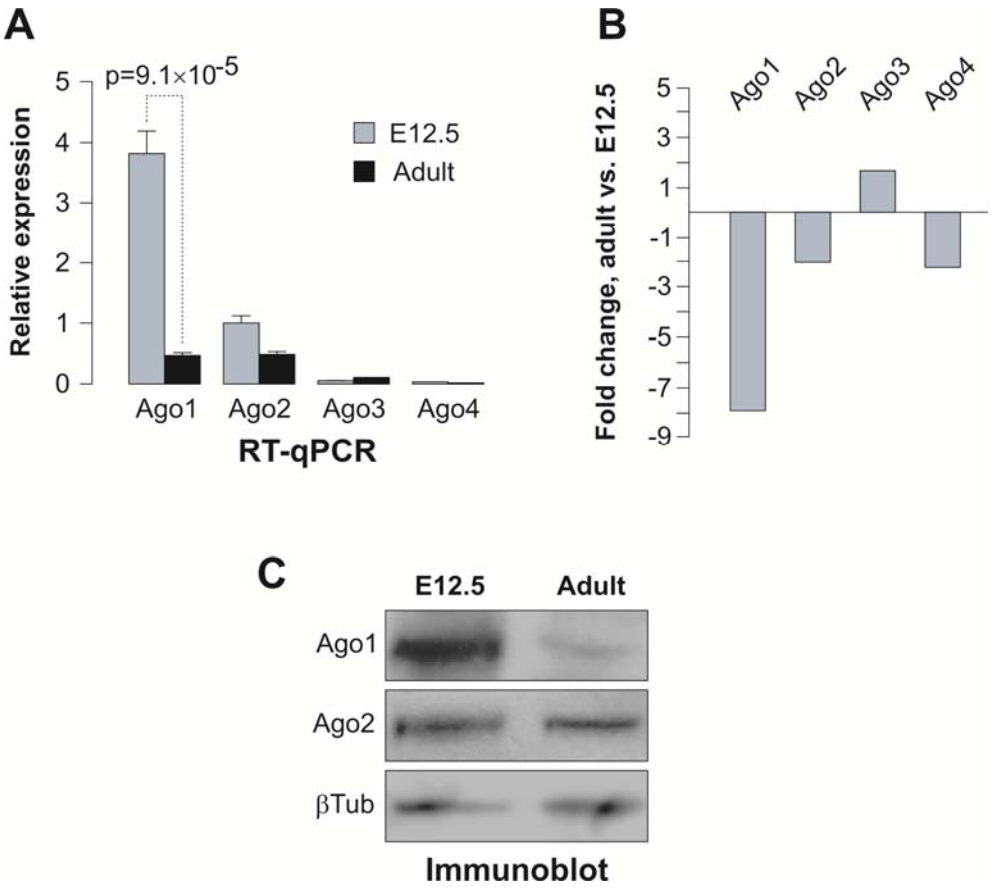

Figure 3.4: Ago2 fractional abundance goes up during the mouse brain development. (**A**) RT-qPCR analysis of the Argonaute expression in E12.5 and adult (P60) mouse brains. Data were averaged from three biological replicates ±SD and analyzed by the t test. (**B**) Quantification of the data in (A) showing a dramatic decrease in the Ago1 expression in the adult brain. Negative fold changes correspond to down-regulation in the adult brain and positive fold changes correspond to up-regulation in the adult brain. (**C**) Immunoblot analysis showing a relatively uniform expression of Ago2 in the E12.5 and adult mouse brains and a reduction in the Ago1 protein levels during mouse brain development. β-tubulin is a loading control.

3.2.2 *Increasing Ago2 fractional abundance enhances the shortening of mature miRNA*

To investigate the effect of this increase in the Ago2 fractional abundance, we analyzed the mature miR-124 in the E12.5, newborn and adult mouse brains (Figure 3.5A). Interestingly, 22-mers were predominant in the E12.5 sample, whereas 21-mers became the most abundant form in the newborn and adult samples (Figure 3.5A-B). This indicated that the change in the Argonaute expression pattern might underlie the miR-124 isoform dynamics during brain development.

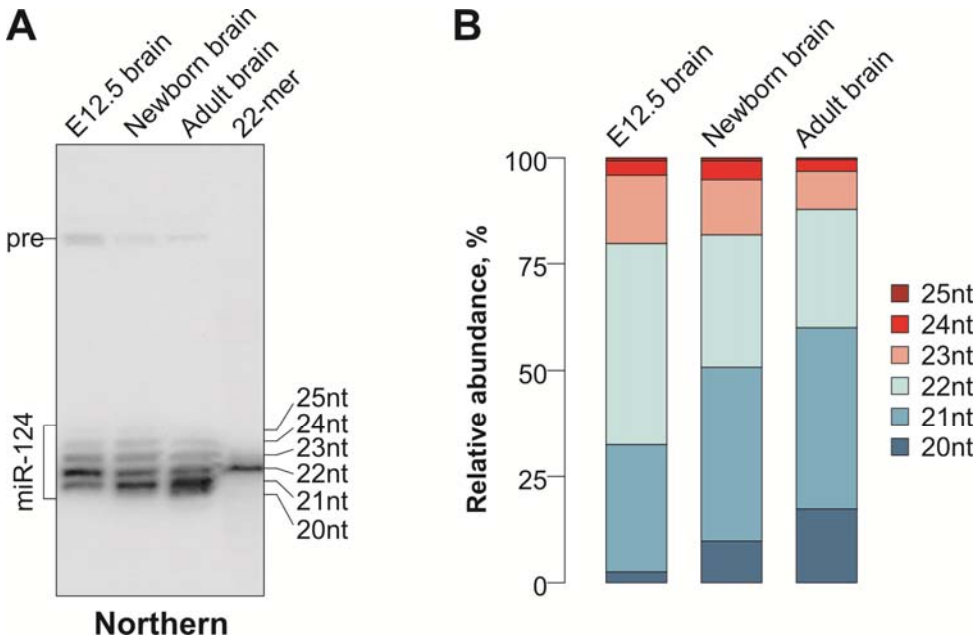

Figure 3.5: Shortening of mature miRNA is in direct relation to the increasing Ago2 fractional abundance during the mouse brain development. (**A**) Northern blot analysis of RNAs from E12.5, newborn (P0) and adult (P60) mouse brains showing progressive shortening of mature miR-124 during development. **(B)** Quantification of the data in (A) showing a change in the percentage of the corresponding miR-124 isoforms (20-25 nt) as a function of development.

3.3 Mature miRNAs are shortened following the Dicer processing step

3.3.1 *Mature miRNAs are shortened in the absence of precursor miRNA, a Dicer substrate*

The Argonaute-dependent change in the miR-124 length could theoretically be due to (i) altered cleavage preferences of Drosha or Dicer or (ii) a post-Dicer trimming of the Argonaute-loaded mature miRNAs. To distinguish between these possibilities, we carried out a pulse-chase experiment, in which miR-124 was expressed from a Dox-repressible promoter in HEK293T cells containing substantial amounts of endogenous AGO2 (Meister *et al*., 2004). The transcription was stopped with Dox 24 hours post transfection and the subsequent changes in the miR-124 RNA were analyzed by Northern blotting (Figure 3.6A). The originally prominent pre-miR-124 precursor band disappeared within 24 hours of the Dox treatment, presumably as a result of the Dicer processing reaction (Figure 3.6A, bottom). This allowed us to monitor the subsequent changes in the mature miR-124 species. Notably, the 22-mer miR-124 species were chased into 21-mers from 24 to 48 hours after adding Dox (Figure 3.6A).

This result was consistent with the model that pre-miR-124 was initially processed by Dicer into 22-mers that were subsequently trimmed to 21-mers.

3.3.2 *Dicer cleaves precursor miRNA giving rise to 22nt size mature miRNA predominantly in vitro*

To directly determine the Dicer cleavage specificity, we incubated the total RNA from the RIPmiR-124-transfected HEK293T cells harvested 24 hours post

transfection with purified human Dicer *in vitro* (Figure 3.6B). Quantification of the newly formed mature miR-124 species processed from the pre-miR-124 substrate confirmed that Dicer indeed generated predominantly 22-mer products (Figure 3.6C).

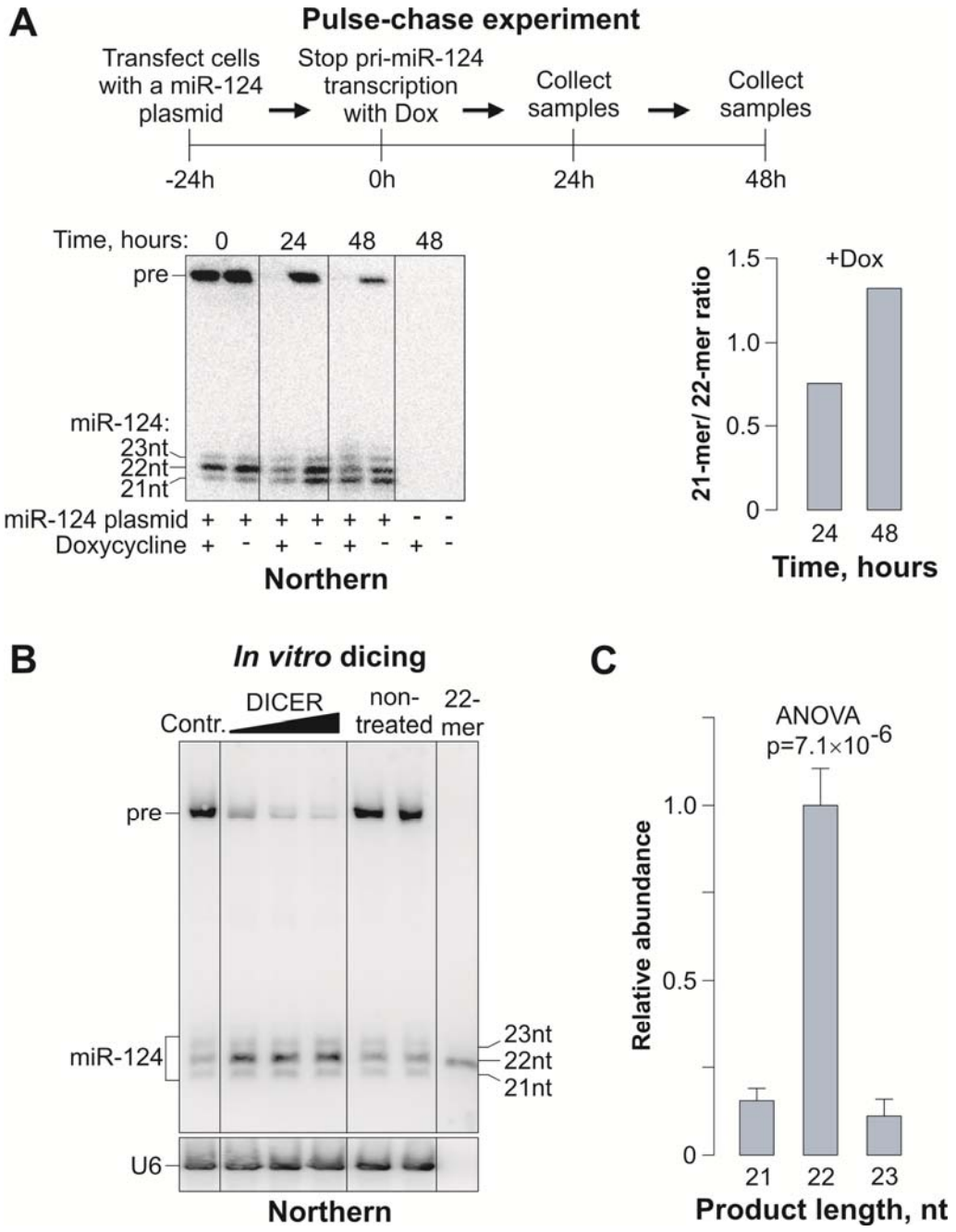

Figure 3.6: Shortening of mature miRNA is independent of precursor processing by Dicer. (**A**) Pulse-chase experiment showing that the mature miR-124 length is reduced after the completion of the Drosha- and Dicer-dependent processing steps. *Top*, the experimental workflow; *bottom left*, Northern blot analysis of the corresponding RNA samples; *bottom right*, quantification of the Northern blot data showing an increase in the 21- to 22-mer ratio in samples from collected 24 and 48 hours after halting the pri-miR-124 transcription by Dox. (**B**) RNA from miR-124-expressing HEK293T cells in (A) at the time point 0 was incubated *in vitro* with increasing amounts of purified human Dicer and the reaction products were analyzed by Northern blotting. (**C**) Quantification of the newly formed products in (B) showing that Dicer generates predominantly 22-mer species. Data are averaged from the three Dicer lanes in (B) ±SD.

3.3.3 *Mature miRNA with 2'-OMe protected on 3' terminus are resistant to shortening*

The 3' termini of some Argonaute-loaded miRNAs are known to undergo enzymatic trimming in Drosophila (Han *et al*., 2011; Liu *et al*., 2011). To test whether miR-124 might be shortened in the mammalian cells through a similar process, we transfected HEK293T cells transiently expressing 3xMyc-tagged AGO2 with synthetic miR-124 22-mer duplexes designed similar to siRNAs and analyzed the lengths of the AGO2-associated miRNAs by Northern blotting 4 and 24 hours post transfection (Figure 3.7A-D). The fraction of the AGO2-bound 21-mers increased over time, indicative of an ongoing trimming reaction. On the other hand, essentially no trimming was detected when we repeated this experiment with 22-mer miR-124, in which the 3'-terminal nucleotide was protected by a 2'-OMe group (Figure 3.7A-C). This suggested that the AGO2-associated 21-mers were derived from the 22-mers as a result of the 3' terminal nucleotide removal.

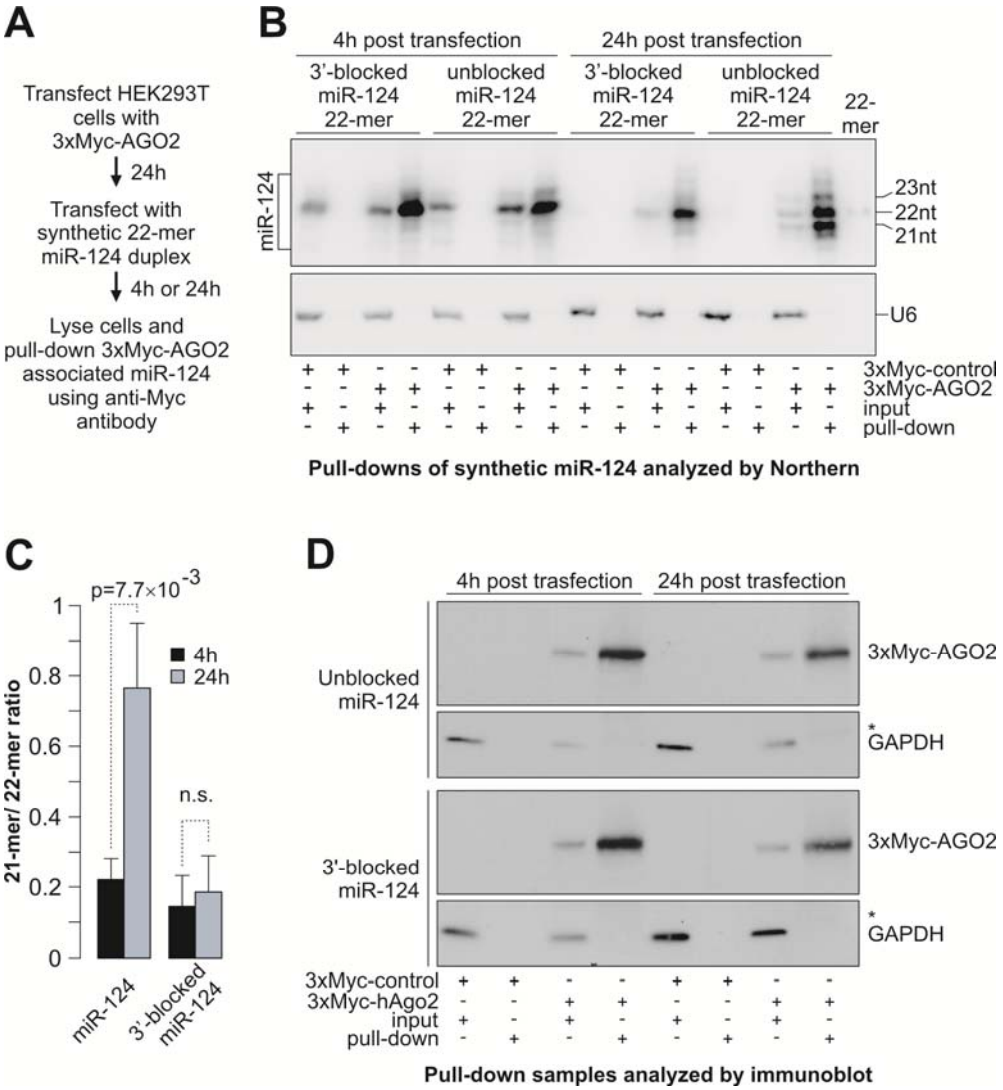

Figure 3.7: AGO2-loaded synthetic 22-mers are efficiently trimmed unless protected at the 3' end. (**A**) Outline of the experiment. (**B**) HEK293T cells expressing 3xMyc-AGO2 were transfected with synthetic siRNA-like duplexes containing either an umodified 22-mer miR-124 or 22-mer protected at the 3' end with a 2'-OMe group. The AGO2/miR-124 complexes were pulled down 4 and 24 hours post transfection and analyzed by Northern blotting. (**C**) Quantification of the data in (B) confirming efficient trimming of the unmodified but not 3'-protected 22-mers loaded into AGO2. Data are averaged from three independent experiments ±SD. (**D**) Immunoblot analysis of the 3xMyc-AGO2/miR-124 pull-down experiment. The 3xMyc-AGO2 expression for (B) was analyzed by immunoblotting with Myc tag-specific antibody and GAPDH antibody was used to control input lane loading and monitor the quality of the pull-down fractions. Asterisks indicate a weak unspecific band detected by the GAPDH antibody in the pull-down fractions.

3.3.4 *miR-124 from all the three precursor paralogs is subjected to trimming*

Next we examined whether the mature miR-124 generated by the processing of all the 3 miR-124 precursors (miR-124-1, 2 and 3) encoded by three gene paralogs is subjected to trimming or not. To this end we transfected RIPmiR constructs for miR-124a-1, 2 and 3 in HEK293T. RNA harvested after 72hours of transfection was subjected to northern blot analysis showed that the levels of mature miR-124 expressed from all the above three paralogs were indistinguishable (Figure 3.8A and C) (Makeyev *et al*., 2007). Most importantly mature miR-124 from each of the three paralogs was subjected to extensive trimming (Figure 3.8A and B). Quantitation of (A) showed no significant difference in trimming efficiency of miR-124 between the three precursor paralogs (Figure 3.8B).

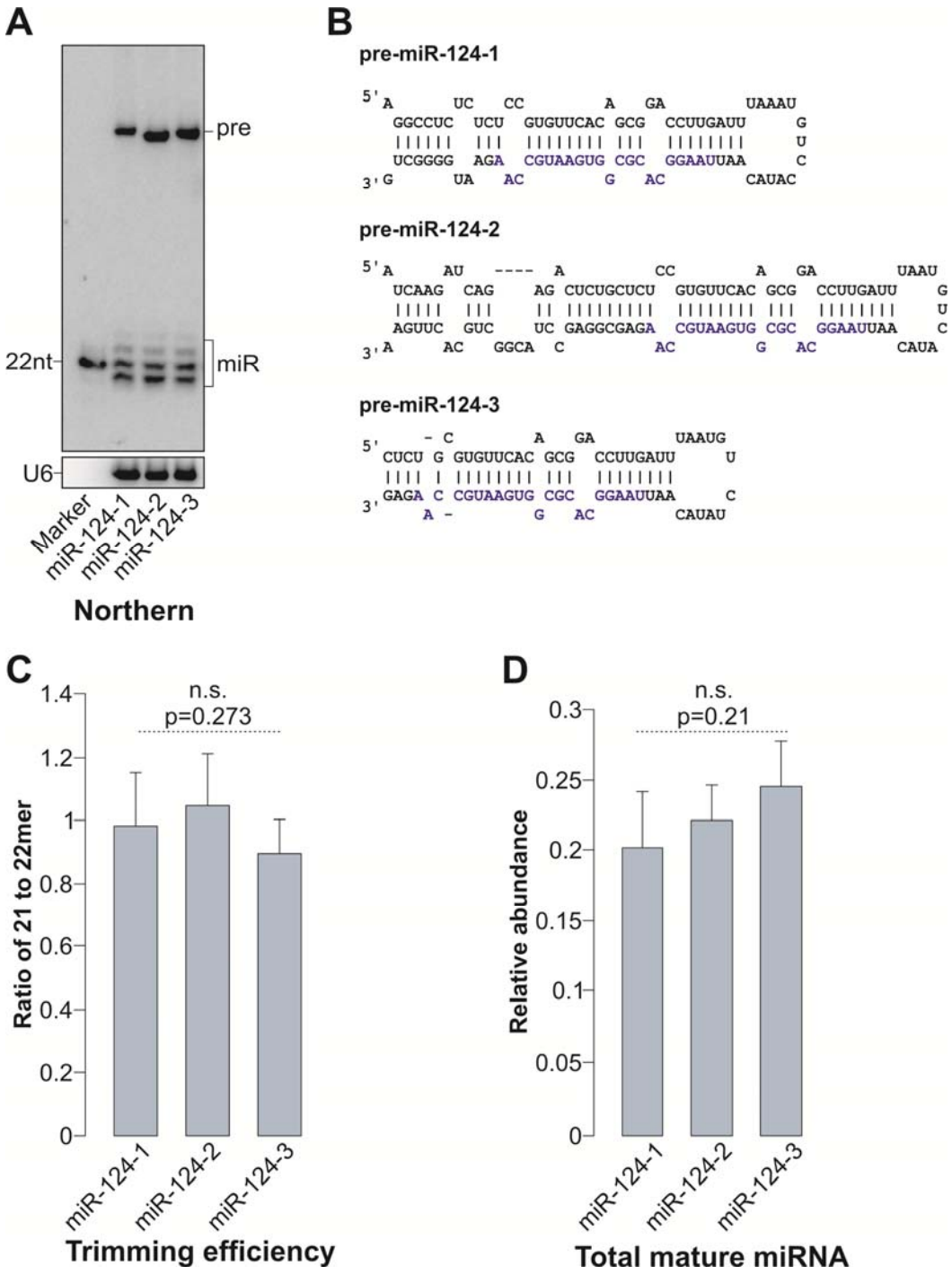

Figure 3.8: Mature miRNA from the three precursor paralogs is trimmed with equal efficiency. (**A**) Northern blot analysis of pre-miR-124-1, 2 and 3 expressed from RIPmiR constructs in HEK293T. The positions of the mature miR and the pre-miR-124 precursor (pre) are marked on the right. U6 snRNA specific probe is used as a loading control. (**B**) Diagram of the pre-miR-124 paralogs with identical mature miRNA sequence (colored in blue) in the 3' arm (miRBase). (**C**) Quantification of the results in (A) showing an extensive trimming (ratio between the 21- and 22-mers) for each of the miR-124-1, 2 and 3 with no significant difference between them. (**D**) Quantification of (A) showing the abundance of total mature miRNA for each of the miR-124-1, 2 and 3 with no significant difference between them. Data for (C) and (D) are averaged from 4 independent transfection experiments ±SD.

3.3.5 *All three miR-124 precursor paralogs predominantly give rise to 22nt size mature miRNA in vitro without any bias*

To directly determine the Dicer cleavage specificity for each of the miR-124 precursors, the pre-miRNA from RIPmiR-124-1, 2 and 3 transfected HEK293T cells harvested at 24 hours post transfection was incubated with purified human Dicer *in vitro* (Figure 3.9B). The pre-miRNA from total RNA of RIPmiR-124-1, 2 and 3 transfected HEK293T cells was extracted after resolving on a 10% PAGE and the gel purified fractions were analyzed by a high resolution northern blot (Figure 3.9A). Pre-miR-124-1, 2 and 3 substrates were then subjected to Dicer cleavage *in vitro* and the mature miRNA thus generated was analyzed by Northern blot. We observed that Dicer indeed generated predominantly 22-mer products irrespective of the precursor substrate (Figure 3.9B).

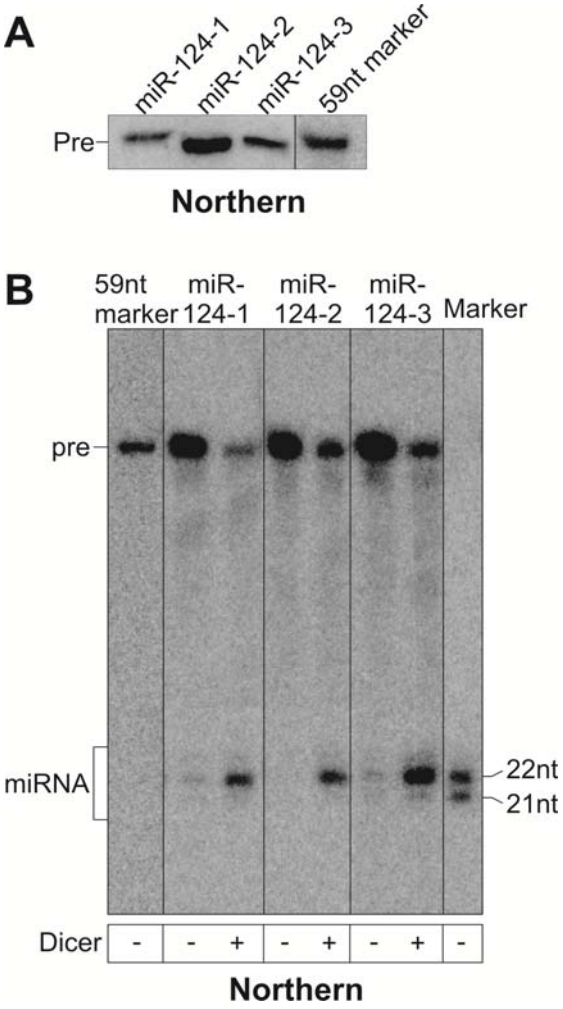

Figure 3.9: Dicer generates predominantly 22-mer mature miR-124 from each of the precursor paralogs. (**A**) High resolution northern blot showing the pre mir-124-1, 2 and 3 extracted from the total RNA of RIPmiR-124-1, 2 and 3 transfected HEK293T cells. (**B**) RNA fraction of ~60nt size from miR-124-1, 2 and 3 expressing HEK293T cells in (A) was incubated *in vitro* with 0.125 units of purified human Dicer in an *in vitro* dicing reaction for 45 minutes and the products were analyzed by Northern blotting showed that Dicer generates predominantly 22-mer species.

3.3.6 *Mature miRNAs are shortened following their loading into AGO2*

Since it was formally possible that different Argonaute proteins might have distinct miRNA loading preferences, we transfected HEK293T cells expressing 3xMyc-tagged AGO1 or AGO2 with an equimolar mixture of the 22- and 21-mer miR-124 duplexes and analyzed the isoform distributions in the Myc-tag pull-down fractions 4 hours post transfection (Figure 3.10A-B). Both AGO1 and AGO2 recruited 22- and 21-mers with comparable efficiencies thus supporting the model that the length of mature miRNAs is altered following their loading into AGO2.

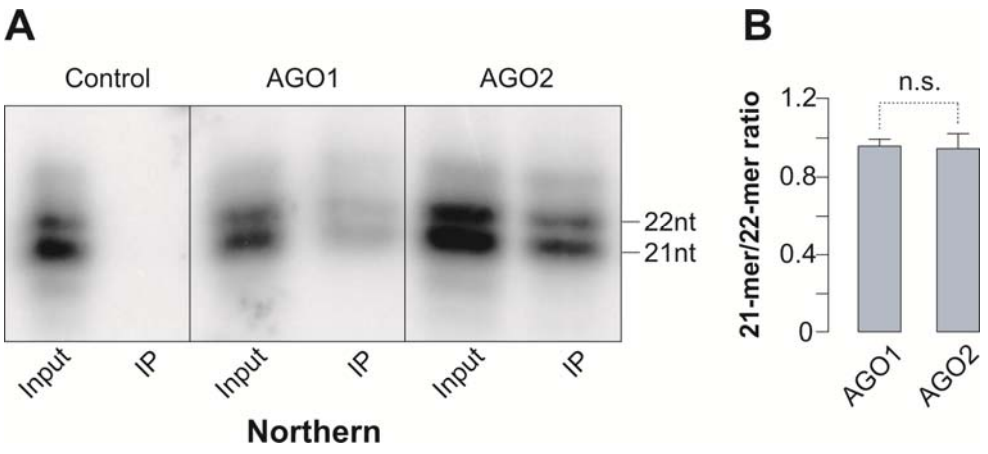

Figure 3.10: miRNA length is reduced following its recruitment to AGO2. (**A**) HEK293T cells were transfected with 3xMyc-AGO1 or 3xMyc-AGO2 expression constructs and the tagged proteins were allowed to be expressed for 24 hours. The cells were then transfected for 4 hours with a mixture of siRNA-like duplexes containing 22- and 21-mer miR-124 strands and the AGO-associated miR-124 RNA was pulled down using an anti-Myc antibody and analyzed by Northern blotting. (**B**) Quantification of the data in (B) averaged from 3 independent transfection experiments ±SD. The loading preferences of AGO1 and AGO2 do not differ significantly (n.s. [not significant with $p>0.05$], t test).

3.4 Mammalian miRNAs undergo large-scale 3’-terminal trimming during nervous system development

3.4.1 *Mature miR-124 is shortened on the 3’ terminus*

To ensure that the 3’-terminal trimming also accounted for the miR-124 isoform dynamics in the developing mouse brain, we analyzed the 3’-terminal sequences of miR-124 at the E12.5 and the adult stages using ligation-mediated RT-PCR (LM-RT-PCR) followed by cloning and sequencing of the miR-124-specific PCR products (Figure 3.11A). All 30 clones derived from the E12.5 sample terminated in ...CCAA3’, which corresponded to the 22-mer sequence 5’UAAGGCACGCGGUGAAUGCCAA3’. On the other hand, ...CCA3’ (21-mer) was the most frequently encountered terminus in the adult clones followed by ...CCAA3’ (22-mer), ...CC3’ (20-mer) and ...C3’ (19-mer) (Figure 3.11A). Primer extension analysis of the E12.5 and adult miR-124 showed that the predominant 5’ end position was 5’UAAGGC... in both samples, thus confirming that the reduced length of miR-124 in the adult brain was due to changes at the 3’ end (Figure 3.11B).

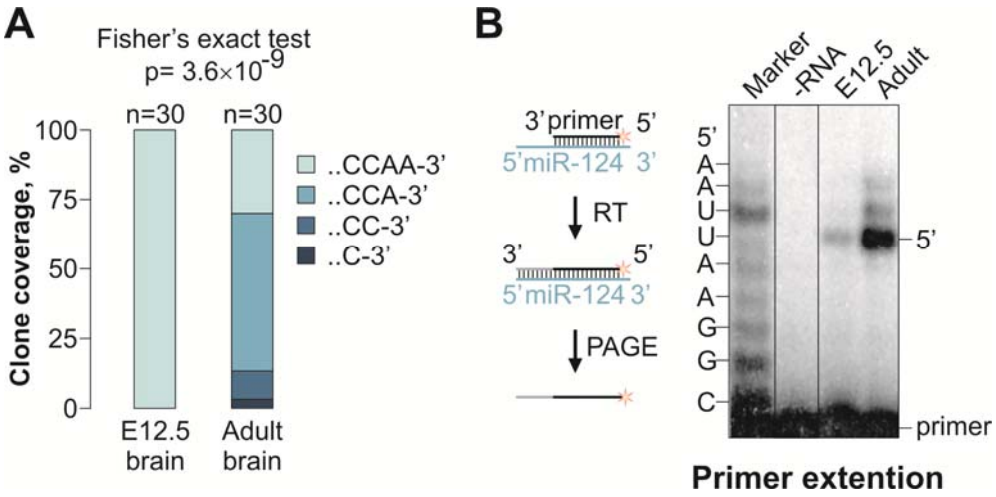

Figure 3.11: The miR-124, 3' end is shortened during nervous system development. (**A**) Extensive shortening of the miR-124, 3' end in the adult mouse brain. The graph shows a summary of 3'-terminal sequences of mature miR-124 determined for 30 miR-124-specific LM-RT-PCR clones from the E12.5 and the adult samples. (**B**) Primer extension assay demonstrates that miR-124 species have relatively uniform 5' termini in both the E12.5 and adult brain. The stronger extension signal in the adult sample correlates with a higher abundance of the mature miR-124 at this stage.

3.4.2 *Deep sequencing uncovered a large fraction of small RNAs that undergo trimming during the nervous system development*

To find out if the 3' ends of other miRNAs are shortened during brain development, we analyzed a small RNA fraction from E12.5 and adult mouse brain by deep sequencing and focused on 193 miRNAs that were detectably expressed in both samples (>100 reads), could be unambiguously distinguished from other miRNAs, and had no non-templated nucleotides at the 3' end. Notably, the empirical cumulative distribution functions (ECDFs) of the overall miRNA length distributions in the two samples differed significantly ($p=7.9\times10^{-6}$, KS test), with the adult miRNAs being shorter than the E12.5 ones (Figure 3.12A). This conclusion was further supported by pair-wise comparisons of the average lengths of specific miRNAs in the adult and E12.5 samples (Figure 3.12B; $p=1.76\times10^{-29}$, Wilcoxon signed rank test; also see Tables 3.1 and 3.2). The differences in the miRNA lengths were clearly due to shortening of the 3' but not the 5' end in the adult sample (Figure 3.12C-D). Notably, Northern blot analyses of select miRNAs confirmed our deep sequencing data (Figure 3.12E-H).

Figure 3.12: Widespread shortening of the miRNA 3' ends during brain development. Statistical analyses of deep sequencing data for 193 miRNAs expressed in the E12.5 and the adult mouse brain and containing no non-templated nucleotides. (**A**) The overall length distribution of miRNAs expressed in the adult brain is shifted towards shorter species as compared to E12.5. (**B**) Average lengths of specific miRNAs tend to decrease in the adult brain as compared to E12.5. (**C**) The miRNA 5' end coordinates do not differ significantly between the two brain samples. (**D**) The 3' end coordinates of the adult miRNAs are diminished significantly as compared to E12.5. **(E-H)** Validation of deep sequencing data by northern blot analysis of a few miRNAs. Select miRNAs from E12.5 (embryonic; E), P0 (newborn; N); and P60 (adult; A) mouse brains were analyzed by Northern blotting. (**E**) miRNAs predicted to be significantly shortened during mouse brain development. (**F**) miRNAs predicted to have relatively stable length during mouse brain development. (**G-H**) Lane density profiles for (E-F), respectively. Developmentally shortened miRNA species are marked by red arrowheads.

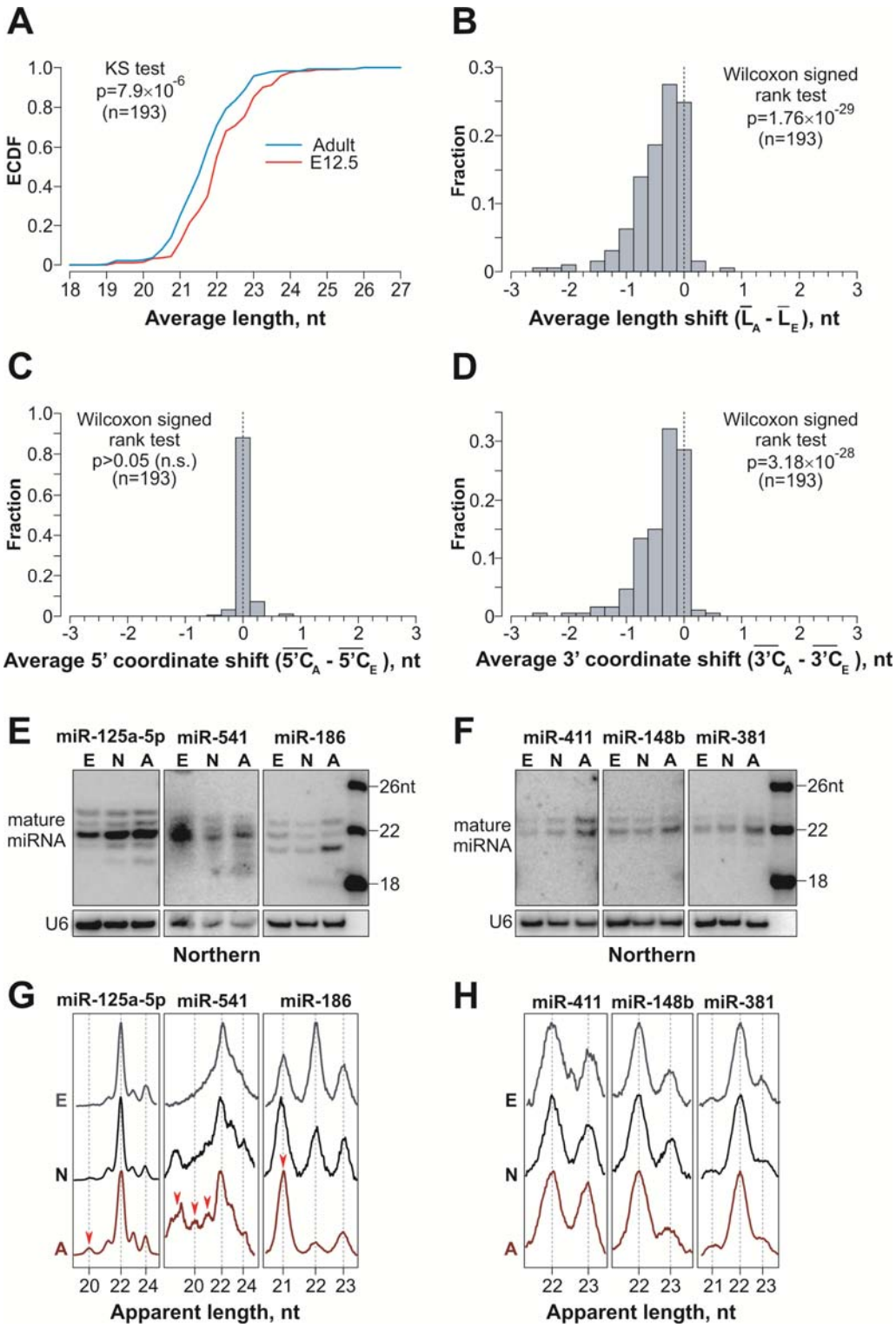
A
KS test
p=7.9×10-6
(n=193)
Adult
E12.5
ECDF
Average length, nt
B
Wilcoxon signed
rank test
p=1.76×10-29
(n=193)
Fraction
Average length shift (L̄A - L̄E), nt
C
Wilcoxon signed
rank test
p>0.05 (n.s.)
(n=193)
Fraction
Average 5' coordinate shift (5'C̄A - 5'C̄E), nt
D
Wilcoxon signed
rank test
p=3.18×10-28
(n=193)
Fraction
Average 3' coordinate shift (3'C̄A - 3'C̄E), nt
E
miR-125a-5p miR-541 miR-186
E N A E N A E N A
mature
miRNA
U6
26nt
22
18
Northern
F
miR-411 miR-148b miR-381
E N A E N A E N A
mature
miRNA
U6
26nt
22
18
Northern
G
miR-125a-5p miR-541 miR-186
E
N
A
Apparent length, nt
H
miR-411 miR-148b miR-381
E
N
A
Apparent length, nt

Table 3.1: Top fifty miRNAs significantly shortened in the adult brain.

miRNA name	Length difference, nt	KS test, D statistic	KS test, p value
mmu-miR-409-5p	-2.5372	0.8003	<2.20E-16
mmu-miR-330*	-1.9902	0.5908	<2.20E-16
mmu-miR-3068	-1.8678	0.9514	<2.20E-16
mmu-miR-598	-1.5090	0.4348	<2.20E-16
mmu-miR-181c	-1.5002	0.5773	<2.20E-16
mmu-miR-139-3p	-1.4001	0.5962	<2.20E-16
mmu-miR-24	-1.2757	0.4474	<2.20E-16
mmu-miR-708*	-1.2492	0.4655	<2.20E-16
mmu-miR-190	-1.1455	0.4662	1.30E-14
mmu-miR-191	-1.0865	0.4234	<2.20E-16
mmu-miR-330	-1.0566	0.4195	<2.20E-16
mmu-miR-181a	-1.0555	0.4542	<2.20E-16
mmu-miR-33	-1.0092	0.9259	<2.20E-16
mmu-miR-125a-5p	-0.9706	0.5371	<2.20E-16
mmu-miR-3057-5p	-0.9465	0.2417	1.65E-13
mmu-miR-181b	-0.9460	0.4312	<2.20E-16
mmu-miR-195	-0.9316	0.4986	<2.20E-16
mmu-miR-192	-0.8823	0.442	<2.20E-16
mmu-miR-1224	-0.8542	0.2597	<2.20E-16
mmu-miR-3099	-0.8390	0.2878	<2.20E-16
mmu-miR-30e	-0.8228	0.2008	<2.20E-16
mmu-miR-666-5p	-0.8123	0.364	<2.20E-16
mmu-miR-26a	-0.7971	0.4004	<2.20E-16
mmu-miR-27b*	-0.7776	0.3361	2.30E-13
mmu-miR-541	-0.7720	0.2596	<2.20E-16
mmu-miR-200b	-0.7705	0.5246	<2.20E-16
mmu-miR-186	-0.7621	0.3026	<2.20E-16
mmu-miR-669c	-0.7146	0.3223	<2.20E-16
mmu-miR-383	-0.7000	0.4619	<2.20E-16
mmu-miR-181d	-0.6940	0.3133	<2.20E-16
mmu-miR-338-5p	-0.6884	0.3152	<2.20E-16
mmu-miR-21	-0.6821	0.4079	<2.20E-16
mmu-miR-16	-0.6814	0.3811	<2.20E-16
mmu-miR-342-5p	-0.6796	0.2333	<2.20E-16
mmu-miR-124	-0.6721	0.2435	<2.20E-16
mmu-miR-218	-0.6672	0.4288	<2.20E-16
mmu-miR-184	-0.6529	0.3686	<2.20E-16
mmu-miR-877	-0.6457	0.2518	<2.20E-16
mmu-miR-130a	-0.6451	0.3201	<2.20E-16
mmu-miR-153	-0.6397	0.2432	<2.20E-16
mmu-miR-30c-2*	-0.6364	0.3203	<2.20E-16
mmu-miR-30a	-0.6310	0.1765	<2.20E-16
mmu-miR-7b	-0.6260	0.3904	<2.20E-16
mmu-miR-433	-0.6254	0.2498	<2.20E-16
mmu-miR-376a*	-0.6208	0.4934	<2.20E-16

mmu-miR-708	-0.5965	0.3629	<2.20E-16
mmu-miR-204	-0.5770	0.2974	2.30E-06
mmu-miR-30b*	-0.5751	0.5233	<2.20E-16
mmu-miR-7a	-0.5736	0.3404	<2.20E-16
mmu-miR-22	-0.5582	0.2252	1.35E-11

Length difference is calculated by subtracting the average miRNA length in the E12.5 sample from that in the adult sample. miRNAs analyzed by Northern blotting (Figure 3.12 E) are shown in bold.

Shifts in the miRNA 3'-terminal coordinates are calculated by subtracting the average E12.5 3' coordinates from the corresponding average adult 3' coordinates. miRNAs trimmed more efficiently than their pre-mRNA "siblings" (and by ≥0.5 nt) are shown on the left (pre-miRNA product 1). Statistical analysis of the data shows that trimming of pre-miRNA products 2 does not correlate significantly with trimming of the corresponding pre-miRNA products 1 (Spearman's correlation coefficient ρ=0.26; p value 0.16).

Table 3.2: miRNAs showing no significant length changes.

miRNA name	Length difference, nt	KS test, D statistic	KS test, p value
mmu-miR-217	-0.1768	0.0742	0.1557
mmu-miR-384-3p	-0.1585	0.0707	0.2633
mmu-miR-323-5p	-0.1313	0.1313	0.06435
mmu-miR-672	-0.1223	0.0613	0.1363
mmu-miR-328	-0.1035	0.0841	0.1766
mmu-miR-337-5p	-0.0780	0.0548	0.8786
mmu-miR-322*	-0.0533	0.0655	0.7105
mmu-miR-138-1*	-0.0480	0.048	0.9927
mmu-miR-376a	-0.0462	0.0515	0.4361
mmu-miR-652	-0.0279	0.0279	0.8938
mmu-miR-376c	-0.0273	0.0563	0.8999
mmu-miR-380-3p	-0.0271	0.0337	0.9745
mmu-miR-381	-0.0256	0.0165	0.2187
mmu-miR-410	-0.0252	0.0171	0.9795
mmu-miR-129-5p	-0.0213	0.0128	0.989
mmu-miR-28*	-0.0209	0.0224	0.7593
mmu-miR-344	-0.0108	0.0054	1
mmu-miR-423-3p	-0.0091	0.0222	1
mmu-miR-148b	-0.0080	0.0045	0.9952
mmu-miR-135b	-0.0068	0.0522	0.9443
mmu-miR-20a	-0.0067	0.0249	0.9913
mmu-miR-135a-2*	-0.0065	0.0881	0.1439
mmu-miR-17	-0.0040	0.0263	0.9967
mmu-miR-34c	-0.0030	0.0025	1
mmu-miR-151-3p	0.0000	0	1
mmu-miR-344d	0.0000	0	1
mmu-miR-541*	0.0000	0	1
mmu-miR-544-5p	0.0000	0	1
mmu-miR-92b	0.0008	0.0131	1
mmu-miR-185	0.0067	0.0067	1
mmu-miR-132	0.0129	0.0302	0.9872
mmu-miR-361	0.0308	0.035	1
mmu-miR-135a-1*	0.0380	0.0397	0.9863
mmu-miR-495	0.0386	0.0386	0.9996
mmu-miR-411*	0.0395	0.0282	0.9992
mmu-miR-362-5p	0.0418	0.0209	1
mmu-miR-496	0.1103	0.1103	0.3775
mmu-miR-335-3p	0.1395	0.0793	0.3252

Length difference is calculated by subtracting the average miRNA length in the E12.5 sample from that in the adult sample. miRNAs analyzed by Northern blotting (Figure 3.12 F) are shown in bold.

Also from a closure look at the deep sequencing data we failed to detect a significant correlation between the trimming efficiencies of mature miRNA "siblings" encoded by the same pre-miRNA in our deep sequencing data (Table 3.3), which is consistent with the model that trimming occurs after the two strands of the precursor miRNA duplex are physically separated.

Table 3.3: Lack of correlation between trimming efficiencies of miRNA pairs produced from the same pre-miRNA precursor

pre-miRNA product 1		pre-miRNA product 2	
miRNA name	**3' coordinate shift, nt**	**miRNA name**	**3' coordinate shift, nt**
mmu-miR-409-5p	-2.537173542	mmu-miR-409-3p	0.105862688
mmu-miR-181b-1*	-2	mmu-miR-181b	-0.94603856
mmu-miR-330*	-1.990232417	mmu-miR-330	-1.056629669
mmu-miR-3068	-1.867808782	mmu-miR-3068*	-0.603754693
mmu-miR-425*	-1.563636364	mmu-miR-425	-0.445631914
mmu-miR-106b*	-1.471512605	mmu-miR-106b	-0.211418035
mmu-miR-139-3p	-1.400130325	mmu-miR-139-5p	-0.284182244
mmu-miR-24	-1.275713312	mmu-miR-24-2*	-0.284615385
mmu-miR-503	-1.27540107	mmu-miR-503*	0
mmu-miR-708*	-1.249244461	mmu-miR-708	-0.596548969
mmu-miR-338-3p	-1.091041515	mmu-miR-338-5p	-0.68835768
mmu-miR-181a	-1.055543879	mmu-miR-181a-2*	0
mmu-miR-125a-5p	-0.970607359	mmu-miR-125a-3p	-0.397138796
mmu-miR-674*	-0.956349206	mmu-miR-674	0.015642841
mmu-miR-541	-0.771993754	mmu-miR-541*	0
mmu-miR-200b	-0.770462089	mmu-miR-200b*	-0.380002236
mmu-miR-329*	-0.687773429	mmu-miR-329	-0.5
mmu-miR-1839-3p	-0.684210526	mmu-miR-1839-5p	-0.157961632
mmu-miR-16	-0.681358991	mmu-miR-16-1*	-0.437229437
mmu-miR-342-5p	-0.679644855	mmu-miR-342-3p	-0.472350731
mmu-miR-325*	-0.675925926	mmu-miR-325	-0.29468599
mmu-miR-124	-0.67206246	mmu-miR-124*	-0.612998648
mmu-miR-218	-0.667239435	mmu-miR-218-2*	-0.315789474
mmu-miR-99b*	-0.653927929	mmu-miR-99b	-0.398142946
mmu-miR-433	-0.625448417	mmu-miR-433*	0
mmu-miR-376a*	-0.620797362	mmu-miR-376a	-0.046211993
mmu-miR-204	-0.577044952	mmu-miR-204*	-0.341059603
mmu-miR-219-5p	-0.571428571	mmu-miR-219-3p	0
mmu-miR-380-5p	-0.516646589	mmu-miR-380-3p	-0.027065527
mmu-miR-676	-0.505933907	mmu-miR-676*	0

To ensure that the above result was not due to a sample preparation artifact, we repeated the statistical analyses with 80 unambiguous miRNAs that were detectably expressed in both the E12.5 and adult samples (>100 reads) and contained 1-3 non-templated nucleotides at their 3' ends (Figure 3.13). These modified miRNA isoforms represented ~10% of the total reads in both samples and the non-templated extensions consisted predominantly of A's and U's (Figure 3.13A), as described earlier (Landgraf *et al*., 2007; Morin *et al*., 2008; Wyman *et al*., 2011). Importantly, when we computationally clipped the non-templated extensions and analyzed the lengths and the 5' and 3' coordinates of the remaining genome-encoded "stumps", a large-scale 3'-terminal trimming was again detected for the adult miRNAs (Figure 3.13B-D). We concluded that the miRNA 3' ends receded in the adult brain but the probability of their subsequent extension by terminal transferases was comparable between the E12.5 and the adult samples.

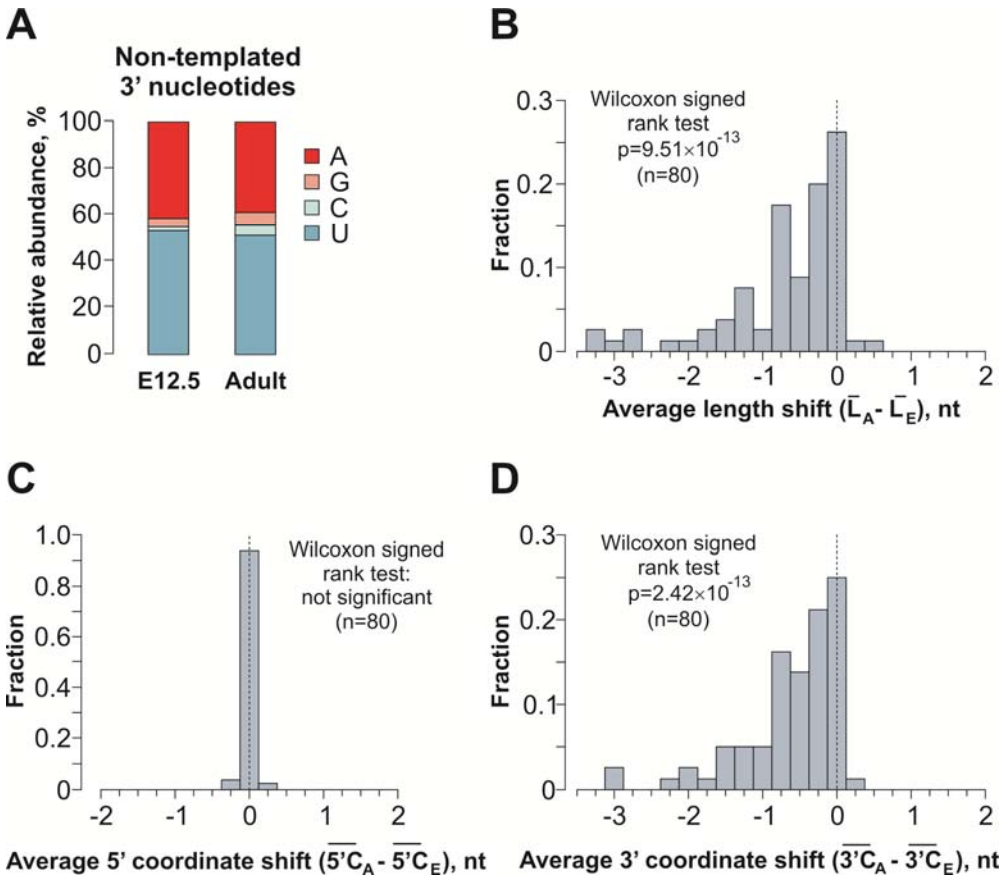

Figure 3.13: Statistical analyses of the deep sequencing reads corresponding to miRNAs with 3'-terminal non-templated extensions. (**A**) The nucleotide composition of the 3'-terminal non-templated extensions in the E12.5 and adult brain miRNAs. (**B**) Average lengths of the genome-encoded "stumps" in 3'-modified miRNAs tend to decrease in the adult brain as compared to E12.5. (**C**) The distributions of the miRNA 5' end coordinates in 3'-modified miRNAs do not differ significantly between the two brain samples. (**D**) The 3' ends of the genome-encoded "stumps" tend to recede in the adult as compared to the E12.5 sample.

3.4.3 *miRNA trimming efficiency depends on the nature of the 3'-terminal nucleotide*

We then returned to the 193 miRNAs devoid of the non-templated extensions and analyzed their 3'-terminal nucleotide usage. All four nucleotides occurred fairly randomly at the 3' ends of the E12.5 miRNAs (Figure 3.14A). However, the 3' termini of the adult miRNAs were noticeably depleted in A's and enriched in U's (Figure 3.14A; $p<2.2\times10^{-16}$, χ^2 test).

To test whether the corresponding nucleotide preferences of the trimming reaction could explain this bias, we prepared a set of miR-124 constructs encoding all four nucleotides at the 3'-terminal position of the mature 22-mer and analyzed the trimming behavior of the corresponding miRNAs in the HEK293T cells after 3 days of transfection (Figure 3.14B-D). Notably, the A3'-terminated (wild type) miR-124 was trimmed most efficiently and the U3' miR-124 was trimmed least efficiently ($p=4.3\times10^{-3}$; ANOVA test; Figure 3.14C-D).

Similar result was observed when the above set of miR-124 constructs encoding all four nucleotides at the 3'-terminal position of the mature 22-mer were expressed from a Dox repressible promoter in HEK293T cells (Figure 3.14E-F). The transcription was stopped by addition of Dox 24 hours post transfection and trimming efficiency of residual miRNA was followed for the successive 3 days in a time course experiment. The result was consistent to the above in which the A3'-terminated (wild type) miR-124 was trimmed most efficiently and the U3' miR-124 was trimmed least efficiently (Figure 3.14E-F).

Figure 3.14: Effect of the 3'-terminal nucleotide identity on miRNA trimming
(**A**) The usage of the 3'-terminal genome-encoded nucleotides is relatively uniform in the E12.5 miRNAs, whereas is becomes significantly depleted in A's and enriched in U's in the adult sample. (**B**) Diagram of the miR-124 expression constructs genetically modified to introduce all 4 nucleotides (arrowheads) at the 3'-terminal position of the mature miRNA (colored sequence). (**C**) To determine their precise lengths, the 3' terminal miR-124 mutants were expressed in HEK293T cells for 72 hours from a constitutive promoter (CMV) and analyzed by Northern blotting alongside the corresponding synthetic 22-mer RNA markers. (**D**) Quantitation of the data from (C) showing, of the four miR-124 variants described in (B), A3' is trimmed most efficiently and U3' is trimmed least efficiently in the HEK293T cells. Data were averaged from 3 independent transfection experiments ±SD. (**E**) Pulse-chase experiment. HEK293T cells were transfected with Dox-repressible constructs encoding the four miR-124 3'-terminal variants and the miRNAs were allowed to be expressed for 24 hours. Dox was then added to the cultures (time point 0) and the miR-124 RNA was analyzed by Northern blotting at the indicated time points. In (E), mature miRNA lengths and the positions of the pre-miR-124 precursors (pre) are shown on the left. U6 is a loading control. (**F**) Quantification of the data in (E) demonstrating distinct trimming behaviours of the four miR-124 variants.

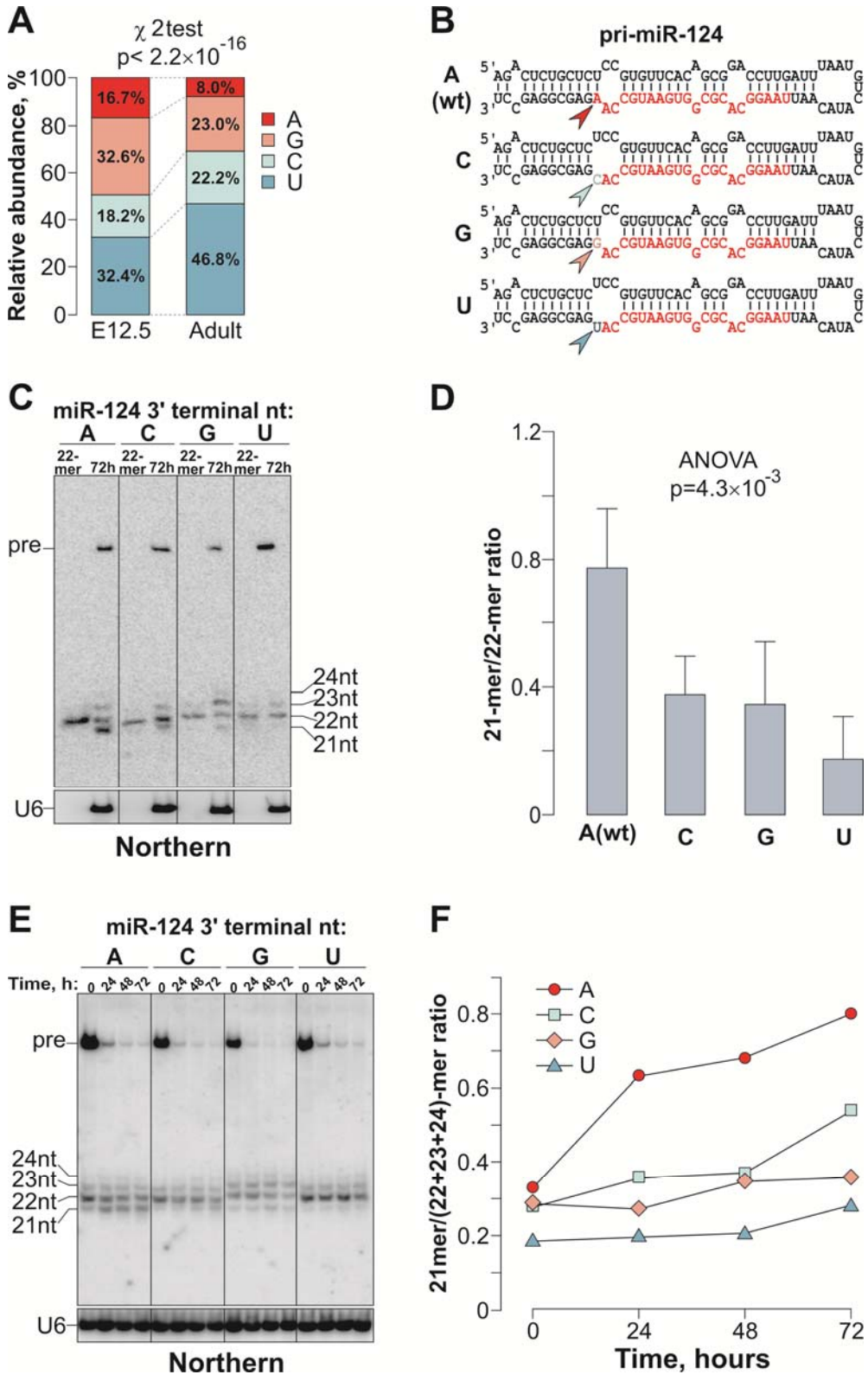
A
χ 2test
p< 2.2×10-16
Relative abundance, %
100
80
60
40
20
0
16.7%
32.6%
18.2%
32.4%
8.0%
23.0%
22.2%
46.8%
A
G
C
U
E12.5
Adult
B
pri-miR-124
A (wt)
C
G
U
C
miR-124 3' terminal nt:
A
C
G
U
22-mer
72h
pre
24nt
23nt
22nt
21nt
U6
Northern
D
ANOVA
p=4.3×10-3
21-mer/22-mer ratio
1.2
0.8
0.4
0
A(wt)
C
G
U
E
miR-124 3' terminal nt:
A
C
G
U
Time, h:
0
24
48
72
pre
24nt
23nt
22nt
21nt
U6
Northern
F
21mer/(22+23+24)-mer ratio
0.8
0.6
0.4
0.2
0
A
C
G
U
0
24
48
72
Time, hours

3.4.4 *miRNA trimming efficiency depends on the interacting Argonaute partner in addition to the nature of the 3'-terminal nucleotide*

Co-expression of the four 3'-terminal miR-124 variants with the 3xMyc-tagged Argonautes showed that AGO2-overexpressing cells trimmed A3' most efficiently and U3' least efficiently (Figure 3.15A-B), similar to the preferences of endogenous HEK293T Argonaute blend. Trimming of all four miR-124 variants was rather inefficient in the presence of over-expressed AGO1, AGO3 or AGO4 (Figure 3.15A-B). These results suggested that the nature of the 3'-terminal nucleotide modulates trimming of AGO2-loaded miRNAs.

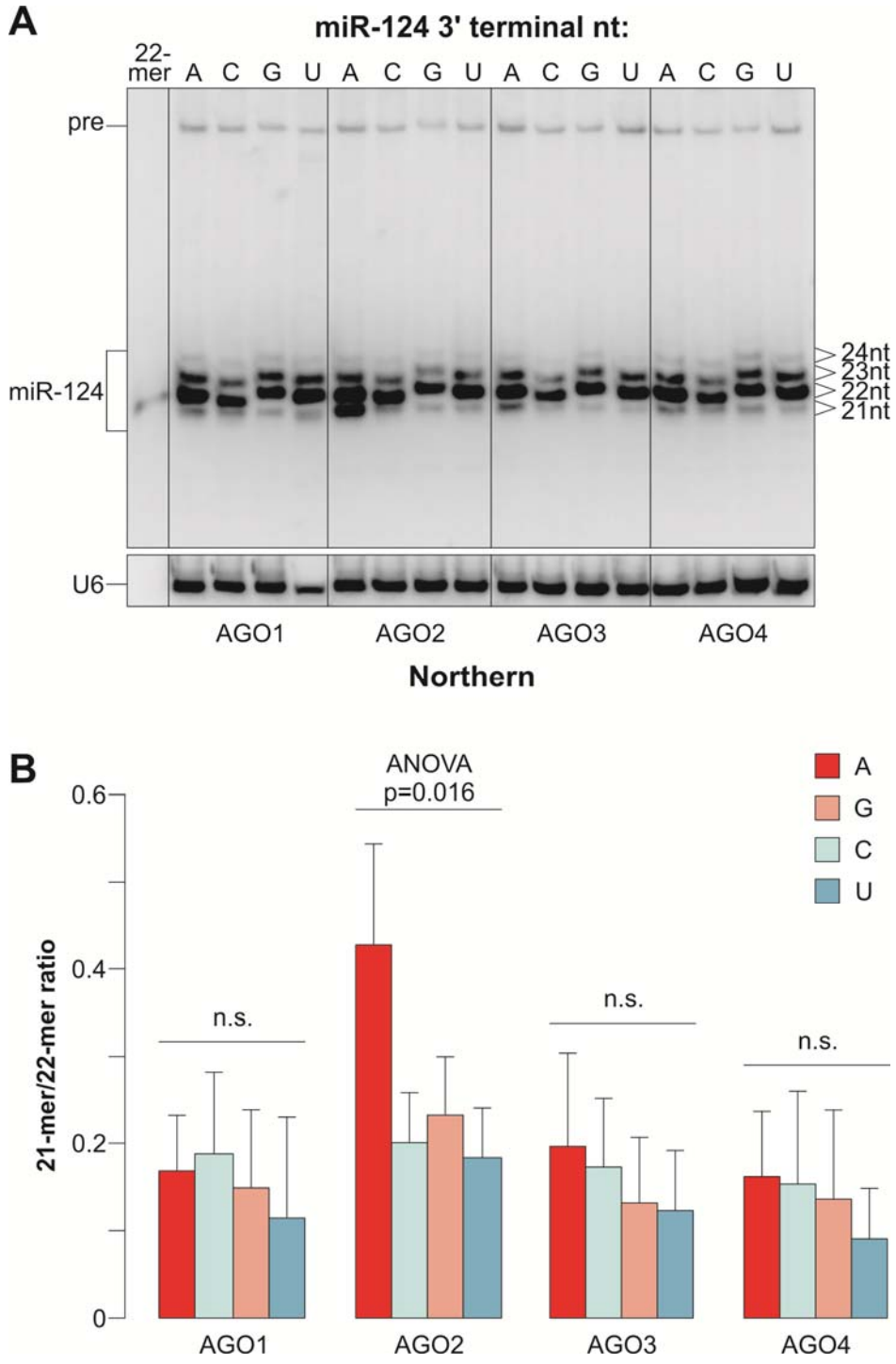

Figure 3.15: Trimming of miRNA is a coordinated mechanism of Argonaute selectivity and 3'-terminal nucleotide identity. (**A**) The four 3'-terminal miR-124 variants were co-expressed in HEK293T cells with the AGO1-4 and the trimming efficiency was analyzed by Northern blotting 48 hours post transfection. (**B**) Quantification of the data in (A) averaged from 3 independent transfection experiments ±SD.

3.5 Specific structural feature of the AGO2 PAZ domain enables efficient miRNA trimming

3.5.1 *PAZ domain interacts with 3' terminal of mature miRNA and plays an important role in trimming*

To elucidate the mechanism for the efficient shortening of AGO2-associated miRNAs, we aligned the amino acid (aa) sequences of human Argonautes and focused on the regions showing the highest divergence (Figure 3.16A). The least conserved element within the PAZ domain sequence corresponded to the AGO1, 300-319 aa segment known to fold into a partially α-helical loop interacting with the small RNA 3' end (Figure 3.16A) (Ma *et al*., 2004). The K313 and Y314 residues were of particular interest since they formed hydrogen bonds with the phosphate groups of the 3' penultimate and ultimate nucleoside monophosphates, respectively (Figure 3.16B). Notably, the KY motif was conserved in AGO1, AGO3 and AGO4 across tetrapod vertebrates, but it was substituted with RH in AGO2 (Figure 3.16A and Figure 3.17).

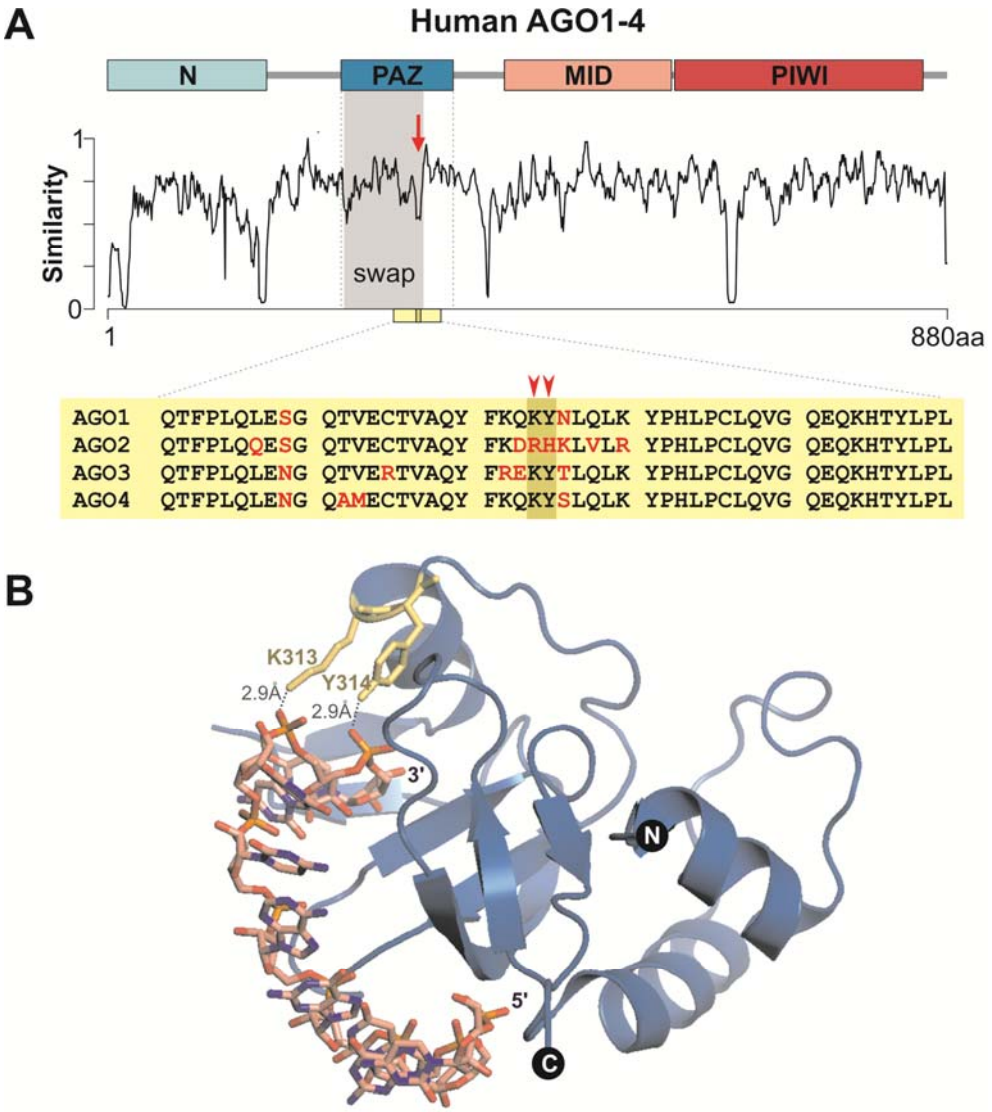

Figure 3.16: Structure of the Argonaute PAZ domain modulates miRNA trimming efficiency. (**A**) Human Argonaute sequence similarity plot. The diagram on the top indicates the positions of the N, PAZ, MID and PIWI domains. The divergent sequence element within the PAZ domain is indicated by the arrow and the sequence swapped between AGO1 and AGO2 in (Figure 3.18, A-C) is highlighted in gray. A fragment of the PAZ sequence alignment is presented at the bottom with non-conserved aa residues shown in red. The position of the AGO1 K313 and Y314 residues is marked by the arrowheads. (**B**) Crystal structure of the AGO1 PAZ domain associated with a small RNA [1SI3; (Ma *et al*., 2004)] showing hydrogen bonds between the K313 and Y314 side chains and the 3' penultimate and ultimate nucleoside triphosphates.

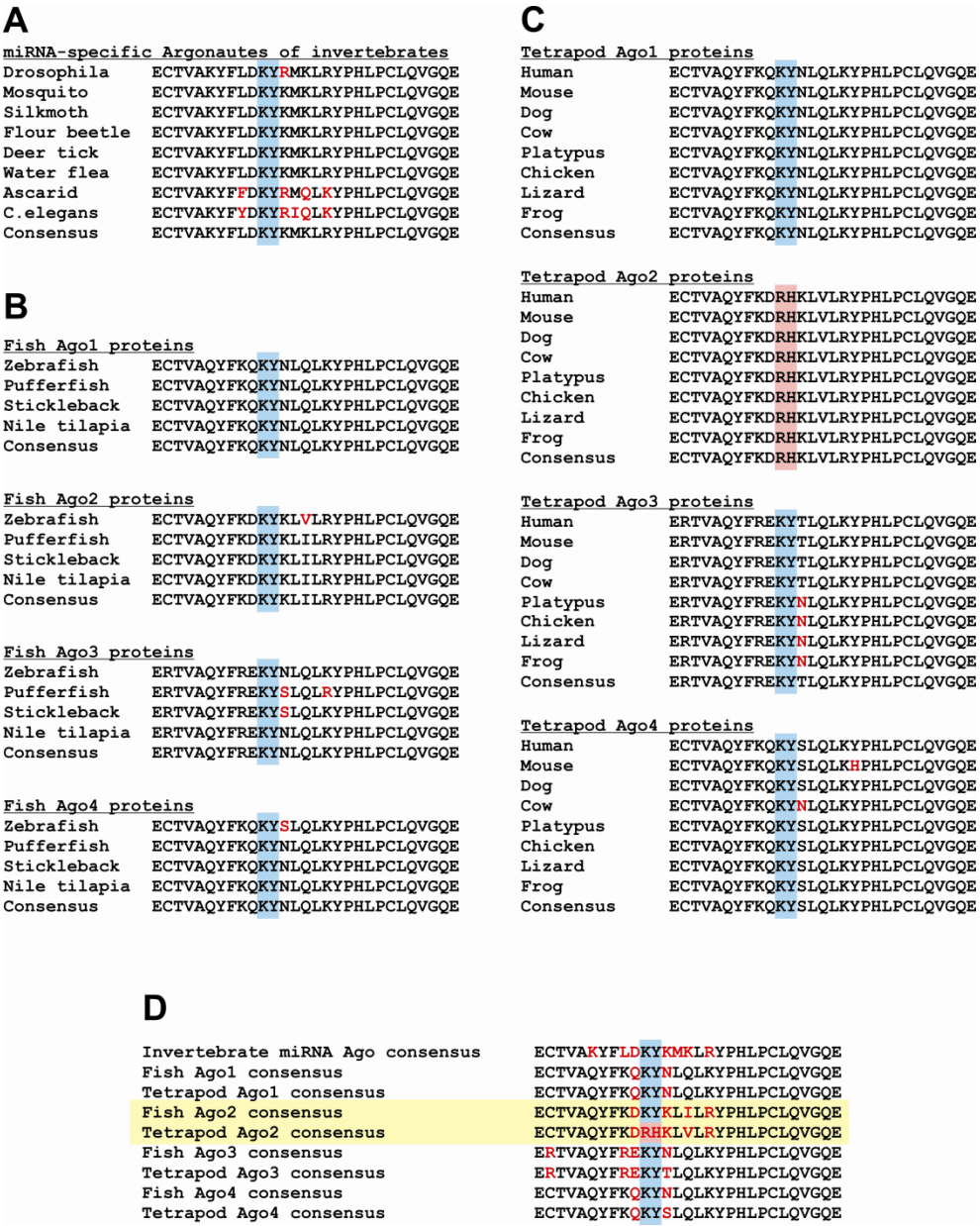

Figure 3.17: Phylogenetic analysis of the miRNA 3' end-binding surface of the metazoan Argonaute PAZ domains. (**A**) Alignment of the putative 3' end-binding segments for miRNA-specific Argonautes of *Drosophila melanogaster* (Ago1) and *Caenorhabditis elegans* (Alg-1), as well as their orthologs from other invertebrates: *Aedes aegypti*, *Bombyx mori*, *Tribolium castaneum*, *Ixodes scapularis*, *Daphnia pulex* and *Ascaris suum*. Similar alignments were generated for (**B**) the Ago1-Ago4 protein families of fishes (*Danio rerio*, *Tetraodon nigroviridis*, *Gasterosteus aculeatus* and *Oreochromis niloticus*) and (**C**) tetrapod vertebrates (*Homo sapiens*, *Mus musculus*, *Canis lupus familiaris*, *Bos taurus*, *Ornithorhynchus anatinus*, *Gallus gallus*, *Anolis carolinensis*, and *Xenopus tropicalis*). (**D**) Alignment of the consensus sequences from (A-C) suggesting that the Ago2-specific RH motif might have diverged from the original KY motif following the expansion of the Ago1-Ago4 paralogs in the vertebrates in an ancestral tetrapod species (compare the fish and the tetrapod Ago2 consensuses). In all panels, non-conserved residues are shown in red and the KY and RH motifs is highlighted in blue and pink, respectively.

3.5.2 *Mature miR-124 trimming is correlated to the PAZ domain of Argonaute*

To address the role of the PAZ domain in the miRNA trimming, we generated reciprocal swap mutants of AGO1 and AGO2 that contained heterologous PAZ domain segments comprising the KY/RH motif (see Figure 3.18A). The engineered AGO1(AGO2 PAZ) and AGO2(AGO1 PAZ) proteins were expressed in HEK293T cells at levels similar to their wild-type counterparts (Figure 3.18A). Strikingly, miR-124 was trimmed more efficiently in the presence of AGO1(AGO2 PAZ) as compared to the wild-type AGO1 protein (Figure 3.18B-C). On the other hand, trimming of AGO2-loaded miR-124 was suppressed by grafting the AGO1 PAZ domain (Figure 3.18B-C).

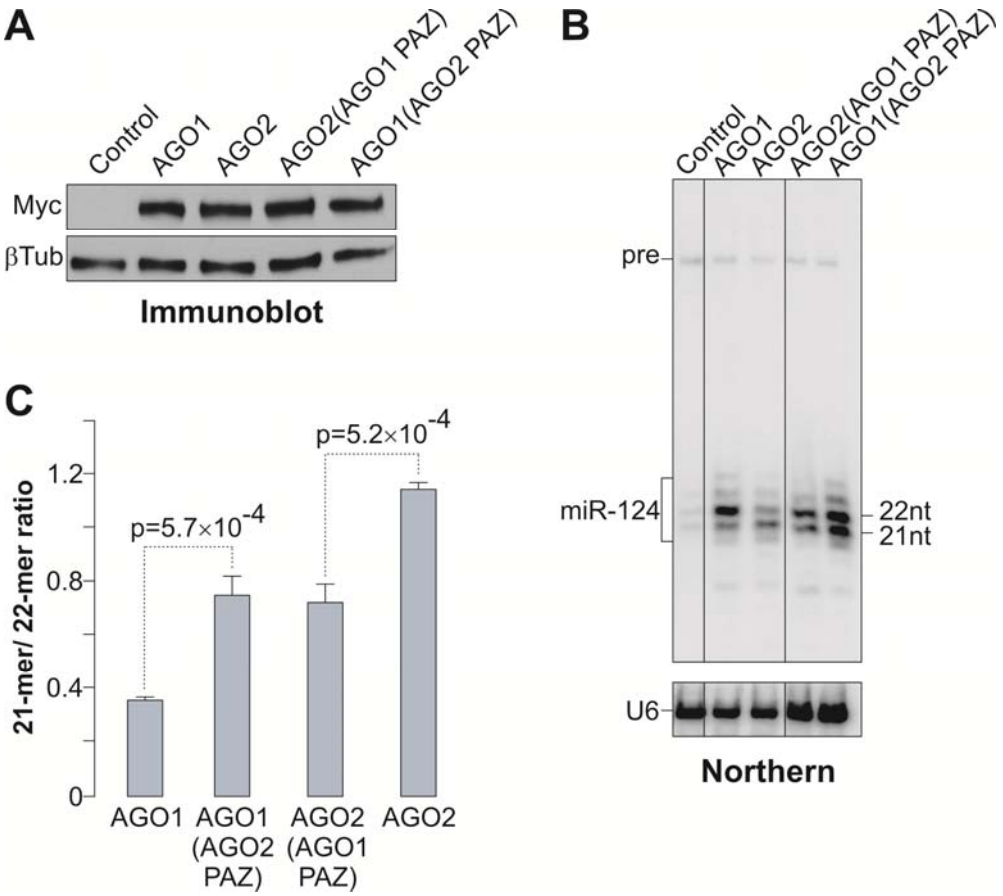

Figure 3.18: PAZ domain affects trimming of mature miRNA. (**A**) Immunoblot analyses showing comparable expression of the wild type AGO1, AGO2 and their reciprocal PAZ domain-swapped mutants. (**B**) Northern blot analyses of miR-124 co-expressed with the corresponding Argonaute proteins (A) in HEK293T cells. Cells were harvested at (B) 72 hours post transfection. (**C**) Quantification of the data in (B) showing the effect of the PAZ domain structure on the miRNA trimming efficiency. Data were averaged from 3 independent transfection experiments ±SD and compared using the t test.

3.5.3 *RH amino acid residues in the PAZ domain play a key role in trimming of AGO2 bound miRNAs*

We hypothesized that the KY residues might stabilize the 3' end of AGO1-, AGO3- and AGO4-bound miRNAs within the PAZ domain and restrict its availability to the yet-to-be identified mammalian miRNA trimming enzyme(s). To test this prediction, we mutated the RH element in AGO2 to KY and co-expressed the mutant protein with miR-124 in HEK293T cells (Figure 3.19A). Satisfyingly, the RH>KY mutation significantly suppressed the trimming of AGO2-loaded miR-124 (Figure 3.19B-C).

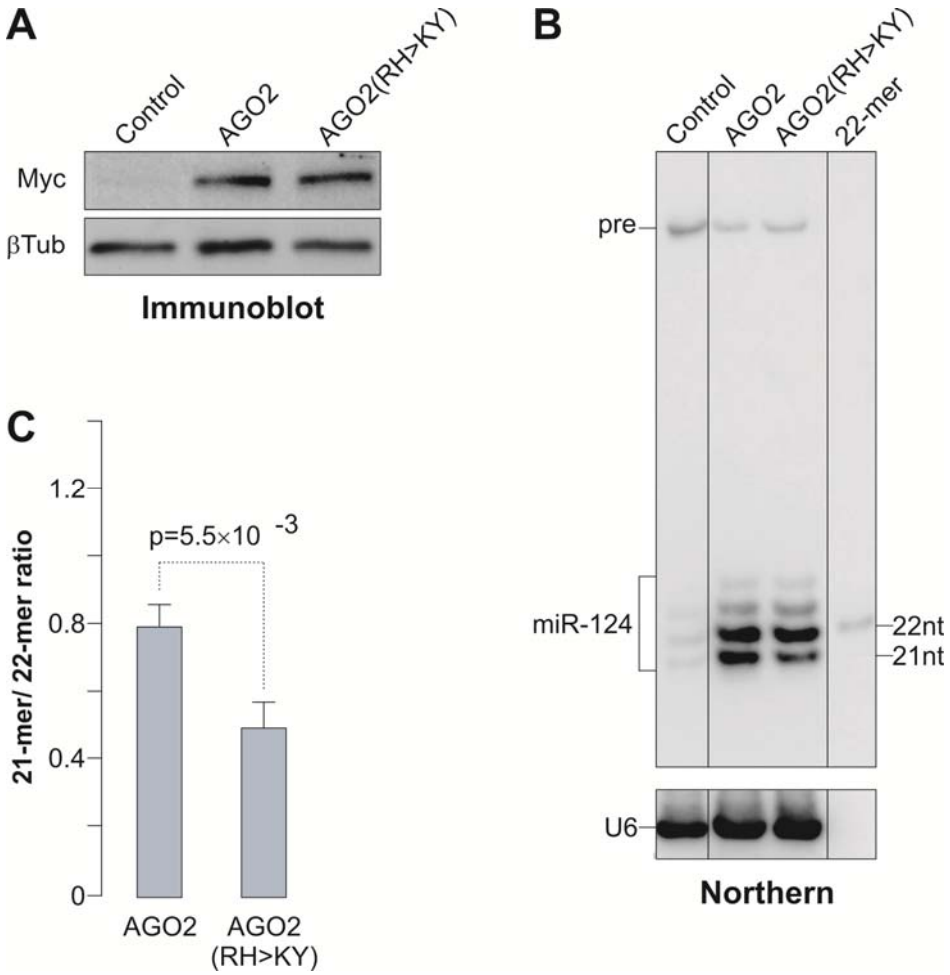

Figure 3.19: RH residues of AGO2 PAZ domain affects trimming of mature miRNA. (**A**) Immunoblot analyses showing comparable expression of the wild type AGO2 and AGO2 (RH>KY) mutant. (**B**) Northern blot analyses of miR-124 co-expressed with the corresponding Argonaute proteins (A) in HEK293T cells. Cells were harvested at (B) 72 hours post transfection. (**C**) Quantification of the data in (B) showing the effect of the PAZ domain structure on the miRNA trimming efficiency. Data were averaged from 3 independent transfection experiments ±SD and compared using the t test.

3.5.4 *KY amino acid residues in the PAZ of AGO1 protects the 3' end of mature miRNA from trimming*

Since KY residues of AGO1 PAZ domain seem to stabilize the 3' end residues in mature miRNA we assumed a reciprocal mutant KY>RH mutant of AGO1 would stimulate the trimming of miR-124. Surprisingly the reciprocal KY>RH mutant of AGO1 stimulated miR-124 trimming (Figure 3.20A-C).

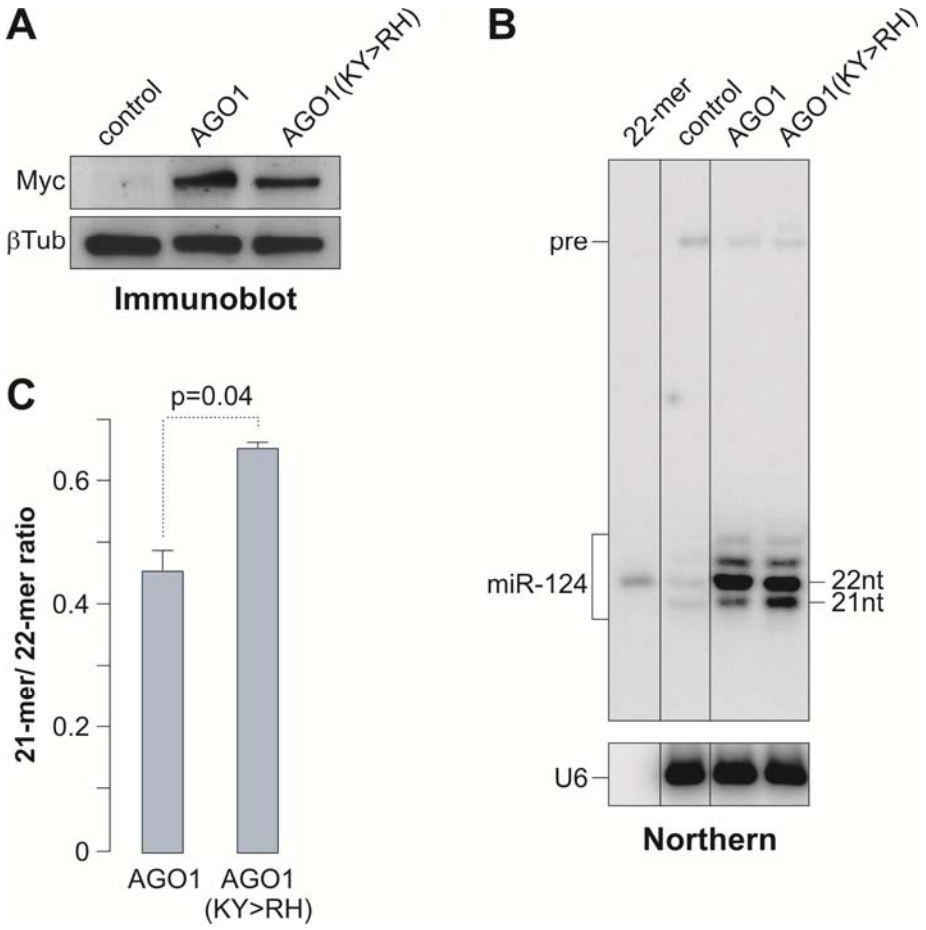

Figure 3.20: KY residues of AGO1 PAZ domain stimulates trimming of mature miRNA. (**A**) Immunoblot analyses showing comparable expression of the wild type AGO1 and AGO1 (KY>RH) mutant. (**B**) Northern blot analyses of miR-124 co-expressed with the corresponding Argonaute proteins (A) in HEK293T cells. Cells were harvested at (B) 72 hours post transfection. (**C**) Quantification of the data in (B) showing the effect of the PAZ domain structure on the miRNA trimming efficiency. Data were averaged from 3 independent transfection experiments ±SD and compared using the t test.

3.5.5 *Trimming is not affected by the slicer inactive mutant of AGO2*

The control mutation (D597A) inactivating the AGO2 slicer activity (Liu *et al*., 2004) had no effect on the miRNA trimming efficiency (Figure 3.21A-C). Therefore, the unusually high trimming propensity of AGO2-loaded miRNAs requires specific structural features of the AGO2 PAZ domain.

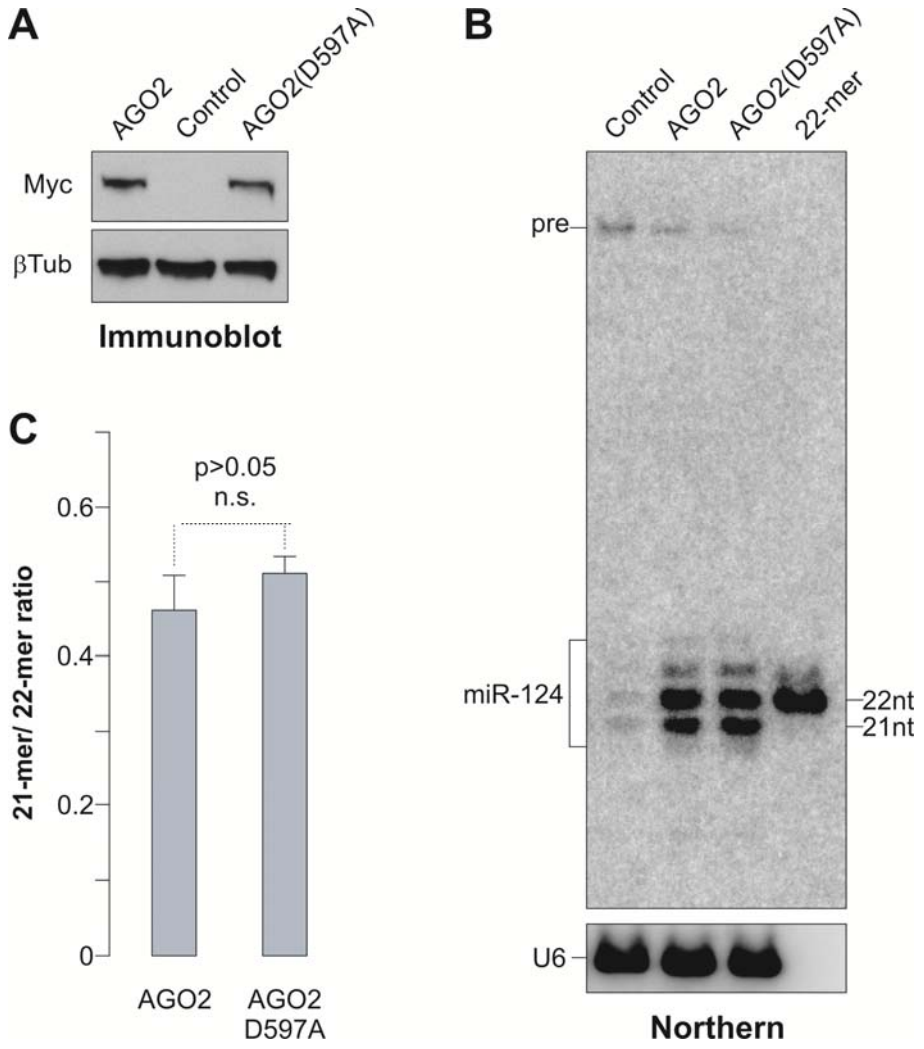

Figure 3.21: Trimming of AGO2-associated miRNA does not require the Slicer activity. (**A**) Immunoblot analysis showing that the wild-type AGO2 and the AGO2 (D597A) mutant proteins are expressed at comparable levels. β-tubulin is a loading control. (**B**) Northern blot analysis of miR-124 co-expressed with either wild-type or the D597A mutant of 3xMyc-AGO2 for 48 hours. U6 is a loading control. (**C**) Quantitation of (A) showing no significant difference in the miR-124 trimming between AGO2 and AGO2(D597A) (n.s. [not significant with $p>0.05$], t test). Data are averaged from 3 independent replicates ±SD.

3.6 AGO1-loaded miR-124 is more potent in inducing neuron-like differentiation of neuroblastoma cells than AGO2-loaded miR-124

3.6.1 *Generation of Neuro2a cell lines stably expressing Ago1 or 2 and shRNA for Ago2*

To address the role of dramatic decrease in the Ago1/Ago2 ratio during nervous system development, we took advantage of the high-efficiency and low-background recombination-mediated cassette exchange (HILO-RMCE) system (Khandelia *et al*., 2011). Using this approach we generated two recombinant populations of mouse Neuro2a (N2a) neuroblastoma cells expressing Dox-inducible cassettes with two intronic shRNAs against the endogenous Ago2 3'UTR followed by a transgenic open reading frame (ORF) of either Ago1 or Ago2 (Figure 3.22A). The sequences recognized by the Ago2-3'UTR-specific shRNAs were absent from the transgenic Ago2 sequence.

The Argonaute expression patterns in the two transgenic N2a populations changed dramatically upon Dox treatment (Figure 3.22B-C). Ago1 was over-expressed and Ago2 was down-regulated in the Ago1(shAgo2-3'UTR) cells, whereas the overall Ago2 levels increased in the Ago2(shAgo2-3'UTR) cells as compared to the control cell population expressing a Dox-inducible EGFP ORF and a firefly-specific shRNA [EGFP(shLuc)] (Figure 3.22B-C).

As expected, in a similar way to Adult mouse brain transiently transfected miR-124 was trimmed more efficiently in the Ago2(shAgo2-3'UTR) as compared to the Ago1(shAgo2-3'UTR) cells (Figure 3.23A-B).

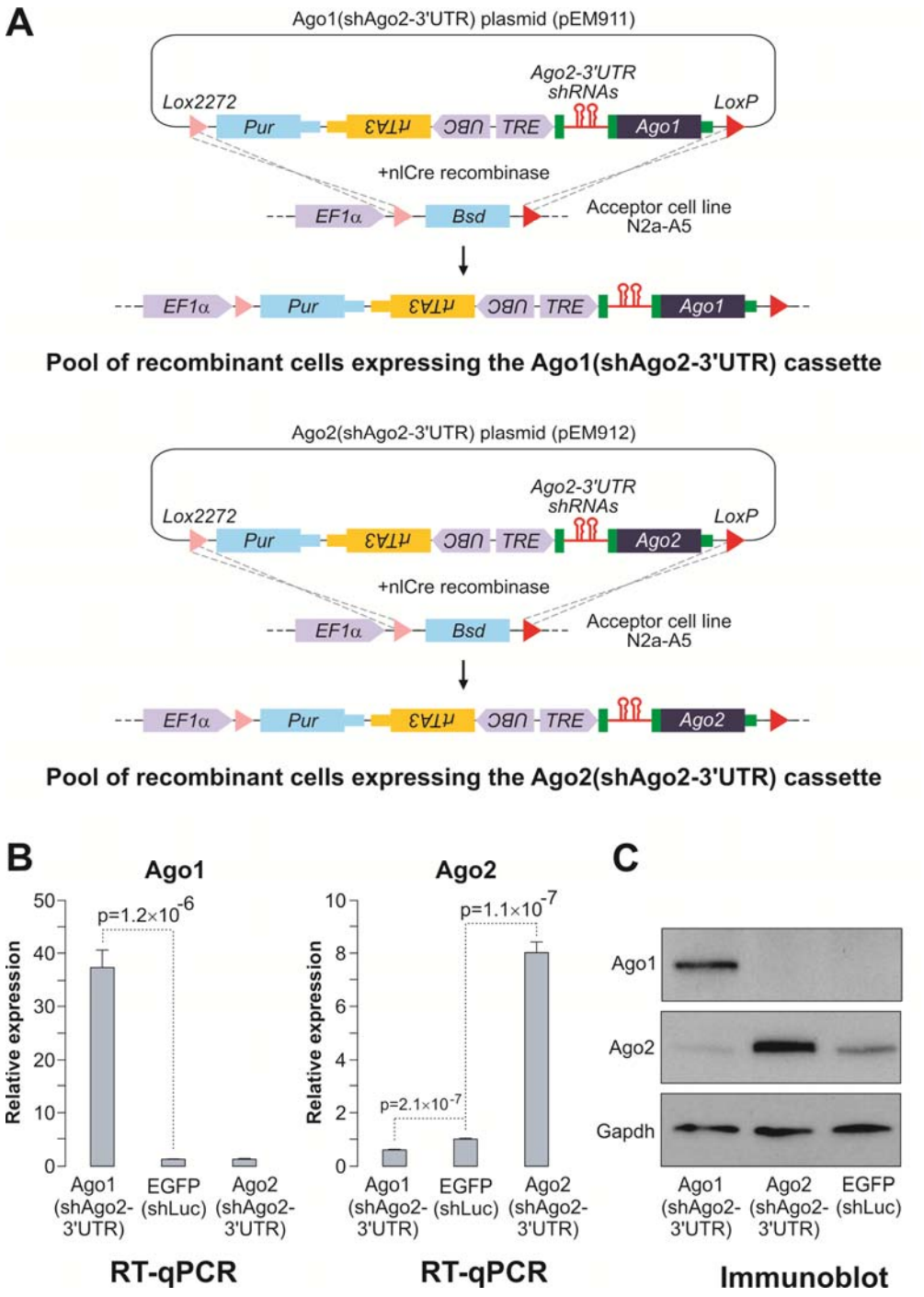

Figure 3.22: Molecular analyses of transgenic N2a cells. (**A**) Diagram of the HILO-RMCE procedure used to obtain pools of transgenic N2a cells expressing Dox-inducible Ago1(shAgo2-3'UTR) and Ago2(shAgo2-3'UTR) cassettes. (**B-C**) Transgenic N2a cells generated as described in (A) or cells containing a Dox-inducible EGFP(shLuc) control transgene were treated with Dox for 72 hours and the Ago1 and Ago2 expression was analyzed by (B) RT-qPCR or (C) immunoblotting. Data in (B) were averaged from 6 independent amplification experiments ±SD and compared using t test.

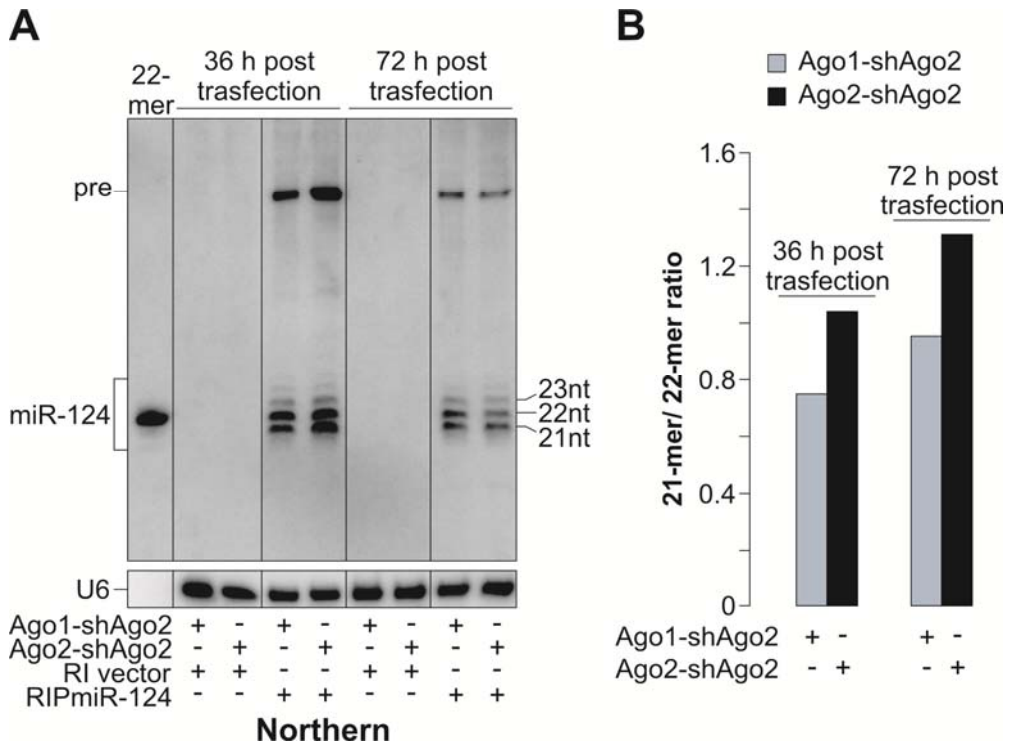

Figure 3.23: Trimming of miR-124 in transgenic N2a cells. (**A**) Argonaute expression patterns were reprogrammed in the Ago1(shAgo2-3'UTR) and Ago2(shAgo2-3'UTR) transgenic N2a populations by 72 hour Dox treatment, the cells were transfected with a constitutive miR-124 expression plasmid (RIPmiR-124) or the corresponding vector control (RI vector) and the miRNA expression was analyzed by Northern blotting at 36 and 72 hours post transfection. Positions of the mature miR-124 and its precursor (pre) are shown on the left. U6 is a loading control. (**B**) Quantification of the data from (A) showing that miR-124 is trimmed consistently better in Ago2-expressing cells as compared to Ago1-expressing cells.

3.6.2 *AGO1-loaded miR-124 potentially induces neuron-like differentiation in neuroblastoma cells*

Since miR-124 expression is known to induce neuron-like differentiation of N2a cells (Makeyev *et al*., 2007), we examined the efficiency of this process in the two Argonaute backgrounds from section 3.6.1. Strikingly, miR-124 expressed in the Dox-treated Ago1(shAgo2-3'UTR) cells was significantly more potent in inducing the neurite outgrowth phenotype as compared to miR-124 expressed in the Dox-treated Ago2(shAgo2-3'UTR) cells (Figure 3.24A-B). This effect was not due to an overall higher activity of miR-124 in the Ago1(shAgo2-3'UTR) cells since miR-124 repressed three of its previously published targets (Ptbp1, Vamp3 and Ctdsp1) equally well in both backgrounds (Figure 3.24C-D). We concluded that the Ago1- and Ago2-loaded miR-124 may have distinct biological activities in the context of mammalian brain development possibly through differential regulation of a subset of targets.

Figure 3.24: AGO1 stimulates miR-124-induced neuronal differentiation of neuroblastoma cells. (**A**) Ago1(shAgo2-3'UTR) and Ago2(shAgo2-3'UTR) cells pre-treated with Dox for 72 hours were transiently transfected with the miR-124 expression plasmid RIPmiR-124 additionally encoding the dsRed2 fluorescent marker or the corresponding control vector (RI vector) and the transfected cell morphology was examined 36 hours post transfection using dsRed2 fluorescence. Note that the expression of RIPmiR-124 leads to the appearance of a larger number of neuron-like cells containing long processes in the Ago1(shAgo2-3'UTR) cells as compared to the Ago2(shAgo2-3'UTR) cells. No differentiated cells are obvious in the RI vector-transfected cultures. (**B**) Quantification of the RIPmiR-124-induced morphological differentiation in Ago1(shAgo2-3'UTR), Ago2(shAgo2-3'UTR) and EGFP(shLuc) cells. Shown are fractions of cells containing at least one primary process longer than the average diameter of the cell soma. Ten randomly selected fields were imaged for each sample and the data were averaged ±SD and compared using the t test. (**C**) Cells were treated as in (A) except a firefly luciferase reporter containing the mouse Ptbp1 3'UTR was co-transfected with the RIPmiR-124 or the RI vector plasmids and the effect of miR-124 on the expression of the reporter gene was assayed as described (Makeyev *et al*., 2007). The experiment was done in triplicate ±SD and the luciferase expression levels in the corresponding RI vector-transfected controls were set to 1. Note that in both Ago1- and Ago2-expressing cells, miR-124 inhibits the expression of Luc-Ptbp1 with equal efficiency (n.s. [not significant with $p>0.05$], t test). (**D**) Ago1(shAgo2-3'UTR) and Ago2(shAgo2-3'UTR) cells pre-treated with Dox for 72 hours were transfected with the wild-type siRNA-like synthetic miR-124 22-mer duplex or a control non-targeting siRNA and the expression of three previously published miR-124 targets (Ptbp1, Ctdsp1, Vamp3; (Karginov *et al*., 2007; Makeyev *et al*., 2007) was analyzed by RT-qPCR 24 hours post transfection. Data are averaged from 6 experiments ±SD and the expression of the corresponding genes in siControl-transfected samples is set to 1. Note that miR-124 reduces the abundance of all three target mRNAs equally well in both Argonaute backgrounds (n.s. [not significant with $p>0.05$], t test).

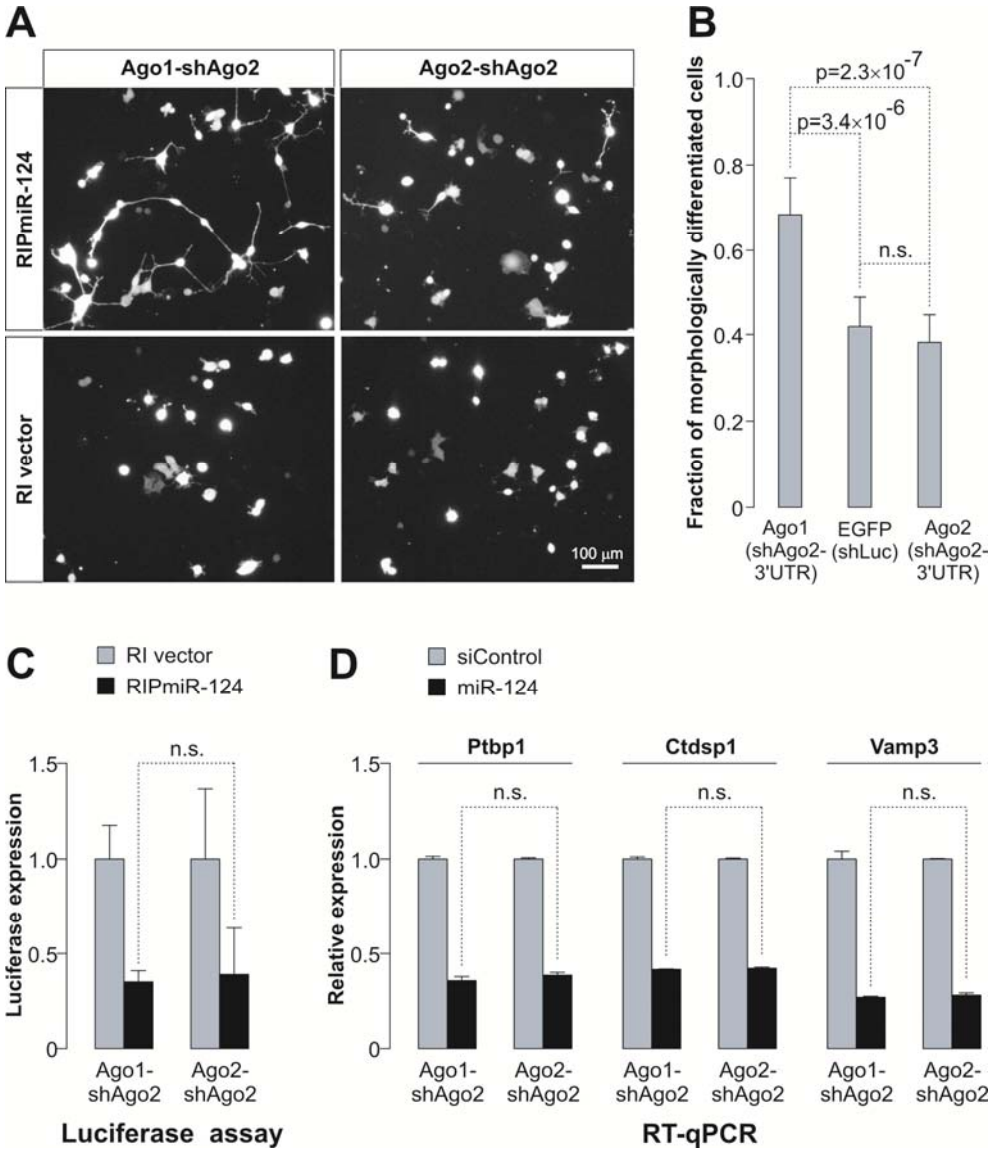
A
Ago1-shAgo2
Ago2-shAgo2
RIPmiR-124
RI vector
100 μm
B
Fraction of morphologically differentiated cells
p=2.3×10-7
p=3.4×10-6
n.s.
Ago1 (shAgo2-3'UTR)
EGFP (shLuc)
Ago2 (shAgo2-3'UTR)
C
RI vector
RIPmiR-124
Luciferase expression
n.s.
Ago1-shAgo2
Ago2-shAgo2
Luciferase assay
D
siControl
miR-124
Relative expression
Ptbp1
Ctdsp1
Vamp3
n.s.
Ago1-shAgo2
Ago2-shAgo2
RT-qPCR

4. DISCUSSION

4.1 Shortening of miRNAs during mouse brain development

miRNAs have emerged as one of the critical post transcriptional regulators of eukaryotic gene expression. Interestingly recent studies indicate that a large fraction of cellular miRNAs themselves are subjected to various modifications resulting in numerous size variants of a given miRNA, referred to as isomiRs (Berezikov *et al*., 2011; Fernandez-Valverde et al; Wyman *et al*., 2011). Multiple post transcriptional mechanisms have been implicated in the regulation of miRNA activity in a range of biological contexts (Krol *et al*., 2010).

Our present study provides an important update to the mammalian catalog of post transcriptional modifications by showing that a large subset of miRNAs undergoes 3'-terminal miRNA trimming during mouse brain development. Moreover, we also provide evidence that in addition to trimming, a fraction of miRNAs in developing nervous system may also undergo the addition of non-templated nucleotides at the 3' terminus. These modifications may lead to two possible functional outcomes: a change in the miRNA targeting properties or its stability (Katoh *et al*., 2009; Xie *et al*., 2012).

4.2 miR-124 undergoes trimming after its loading to RISC complex

miR-124 is an important brain-specific miRNA whose expression elevates during the mouse brain development (Krichevsky *et al*., 2003; Miska *et al*., 2004; Smirnova *et al*., 2005). We also observed a progressive trimming of mature miR-124 during mouse brain development (Figure 3.5). Several lines of evidence strongly suggest that, similar to the situation in *Drosophila* (Han *et al*., 2011; Liu *et al*., 2011), mammalian trimming occurs after the pre-miRNA dicing step after the recruitment of

mature miRNAs into Argonaute-containing complexes. Firstly, miR-124 was trimmed even in the absence of detectable amounts of the pre-mRNA precursor (Figure 3.6A) and secondly, AGO2-loaded synthetic miRNAs were efficiently trimmed whereas the end blocked synthetic miRNAs were protected from trimming (Figure 3.7A-C). Furthermore the pre-miR-124 predominantly gives rise to 22 nt mature miR-124 in an *in vitro* dicing reaction (Figure 3.6B-C). Taken together our data convincingly indicates that the trimmed species of miR-124 arise after Dicer cleavage and after loading of mature miRNA onto the RISC complex.

The mature miR-124 pool in the cell arises from three precursor paralogs (pri-miR-124a-1, -2, and -3) that differ by a few nucleotides in the pre-miRNA loop region. Notably, not only all the three precursor paralogs give rise to mature miR-124 at similar levels (Figure 3.8A and C) (Makeyev *et al*., 2007), but the mature miR-124 derived from each of the precursor paralogs is trimmed with identical efficiency (Figure 3.8A and B). Furthermore, all the three precursors give rise to predominantly 22 nt mature miRNA species *in vitro* (Figure 3.9B). Our data thus strongly suggests that trimming of miRNA is a post dicing event and mature miRNA is the substrate for trimming.

4.3 Argonaute association determines miRNA trimming

A surprising conclusion from our work is that, of the four mammalian Argonaute paralogs, only Ago2-loaded miRNAs undergo efficient 3'-terminal trimming (Figure 3.1, 3.2 and 3.3). Given the increase in fractional abundance of Ago2 during brain development due to dramatic down-regulation of Ago1 (Figure 3.4), this provides a molecular mechanism for the large-scale resection of the miRNA 3' ends in adult mouse brain.

We link the efficient trimming of Ago2-loaded miRNAs to the unusual structure of the Ago2 PAZ domain featuring the RH residues in its miRNA 3'-interaction loop instead of the KY motif conserved across other miRNA-specific Argonautes (Figure 3.16 and 3.17). A likely outcome of the KY>RH substitution could be a loss of at least one of the two hydrogen bonds between the KY residues and the miRNA 3'end due to the relatively small size and the lack of hydroxyl in the histidine side chain. This might theoretically weaken the interaction of the miRNA 3' end with the PAZ domain thus making it more accessible to a trimming exonuclease (Figure 3.18, 3.19 and 3.20). Based on our phylogenetic analyses, it is tempting to speculate that the Ago2 RH motif might have emerged in an ancestor of the tetrapod vertebrates as an adaptation enabling developmental control of the miRNA trimming. Additional experimental work would be required to show whether all tetrapod miRNAs loaded to the cognate Ago2 proteins have an increased trimming propensity.

4.4 Nature of the 3' terminal nucleotide alters the trimming efficiency of miR-124

Trimming reaction shows a 3'-terminal nucleotide bias. Indeed, 3'-terminal 'A' is substantially more accessible to trimming than the other three nucleotides. In addition to this, the miR-124 with terminal A nucleotide replaced, showed significant decrease in the trimming efficiency even in the presence of Ago2 unlike wild type miR-124 (Figure 3.14C-F).

Also 3' termini of the adult miRNAs were noticeably depleted in A's and enriched in U's (Fig. 4A; $p<2.2\times10^{-16}$, χ^2 test) (Figure 3.14A). Considering the above observations we propose that the trimming machinery favors miRNAs having a specific nucleotide at the 3' end as well as association with AGO2 but not AGO1, 3, or 4 (Figure 3.15A and B).

Further work will be required to establish the identity of the enzyme(s) trimming the mammalian miRNA 3' ends. An obvious starting point of these studies would be characterization of the mammalian Nibbler homologs (Han *et al*., 2011; Liu *et al*., 2011). Our observation that the nature of the miRNA 3' terminal nucleotide affects the efficiency of the trimming reaction (Figure 3.14 and 3.15) might reflect biochemical preferences of this hypothetical 3'-to'5' exonuclease and possibly facilitate its identification.

4.5 Biological significance of miRNA trimming

A growing body of evidence suggests that the 3'-terminus of a miRNA may modulate its interaction with cognate mRNAs in addition to the 5'-proximal "seed" sequence (Bartel, 2009; Brennecke *et al*., 2005; Broderick *et al*., 2011). It is therefore conceivable that the removal of one or two nucleotides from the 3' terminus could diminish the miRNA binding affinity to a subset of targets requiring 3' compensatory interactions. The higher biological activity of Ago1-associated miR-124 in neuroblastoma cells observed in our study (Figure 3.24) would generally be consistent with this model. Indeed, trimming of Ago2-loaded miR-124 might diminish its target repertoire thus potentially leading to a loss of important differentiation-specific targets (Figure 4.1). We are currently investigating the effect of Argonaute identity on the miR-124 targeting properties and potential significance of the stronger differentiation phenotype of Ago1-loaded miR-124 for mouse brain development. Another future line of research would be to examine possible effect of trimming on the miRNA half-life.

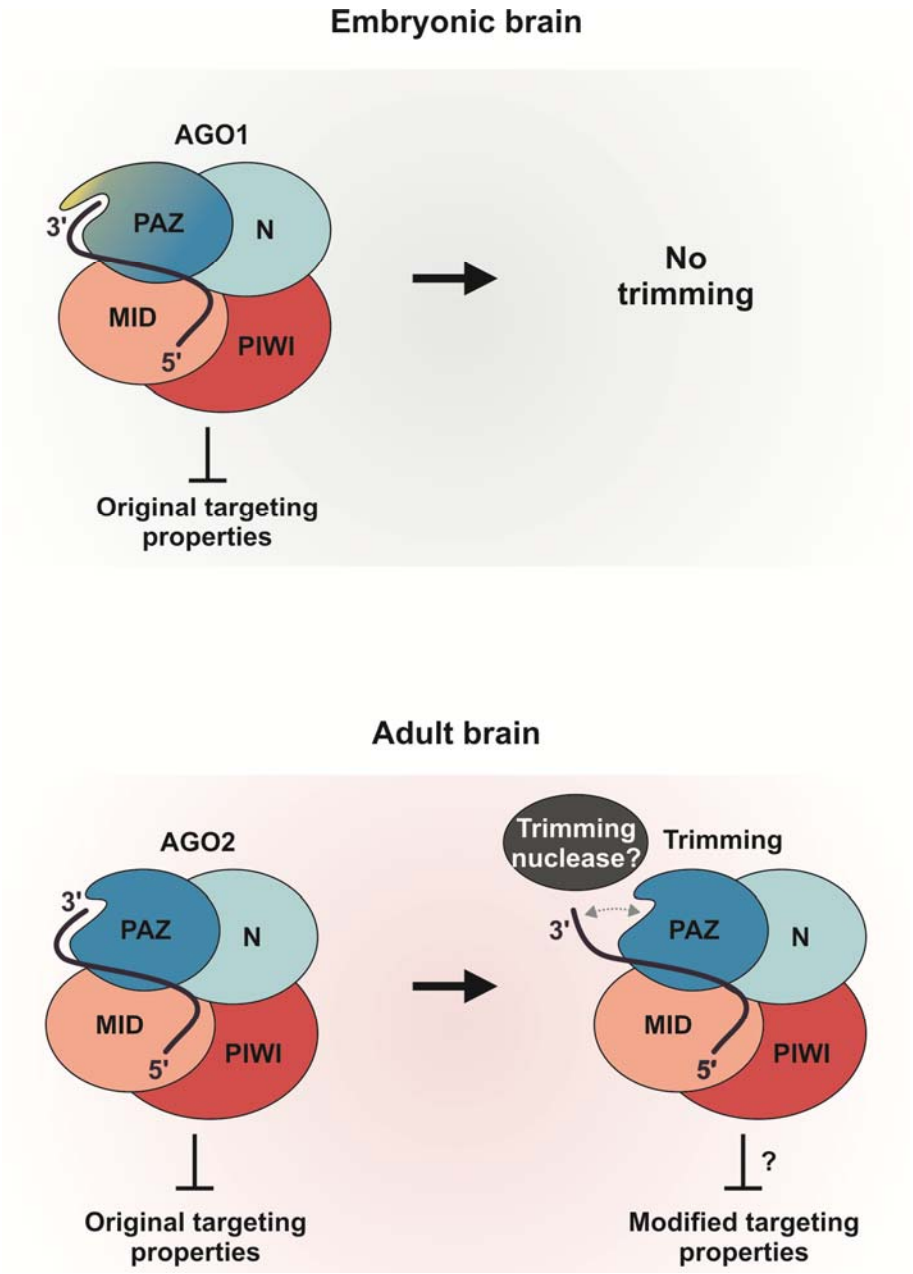

Figure 4.1: Proposed model outlining the role of mammalian Argonaute identity in miRNA trimming. Trimming of miRNAs recruited to AGO2 in adult brain might diminish the regulation of select targets which determine the differentiation (on top) unlike the miRNAs recruited to AGO1 in embryonic brain that do not undergo trimming (bottom).

In conclusion, the present work uncovers pervasive 3'-terminal trimming of mammalian miRNAs and suggests that the efficiency of this process might be developmentally regulated by changes in fractional abundance of Ago2, the only mammalian Argonaute compatible with efficient trimming reaction. Identification of the mammalian miRNA trimming enzyme(s) and understanding the possible functions of trimmed miRNAs in mammals and *Drosophila* will be important questions for future studies.

6. REFERENCES

Aalto AP, Pasquinelli AE (2012) Small non-coding RNAs mount a silent revolution in gene expression. *Curr Opin Cell Biol*

Ambros V (2004) The functions of animal microRNAs. *Nature* **431:** 350-355

Ameres SL, Horwich MD, Hung J-H, Xu J, Ghildiyal M, Weng Z, Zamore PD (2010) Target RNA-Directed Trimming and Tailing of Small Silencing RNAs. *Science* **328:** 1534-1539

Andersson MG, Haasnoot PC, Xu N, Berenjian S, Berkhout B, Akusjarvi G (2005) Suppression of RNA interference by adenovirus virus-associated RNA. *J Virol* **79:** 9556-9565

Aravin AA, Lagos-Quintana M, Yalcin A, Zavolan M, Marks D, Snyder B, Gaasterland T, Meyer J, Tuschl T (2003) The Small RNA Profile during Drosophila melanogaster Development. *Developmental Cell* **5:** 337-350

Ashraf SI, McLoon AL, Sclarsic SM, Kunes S (2006) Synaptic protein synthesis associated with memory is regulated by the RISC pathway in Drosophila. *Cell* **124:** 191-205

Babiarz JE, Ruby JG, Wang Y, Bartel DP, Blelloch R (2008) Mouse ES cells express endogenous shRNAs, siRNAs, and other Microprocessor-independent, Dicer-dependent small RNAs. *Genes & Development* **22:** 2773-2785

Bachellerie JP, Cavaille J, Huttenhofer A (2002) The expanding snoRNA world. *Biochimie* **84:** 775-790

Bail S, Swerdel M, Liu H, Jiao X, Goff LA, Hart RP, Kiledjian M (2010) Differential regulation of microRNA stability. *RNA* **16:** 1032-1039

Bartel DP (2004) MicroRNAs: Genomics, Biogenesis, Mechanism, and Function. *Cell* **116:** 281-297

Bartel DP (2009) MicroRNAs: target recognition and regulatory functions. *Cell* **136:** 215-233

Baskerville S, Bartel DP (2005) Microarray profiling of microRNAs reveals frequent coexpression with neighboring miRNAs and host genes. *RNA* **11:** 241-247

Bazzini AA, Lee MT, Giraldez AJ (2012) Ribosome Profiling Shows That miR-430 Reduces Translation Before Causing mRNA Decay in Zebrafish. *Science* **336:** 233-237

Behm-Ansmant I, Rehwinkel J, Doerks T, Stark A, Bork P, Izaurralde E (2006) mRNA degradation by miRNAs and GW182 requires both CCR4:NOT deadenylase and DCP1:DCP2 decapping complexes. *Genes & Development* **20:** 1885-1898

Berezikov E, Robine N, Samsonova A, Westholm JO, Naqvi A, Hung JH, Okamura K, Dai Q, Bortolamiol-Becet D, Martin R, Zhao Y, Zamore PD, Hannon GJ, Marra MA, Weng Z, Perrimon N, Lai EC (2011) Deep annotation of Drosophila melanogaster microRNAs yields insights into their processing, modification, and emergence. *Genome Res* **21:** 203-215

Bernstein E, Caudy AA, Hammond SM, Hannon GJ (2001) Role for a bidentate ribonuclease in the initiation step of RNA interference. *Nature* **409:** 363-366

Bernstein E, Kim SY, Carmell MA, Murchison EP, Alcorn H, Li MZ, Mills AA, Elledge SJ, Anderson KV, Hannon GJ (2003) Dicer is essential for mouse development. *Nat Genet* **35:** 215-217

Bishop JM, Levinson WE, Quintrell N, Sullivan D, Fanshier L, Jackson J (1970a) The low molecular weight RNAs of Rous sarcoma virus. I. The 4 S RNA. *Virology* **42:** 182-195

Bishop JM, Levinson WE, Sullivan D, Fanshier L, Quintrell N, Jackson J (1970b) The low molecular weight RNAs of Rous sarcoma virus. II. The 7 S RNA. *Virology* **42:** 927-937

Blackshaw S, Harpavat S, Trimarchi J, Cai L, Huang H, Kuo WP, Weber G, Lee K, Fraioli RE, Cho SH, Yung R, Asch E, Ohno-Machado L, Wong WH, Cepko CL (2004) Genomic analysis of mouse retinal development. *PLoS Biol* **2:** E247

Bohnsack MT, Czaplinski K, Görlich D (2004) Exportin 5 is a RanGTP-dependent dsRNA-binding protein that mediates nuclear export of pre-miRNAs. *RNA* **10:** 185-191

Borchert GM, Lanier W, Davidson BL (2006) RNA polymerase III transcribes human microRNAs. *Nat Struct Mol Biol* **13:** 1097-1101

Boutz PL, Chawla G, Stoilov P, Black DL (2007) MicroRNAs regulate the expression of the alternative splicing factor nPTB during muscle development. *Genes & Development* **21:** 71-84

Bracht J, Hunter S, Eachus R, Weeks P, Pasquinelli AE (2004) Trans-splicing and polyadenylation of let-7 microRNA primary transcripts. *RNA* **10:** 1586-1594

Brennecke J, Stark A, Russell RB, Cohen SM (2005) Principles of microRNA-target recognition. *PLoS Biol* **3:** e85

Broderick JA, Salomon WE, Ryder SP, Aronin N, Zamore PD (2011) Argonaute protein identity and pairing geometry determine cooperativity in mammalian RNA silencing. *RNA* **17:** 1858-1869

Brodersen P, Voinnet O (2009) Revisiting the principles of microRNA target recognition and mode of action. *Nat Rev Mol Cell Biol* **10:** 141-148

Bushati N, Cohen SM (2007a) microRNA Functions. *Annu Rev Cell Dev Biol* **23:** 175-205

Cai X, Hagedorn CH, Cullen BR (2004) Human microRNAs are processed from capped, polyadenylated transcripts that can also function as mRNAs. *RNA* **10:** 1957-1966

Cao X, Pfaff SL, Gage FH (2007) A functional study of miR-124 in the developing neural tube. *Genes & Development* **21:** 531-536

Carrington J, Ambros V (2003) Role of microRNAs in plant and animal development. *Science* **301:** 336 - 338

Carmell MA, Xuan Z, Zhang MQ, Hannon GJ (2002) The Argonaute family: tentacles that reach into RNAi, developmental control, stem cell maintenance, and tumorigenesis. *Genes & Development* **16:** 2733-2742

Chang S, Johnston RJ, Jr., Frokjaer-Jensen C, Lockery S, Hobert O (2004) MicroRNAs act sequentially and asymmetrically to control chemosensory laterality in the nematode. *Nature* **430:** 785-789

Chapman EJ, Carrington JC (2007) Specialization and evolution of endogenous small RNA pathways. *Nat Rev Genet* **8:** 884-896

Chatterjee S, Großhans H (2009) Active turnover modulates mature microRNA activity in Caenorhabditis elegans. *Nature* **461:** 546-549

Cheloufi S, Dos Santos CO, Chong MMW, Hannon GJ (2010) A dicer-independent miRNA biogenesis pathway that requires Ago catalysis. *Nature* **465:** 584-589

Chen J-F, Mandel EM, Thomson JM, Wu Q, Callis TE, Hammond SM, Conlon FL, Wang D-Z (2006) The role of microRNA-1 and microRNA-133 in skeletal muscle proliferation and differentiation. *Nat Genet* **38:** 228-233

Chendrimada TP, Gregory RI, Kumaraswamy E, Norman J, Cooch N, Nishikura K, Shiekhattar R (2005) TRBP recruits the Dicer complex to Ago2 for microRNA processing and gene silencing. *Nature* **436:** 740-744

Chi SW, Zang JB, Mele A, Darnell RB (2009) Argonaute HITS-CLIP decodes microRNA-mRNA interaction maps. *Nature* **460:** 479-486

Cifuentes D, Xue H, Taylor DW, Patnode H, Mishima Y, Cheloufi S, Ma E, Mane S, Hannon GJ, Lawson ND, Wolfe SA, Giraldez AJ (2010) A Novel miRNA Processing Pathway Independent of Dicer Requires Argonaute2 Catalytic Activity. *Science* **328:** 1694-1698

Conaco C, Otto S, Han J-J, Mandel G (2006) Reciprocal actions of REST and a microRNA promote neuronal identity. *Proc Natl Acad Sci U S A* **103:** 2422-2427

Czech B, Hannon GJ (2011) Small RNA sorting: matchmaking for Argonautes. *Nat Rev Genet* **12:** 19-31

Denli AM, Tops BB, Plasterk RH, Ketting RF, Hannon GJ (2004) Processing of primary microRNAs by the Microprocessor complex. *Nature* **432:** 231-235

Diederichs S, Haber DA (2007) Dual role for argonautes in microRNA processing and posttranscriptional regulation of microRNA expression. *Cell* **131:** 1097-1108

Djuranovic S, Nahvi A, Green R (2012) miRNA-Mediated Gene Silencing by Translational Repression Followed by mRNA Deadenylation and Decay. *Science* **336:** 237-240

Doench JG, Sharp PA (2004) Specificity of microRNA target selection in translational repression. *Genes & Development* **18:** 504-511

Du T, Zamore PD (2005) microPrimer: the biogenesis and function of microRNA. *Development* **132:** 4645-4652

Elbashir SM, Harborth J, Lendeckel W, Yalcin A, Weber K, Tuschl T (2001a) Duplexes of 21-nucleotide RNAs mediate RNA interference in cultured mammalian cells. *Nature* **411:** 494-498

Elbashir SM, Lendeckel W, Tuschl T (2001b) RNA interference is mediated by 21- and 22-nucleotide RNAs. *Genes & Development* **15:** 188-200

Eulalio A, Behm-Ansmant I, Izaurralde E (2007) P bodies: at the crossroads of post-transcriptional pathways. *Nat Rev Mol Cell Biol* **8:** 9-22

Fernandez-Valverde SL, Taft RJ, Mattick JS (2010) Dynamic isomiR regulation in Drosophila development. *RNA* **16:** 1881-1888

Filipowicz W, Bhattacharyya SN, Sonenberg N (2008) Mechanisms of post-transcriptional regulation by microRNAs: are the answers in sight? *Nat Rev Genet* **9:** 102-114

Fineberg SK, Kosik KS, Davidson BL (2009) MicroRNAs potentiate neural development. *Neuron* **64:** 303-309

Fire A, Xu S, Montgomery MK, Kostas SA, Driver SE, Mello CC (1998) Potent and specific genetic interference by double-stranded RNA in Caenorhabditis elegans. *Nature* **391:** 806-811

Friedlander MR, Chen W, Adamidi C, Maaskola J, Einspanier R, Knespel S, Rajewsky N (2008) Discovering microRNAs from deep sequencing data using miRDeep. *Nat Biotechnol* **26:** 407-415

Garneau NL, Wilusz J, Wilusz CJ (2007) The highways and byways of mRNA decay. *Nat Rev Mol Cell Biol* **8:** 113-126

Giraldez AJ, Cinalli RM, Glasner ME, Enright AJ, Thomson JM, Baskerville S, Hammond SM, Bartel DP, Schier AF (2005) MicroRNAs Regulate Brain Morphogenesis in Zebrafish. *Science* **308:** 833-838

Giraldez AJ, Mishima Y, Rihel J, Grocock RJ, Van Dongen S, Inoue K, Enright AJ, Schier AF (2006) Zebrafish MiR-430 Promotes Deadenylation and Clearance of Maternal mRNAs. *Science* **312:** 75-79

Girard A, Sachidanandam R, Hannon GJ, Carmell MA (2006) A germline-specific class of small RNAs binds mammalian Piwi proteins. *Nature* **442:** 199-202

Gregory RI, Chendrimada TP, Cooch N, Shiekhattar R (2005) Human RISC Couples MicroRNA Biogenesis and Posttranscriptional Gene Silencing. **123:** 631-640

Gregory RI, Yan K-p, Amuthan G, Chendrimada T, Doratotaj B, Cooch N, Shiekhattar R (2004) The Microprocessor complex mediates the genesis of microRNAs. *Nature* **432:** 235-240

Grimson A, Farh KK, Johnston WK, Garrett-Engele P, Lim LP, Bartel DP (2007) MicroRNA targeting specificity in mammals: determinants beyond seed pairing. *Mol Cell* **27:** 91-105

Grivna ST, Beyret E, Wang Z, Lin H (2006) A novel class of small RNAs in mouse spermatogenic cells. *Genes & Development* **20:** 1709-1714

Guo H, Ingolia NT, Weissman JS, Bartel DP (2010) Mammalian microRNAs predominantly act to decrease target mRNA levels. *Nature* **466:** 835-840

Hagan JP, Piskounova E, Gregory RI (2009) Lin28 recruits the TUTase Zcchc11 to inhibit let-7 maturation in mouse embryonic stem cells. *Nat Struct Mol Biol* **16:** 1021-1025

Han BW, Hung JH, Weng Z, Zamore PD, Ameres SL (2011) The 3'-to-5' exoribonuclease Nibbler shapes the 3' ends of microRNAs bound to Drosophila Argonaute1. *Curr Biol* **21:** 1878-1887

Han J, Lee Y, Yeom K-H, Kim Y-K, Jin H, Kim VN (2004) The Drosha-DGCR8 complex in primary microRNA processing. *Genes & Development* **18:** 3016-3027

Han J, Lee Y, Yeom KH, Nam JW, Heo I, Rhee JK, Sohn SY, Cho Y, Zhang BT, Kim VN (2006) Molecular basis for the recognition of primary microRNAs by the Drosha-DGCR8 complex. *Cell* **125:** 887-901

Hébert SS, Papadopoulou AS, Smith P, Galas M-C, Planel E, Silahtaroglu AN, Sergeant N, Buée L, De Strooper B (2010) Genetic ablation of Dicer in adult forebrain neurons results in abnormal tau hyperphosphorylation and neurodegeneration. *Hum Mol Genet* **19:** 3959-3969

Hendrickson DG, Hogan DJ, McCullough HL, Myers JW, Herschlag D, Ferrell JE, Brown PO (2009) Concordant regulation of translation and mRNA abundance for hundreds of targets of a human microRNA. *PLoS Biol* **7:** e1000238

Heo I, Joo C, Kim Y-K, Ha M, Yoon M-J, Cho J, Yeom K-H, Han J, Kim VN (2009) TUT4 in Concert with Lin28 Suppresses MicroRNA Biogenesis through Pre-MicroRNA Uridylation. **138:** 696-708

Hock J, Meister G (2008) The Argonaute protein family. *Genome Biol* **9:** 210

Holley RW, Apgar J, Everett GA, Madison JT, Marquisee M, Merrill SH, Penswick JR, Zamir A (1965) Structure of a Ribonucleic Acid. *Science* **147:** 1462-1465

Horwich MD, Li C, Matranga C, Vagin V, Farley G, Wang P, Zamore PD (2007) The Drosophila RNA Methyltransferase, DmHen1, Modifies Germline piRNAs and Single-Stranded siRNAs in RISC. *Current Biology* **17:** 1265-1272

Houwing S, Kamminga LM, Berezikov E, Cronembold D, Girard A, van den Elst H, Filippov DV, Blaser H, Raz E, Moens CB, Plasterk RHA, Hannon GJ, Draper BW, Ketting RF (2007) A Role for Piwi and piRNAs in Germ Cell Maintenance and Transposon Silencing in Zebrafish. *Cell* **129:** 69-82

Huang T, Liu Y, Huang M, Zhao X, Cheng L (2010) Wnt1-cre-mediated Conditional Loss of Dicer Results in Malformation of the Midbrain and Cerebellum and Failure of

Neural Crest and Dopaminergic Differentiation in Mice. *Journal of Molecular Cell Biology* **2:** 152-163

Humphreys DT, Westman BJ, Martin DIK, Preiss T (2005) MicroRNAs control translation initiation by inhibiting eukaryotic initiation factor 4E/cap and poly(A) tail function. *Proc Natl Acad Sci U S A* **102:** 16961-16966

Hutvagner G, Simard MJ (2008) Argonaute proteins: key players in RNA silencing. *Nat Rev Mol Cell Biol* **9:** 22-32

Hutvagner G, Zamore PD (2002) A microRNA in a Multiple-Turnover RNAi Enzyme Complex. *Science* **297:** 2056-2060

Jones MR, Quinton LJ, Blahna MT, Neilson JR, Fu S, Ivanov AR, Wolf DA, Mizgerd JP (2009) Zcchc11-dependent uridylation of microRNA directs cytokine expression. *Nat Cell Biol* **11:** 1157-1163

Johnston RJ, Hobert O (2003) A microRNA controlling left/right neuronal asymmetry in Caenorhabditis elegans. *Nature* **426:** 845-849

Johnston RJ, Jr., Chang S, Etchberger JF, Ortiz CO, Hobert O (2005) MicroRNAs acting in a double-negative feedback loop to control a neuronal cell fate decision. *Proc Natl Acad Sci U S A* **102:** 12449-12454

Jones-Rhoades MW, Bartel DP, Bartel B (2006) MicroRNAs and their regulatory roles in plants. *Annual Review of Plant Biology* **57:** 19-53

Jones AL, Thomas CL, Maule AJ (1998) De novo methylation and co-suppression induced by a cytoplasmically replicating plant RNA virus. *Embo J* **17:** 6385-6393

Joshua-Tor L, Hannon GJ (2011) Ancestral roles of small RNAs: an Ago-centric perspective. *Cold Spring Harb Perspect Biol* **3:** a003772

Kai ZS, Pasquinelli AE (2010) MicroRNA assassins: factors that regulate the disappearance of miRNAs. *Nat Struct Mol Biol* **17:** 5-10

Karginov FV, Conaco C, Xuan Z, Schmidt BH, Parker JS, Mandel G, Hannon GJ (2007) A biochemical approach to identifying microRNA targets. *Proc Natl Acad Sci U S A* **104:** 19291-19296

Kataoka Y, Takeichi M, Uemura T (2001) Developmental roles and molecular characterization of a Drosophila homologue of Arabidopsis Argonaute1, the founder of a novel gene superfamily. *Genes to Cells* **6:** 313-325

Katoh T, Sakaguchi Y, Miyauchi K, Suzuki T, Kashiwabara S-i, Baba T, Suzuki T (2009) Selective stabilization of mammalian microRNAs by 3′ adenylation mediated by the cytoplasmic poly(A) polymerase GLD-2. *Genes & Development* **23:** 433-438

Kawahara H, Imai T, Okano H (2012) MicroRNAs in Neural Stem Cells and Neurogenesis. *Front Neurosci* **6:** 30

Kawamura Y, Saito K, Kin T, Ono Y, Asai K, Sunohara T, Okada TN, Siomi MC, Siomi H (2008) Drosophila endogenous small RNAs bind to Argonaute 2 in somatic cells. *Nature* **453:** 793-797

Ketting RF, Fischer SEJ, Bernstein E, Sijen T, Hannon GJ, Plasterk RHA (2001) Dicer functions in RNA interference and in synthesis of small RNA involved in developmental timing in C. elegans. *Genes & Development* **15:** 2654-2659

Khandelia P, Yap K, Makeyev EV (2011) Streamlined platform for short hairpin RNA interference and transgenesis in cultured mammalian cells. *Proc Natl Acad Sci U S A* **108:** 12799-12804

Khvorova A, Reynolds A, Jayasena SD (2003) Functional siRNAs and miRNAs Exhibit Strand Bias. **115:** 209-216

Kim J, Inoue K, Ishii J, Vanti WB, Voronov SV, Murchison E, Hannon G, Abeliovich A (2007) A MicroRNA Feedback Circuit in Midbrain Dopamine Neurons. *Science* **317:** 1220-1224

Kim J, Krichevsky A, Grad Y, Hayes GD, Kosik KS, Church GM, Ruvkun G (2004) Identification of many microRNAs that copurify with polyribosomes in mammalian neurons. *Proceedings of the National Academy of Sciences* **101:** 360-365

Kim VN (2005) MicroRNA biogenesis: coordinated cropping and dicing. *Nat Rev Mol Cell Biol* **6:** 376-385

Kim VN, Han J, Siomi MC (2009) Biogenesis of small RNAs in animals. *Nat Rev Mol Cell Biol* **10:** 126-139

Kim VN, Nam JW (2006) Genomics of microRNA. *Trends Genet* **22:** 165-173

Kim Y-K, Kim VN (2007) Processing of intronic microRNAs. *Embo J* **26:** 775-783

Kiriakidou M, Tan GS, Lamprinaki S, De Planell-Saguer M, Nelson PT, Mourelatos Z (2007) An mRNA m7G Cap Binding-like Motif within Human Ago2 Represses Translation. *Cell* **129:** 1141-1151

Knight SW, Bass BL (2001) A Role for the RNase III Enzyme DCR-1 in RNA Interference and Germ Line Development in Caenorhabditis elegans. *Science* **293:** 2269-2271

Kosik KS (2006) The neuronal microRNA system. *Nat Rev Neurosci* **7:** 911-920

Krichevsky A, King K, Donahue C, Khrapko K, Kosik K (2003) A microRNA array reveals extensive regulation of microRNAs during brain development. *RNA* **9:** 1274 - 1281

Krichevsky AM, Sonntag KC, Isacson O, Kosik KS (2006) Specific microRNAs modulate embryonic stem cell-derived neurogenesis. *Stem Cells* **24:** 857-864

Krol J, Loedige I, Filipowicz W (2010) The widespread regulation of microRNA biogenesis, function and decay. *Nat Rev Genet* **11:** 597-610

Lagos-Quintana M, Rauhut R, Lendeckel W, Tuschl T (2001) Identification of novel genes coding for small expressed RNAs. *Science* **294:** 853 - 858

Lagos-Quintana M, Rauhut R, Meyer J, Borkhardt A, Tuschl T (2003) New microRNAs from mouse and human. *RNA* **9:** 175-179

Lagos-Quintana M, Rauhut R, Yalcin A, Meyer J, Lendeckel W, Tuschl T (2002) Identification of tissue-specific microRNAs from mouse. *Curr Biol* **12:** 735 - 739

Landgraf P, Rusu M, Sheridan R, Sewer A, Iovino N, Aravin A, Pfeffer S, Rice A, Kamphorst AO, Landthaler M, Lin C, Socci ND, Hermida L, Fulci V, Chiaretti S, Foa R, Schliwka J, Fuchs U, Novosel A, Muller RU, Schermer B, Bissels U, Inman J, Phan Q, Chien M, Weir DB, Choksi R, De Vita G, Frezzetti D, Trompeter HI, Hornung V, Teng G, Hartmann G, Palkovits M, Di Lauro R, Wernet P, Macino G, Rogler CE, Nagle JW, Ju J, Papavasiliou FN, Benzing T, Lichter P, Tam W, Brownstein MJ, Bosio A, Borkhardt A, Russo JJ, Sander C, Zavolan M, Tuschl T (2007) A mammalian microRNA expression atlas based on small RNA library sequencing. *Cell* **129:** 1401-1414

Langmead B, Trapnell C, Pop M, Salzberg SL (2009) Ultrafast and memory-efficient alignment of short DNA sequences to the human genome. *Genome Biol* **10:** R25

Lau N, Lim L, Weinstein E, Bartel D (2001) An abundant class of tiny RNAs with probable regulatory roles in Caenorhabditis elegans. *Science* **294:** 858 - 862

Lee RC, Feinbaum RL, Ambros V (1993) The C. elegans heterochronic gene lin-4 encodes small RNAs with antisense complementarity to lin-14. *Cell* **75:** 843-854

Lee Y, Hur I, Park SY, Kim YK, Suh MR, Kim VN (2006) The role of PACT in the RNA silencing pathway. *Embo J* **25:** 522-532

Lee Y, Jeon K, Lee J, Kim S, Kim V (2002) MicroRNA maturation: stepwise processing and subcellular localization. *Embo J* **21:** 4663 - 4670

Lee Y, Kim M, Han J, Yeom K-H, Lee S, Baek SH, Kim VN (2004) MicroRNA genes are transcribed by RNA polymerase II. *Embo J* **23:** 4051-4060

Leung AK, Sharp PA (2010) MicroRNA functions in stress responses. *Mol Cell* **40:** 205-215

Lewis BP, Burge CB, Bartel DP (2005) Conserved seed pairing, often flanked by adenosines, indicates that thousands of human genes are microRNA targets. *Cell* **120:** 15-20

Li Y, Wang F, Lee JA, Gao FB (2006) MicroRNA-9a ensures the precise specification of sensory organ precursors in Drosophila. *Genes & Development* **20:** 2793-2805

Lim LP, Lau NC, Garrett-Engele P, Grimson A, Schelter JM, Castle J, Bartel DP, Linsley PS, Johnson JM (2005) Microarray analysis shows that some microRNAs downregulate large numbers of target mRNAs. *Nature* **433:** 769-773

Lingel A, Simon B, Izaurralde E, Sattler M (2004) Nucleic acid 3'-end recognition by the Argonaute2 PAZ domain. *Nat Struct Mol Biol* **11:** 576-577

Liu C, Zhao X (2009) MicroRNAs in adult and embryonic neurogenesis. *Neuromolecular Med* **11:** 141-152

Liu J, Carmell MA, Rivas FV, Marsden CG, Thomson JM, Song J-J, Hammond SM, Joshua-Tor L, Hannon GJ (2004) Argonaute2 Is the Catalytic Engine of Mammalian RNAi. *Science* **305:** 1437-1441

Liu J, Valencia-Sanchez MA, Hannon GJ, Parker R (2005) MicroRNA-dependent localization of targeted mRNAs to mammalian P-bodies. *Nat Cell Biol* **7:** 719-723

Liu N, Abe M, Sabin LR, Hendriks GJ, Naqvi AS, Yu Z, Cherry S, Bonini NM (2011) The exoribonuclease Nibbler controls 3' end processing of microRNAs in Drosophila. *Curr Biol* **21:** 1888-1893

Lund E, Guttinger S, Calado A, Dahlberg JE, Kutay U (2004) Nuclear Export of MicroRNA Precursors. *Science* **303:** 95-98

Ma J-B, Ye K, Patel DJ (2004) Structural basis for overhang-specific small interfering RNA recognition by the PAZ domain. *Nature* **429:** 318-322

Magill ST, Cambronne XA, Luikart BW, Lioy DT, Leighton BH, Westbrook GL, Mandel G, Goodman RH (2010) microRNA-132 regulates dendritic growth and arborization of newborn neurons in the adult hippocampus. *Proc Natl Acad Sci U S A* **107:** 20382-20387

Makeyev EV, Maniatis T (2008) Multilevel Regulation of Gene Expression by MicroRNAs. *Science* **319:** 1789-1790

Makeyev EV, Zhang J, Carrasco MA, Maniatis T (2007) The MicroRNA miR-124 Promotes Neuronal Differentiation by Triggering Brain-Specific Alternative Pre-mRNA Splicing. **27:** 435-448

Martinez J, Tuschl T (2004) RISC is a 5′ phosphomonoester-producing RNA endonuclease. *Genes & Development* **18:** 975-980

Matera AG, Terns RM, Terns MP (2007) Non-coding RNAs: lessons from the small nuclear and small nucleolar RNAs. *Nat Rev Mol Cell Biol* **8:** 209-220

Meister G, Landthaler M, Patkaniowska A, Dorsett Y, Teng G, Tuschl T (2004) Human Argonaute2 Mediates RNA Cleavage Targeted by miRNAs and siRNAs. *Mol Cell* **15:** 185-197

Meister G, Landthaler M, Peters L, Chen PY, Urlaub H, Luhrmann R, Tuschl T (2005) Identification of novel argonaute-associated proteins. *Curr Biol* **15:** 2149-2155

Meister G, Tuschl T (2004) Mechanisms of gene silencing by double-stranded RNA. *Nature* **431:** 343-349

Melton C, Judson RL, Blelloch R (2010) Opposing microRNA families regulate self-renewal in mouse embryonic stem cells. *Nature* **463:** 621-626

Miska EA, Alvarez-Saavedra E, Townsend M, Yoshii A, Sestan N, Rakic P, Constantine-Paton M, Horvitz HR (2004) Microarray analysis of microRNA expression in the developing mammalian brain. *Genome Biol* **5:** R68

Morin RD, O'Connor MD, Griffith M, Kuchenbauer F, Delaney A, Prabhu AL, Zhao Y, McDonald H, Zeng T, Hirst M, Eaves CJ, Marra MA (2008) Application of massively parallel sequencing to microRNA profiling and discovery in human embryonic stem cells. *Genome Res* **18:** 610-621

Morlando M, Ballarino M, Gromak N, Pagano F, Bozzoni I, Proudfoot NJ (2008) Primary microRNA transcripts are processed co-transcriptionally. *Nat Struct Mol Biol* **15:** 902-909

Mourelatos Z, Dostie J, Paushkin S, Sharma A, Charroux B, Abel L, Rappsilber J, Mann M, Dreyfuss G (2002) miRNPs: a novel class of ribonucleoproteins containing numerous microRNAs. *Genes Dev* **16:** 720 - 728

Nilsen TW (2007) Mechanisms of microRNA-mediated gene regulation in animal cells. *Trends Genet* **23:** 243-249

Nottrott S, Simard MJ, Richter JD (2006) Human let-7a miRNA blocks protein production on actively translating polyribosomes. *Nat Struct Mol Biol* **13:** 1108-1114

O'Donnell KA, Wentzel EA, Zeller KI, Dang CV, Mendell JT (2005) c-Myc-regulated microRNAs modulate E2F1 expression. *Nature* **435:** 839-843

Okamura K, Chung WJ, Ruby JG, Guo H, Bartel DP, Lai EC (2008) The Drosophila hairpin RNA pathway generates endogenous short interfering RNAs. *Nature* **453:** 803-806

Okamura K, Hagen JW, Duan H, Tyler DM, Lai EC (2007) The Mirtron Pathway Generates microRNA-Class Regulatory RNAs in Drosophila. **130:** 89-100

Pawlicki JM, Steitz JA (2008) Primary microRNA transcript retention at sites of transcription leads to enhanced microRNA production. *J Cell Biol* **182:** 61-76

Peters L, Meister G (2007) Argonaute proteins: mediators of RNA silencing. *Mol Cell* **26:** 611-623

Petersen CP, Bordeleau ME, Pelletier J, Sharp PA (2006) Short RNAs repress translation after initiation in mammalian cells. *Mol Cell* **21:** 533-542

Pfeffer S, Sewer A, Lagos-Quintana M, Sheridan R, Sander C, Grasser FA, van Dyk LF, Ho CK, Shuman S, Chien M, Russo JJ, Ju J, Randall G, Lindenbach BD, Rice CM, Simon V, Ho DD, Zavolan M, Tuschl T (2005) Identification of microRNAs of the herpesvirus family. *Nat Methods* **2:** 269-276

Pillai RS, Bhattacharyya SN, Artus CG, Zoller T, Cougot N, Basyuk E, Bertrand E, Filipowicz W (2005) Inhibition of Translational Initiation by Let-7 MicroRNA in Human Cells. *Science* **309:** 1573-1576

Ponomarev ED, Veremeyko T, Barteneva N, Krichevsky AM, Weiner HL (2011) MicroRNA-124 promotes microglia quiescence and suppresses EAE by deactivating macrophages via the C/EBP-[alpha]-PU.1 pathway. *Nat Med* **17:** 64-70

Ramachandran V, Chen X (2008) Degradation of microRNAs by a Family of Exoribonucleases in Arabidopsis. *Science* **321:** 1490-1492

Rau F, Freyermuth F, Fugier C, Villemin J-P, Fischer M-C, Jost B, Dembele D, Gourdon G, Nicole A, Duboc D, Wahbi K, Day JW, Fujimura H, Takahashi MP, Auboeuf D, Dreumont N, Furling D, Charlet-Berguerand N (2011) Misregulation of miR-1 processing is associated with heart defects in myotonic dystrophy. *Nat Struct Mol Biol* **18:** 840-845

Ruby JG, Jan CH, Bartel DP (2007) Intronic microRNA precursors that bypass Drosha processing. *Nature* **448:** 83-86

Saito K, Ishizuka A, Siomi H, Siomi MC (2005) Processing of pre-microRNAs by the Dicer-1-Loquacious complex in Drosophila cells. *PLoS Biol* **3:** e235

Saito Y, Liang G, Egger G, Friedman JM, Chuang JC, Coetzee GA, Jones PA (2006) Specific activation of microRNA-127 with downregulation of the proto-oncogene BCL6 by chromatin-modifying drugs in human cancer cells. *Cancer Cell* **9:** 435-443

Sambrook,J. and Russell,R.W. (2001) Molecular Cloning: A Laboratory Manual, 3rd edn. Cold Spring Harbor Laboratory Press, Cold Spring Harbor, NY.

Sanuki R, Onishi A, Koike C, Muramatsu R, Watanabe S, Muranishi Y, Irie S, Uneo S, Koyasu T, Matsui R, Cherasse Y, Urade Y, Watanabe D, Kondo M, Yamashita T, Furukawa T (2011) miR-124a is required for hippocampal axogenesis and retinal cone survival through Lhx2 suppression. *Nat Neurosci* **14:** 1125-1134

Schaefer A, O'Carroll D, Tan CL, Hillman D, Sugimori M, Llinas R, Greengard P (2007) Cerebellar neurodegeneration in the absence of microRNAs. *J Exp Med* **204:** 1553-1558

Schmid M, Jensen TH (2008) The exosome: a multipurpose RNA-decay machine. *Trends in Biochemical Sciences* **33:** 501-510

Schratt GM, Tuebing F, Nigh EA, Kane CG, Sabatini ME, Kiebler M, Greenberg ME (2006) A brain-specific microRNA regulates dendritic spine development. *Nature* **439:** 283-289

Schwamborn JC, Berezikov E, Knoblich JA (2009) The TRIM-NHL protein TRIM32 activates microRNAs and prevents self-renewal in mouse neural progenitors. *Cell* **136:** 913-925

Schwarz DS, Hutvágner G, Du T, Xu Z, Aronin N, Zamore PD (2003) Asymmetry in the Assembly of the RNAi Enzyme Complex. **115:** 199-208

Sempere L, Freemantle S, Pitha-Rowe I, Moss E, Dmitrovsky E, Ambros V (2004) Expression profiling of mammalian microRNAs uncovers a subset of brain-expressed microRNAs with possible roles in murine and human neuronal differentiation. *Genome Biol* **5:** R13

Smirnova L, Grafe A, Seiler A, Schumacher S, Nitsch R, Wulczyn FG (2005) Regulation of miRNA expression during neural cell specification. *Eur J Neurosci* **21:** 1469-1477

Smith P, Al Hashimi A, Girard J, Delay C, Hebert SS (2011) In vivo regulation of amyloid precursor protein neuronal splicing by microRNAs. *J Neurochem* **116:** 240-247

Song J-J, Liu J, Tolia NH, Schneiderman J, Smith SK, Martienssen RA, Hannon GJ, Joshua-Tor L (2003) The crystal structure of the Argonaute2 PAZ domain reveals an RNA binding motif in RNAi effector complexes. *Nat Struct Mol Biol* **10:** 1026-1032

Song J-J, Smith SK, Hannon GJ, Joshua-Tor L (2004) Crystal Structure of Argonaute and Its Implications for RISC Slicer Activity. *Science* **305:** 1434-1437

Spellman R, Smith CWJ (2006) Novel modes of splicing repression by PTB. *Trends in Biochemical Sciences* **31:** 73-76

Stefani G, Slack FJ (2008) Small non-coding RNAs in animal development. *Nature Reviews Molecular Cell Biology* **9:** 219-230

Tian Z, Greene AS, Pietrusz JL, Matus IR, Liang M (2008) MicroRNA–target pairs in the rat kidney identified by microRNA microarray, proteomic, and bioinformatic analysis. *Genome Res* **18:** 404-411

Vagin VV, Sigova A, Li C, Seitz H, Gvozdev V, Zamore PD (2006) A distinct small RNA pathway silences selfish genetic elements in the germline. *Science* **313:** 320-324

Valencia-Sanchez MA, Liu J, Hannon GJ, Parker R (2006) Control of translation and mRNA degradation by miRNAs and siRNAs. *Genes & Development* **20:** 515-524

Visvanathan J, Lee S, Lee B, Lee JW, Lee S-K (2007) The microRNA miR-124 antagonizes the anti-neural REST/SCP1 pathway during embryonic CNS development. *Genes & Development* **21:** 744-749

Watanabe T, Takeda A, Tsukiyama T, Mise K, Okuno T, Sasaki H, Minami N, Imai H (2006) Identification and characterization of two novel classes of small RNAs in the mouse germline: retrotransposon-derived siRNAs in oocytes and germline small RNAs in testes. *Genes & Development* **20:** 1732-1743

Watanabe T, Totoki Y, Toyoda A, Kaneda M, Kuramochi-Miyagawa S, Obata Y, Chiba H, Kohara Y, Kono T, Nakano T, Surani MA, Sakaki Y, Sasaki H (2008) Endogenous siRNAs from naturally formed dsRNAs regulate transcripts in mouse oocytes. *Nature* **453:** 539-543

Wienholds E, Plasterk RH (2005) MicroRNA function in animal development. *FEBS Lett* **579:** 5911-5922

Wightman B, Ha I, Ruvkun G (1993) Posttranscriptional regulation of the heterochronic gene lin-14 by lin-4 mediates temporal pattern formation in C. elegans. *Cell* **75:** 855-862

Wu L, Fan J, Belasco JG (2006) MicroRNAs direct rapid deadenylation of mRNA. *Proc Natl Acad Sci U S A* **103:** 4034-4039

Wyman SK, Knouf EC, Parkin RK, Fritz BR, Lin DW, Dennis LM, Krouse MA, Webster PJ, Tewari M (2011) Post-transcriptional generation of miRNA variants by multiple nucleotidyl transferases contributes to miRNA transcriptome complexity. *Genome Res* **21:** 1450-1461

Xie J, Ameres SL, Friedline R, Hung J-H, Zhang Y, Xie Q, Zhong L, Su Q, He R, Li M, Li H, Mu X, Zhang H, Broderick JA, Kim JK, Weng Z, Flotte TR, Zamore PD, Gao G (2012) Long-term, efficient inhibition of microRNA function in mice using rAAV vectors. *Nat Meth* **9:** 403-409

Yan KS, Yan S, Farooq A, Han A, Zeng L, Zhou M-M (2003) Structure and conserved RNA binding of the PAZ domain. *Nature* **426:** 469-474

Yang J-S, Maurin T, Robine N, Rasmussen KD, Jeffrey KL, Chandwani R, Papapetrou EP, Sadelain M, O'Carroll D, Lai EC (2010) Conserved vertebrate mir-451 provides a platform for Dicer-independent, Ago2-mediated microRNA biogenesis. *Proceedings of the National Academy of Sciences* **107:** 15163-15168

Yigit E, Batista PJ, Bei Y, Pang KM, Chen CC, Tolia NH, Joshua-Tor L, Mitani S, Simard MJ, Mello CC (2006) Analysis of the C. elegans Argonaute family reveals that distinct Argonautes act sequentially during RNAi. *Cell* **127:** 747-757

Yu B, Yang Z, Li J, Minakhina S, Yang M, Padgett RW, Steward R, Chen X (2005) Methylation as a Crucial Step in Plant microRNA Biogenesis. *Science* **307:** 932-935

Yu J, Wang F, Yang GH, Wang FL, Ma YN, Du ZW, Zhang JW (2006) Human microRNA clusters: genomic organization and expression profile in leukemia cell lines. *Biochem Biophys Res Commun* **349:** 59-68

Zeng Y (2006) Principles of micro-RNA production and maturation. *Oncogene* **25:** 6156-6162

Zeng Y, Cullen BR (2005) Efficient processing of primary microRNA hairpins by Drosha requires flanking nonstructured RNA sequences. *J Biol Chem* **280:** 27595-27603

Zhao LJ, Jian H, Zhu H (2003) Specific gene inhibition by adenovirus-mediated expression of small interfering RNA. *Gene* **316:** 137-141

Zhao Y, Samal E, Srivastava D (2005) Serum response factor regulates a muscle-specific microRNA that targets Hand2 during cardiogenesis. *Nature* **436:** 214-220

Zhao Y, Srivastava D (2007) A developmental view of microRNA function. *Trends in Biochemical Sciences* **32:** 189-197

Zieve G, Penman S (1976) Small RNA species of the HeLa cell: metabolism and subcellular localization. *Cell* **8:** 19-31

6. PUBLICATION

Juvvuna PK, Khandelia P, Lee LM, Makeyev EV (2012) Argonaute identity defines the length of mature mammalian microRNAs. *Nucleic Acids Research,* (doi: 10.1093/nar/gks293)

Nucleic Acids Research Advance Access published April 13, 2012

Nucleic Acids Research, 2012, 1–13
doi:10.1093/nar/gks293

Argonaute identity defines the length of mature mammalian microRNAs

Prasanna Kumar Juvvuna[1], Piyush Khandelia[1], Li Ming Lee[1,2] and Eugene V. Makeyev[1,*]

[1]School of Biological Sciences and [2]C.N. Yang Scholars Programme, Nanyang Technological University, 60 Nanyang Drive, SBS-02n-45, Singapore 637551

Received December 29, 2011; Revised March 15, 2012; Accepted March 19, 2012